AD-A273 999

Detection Performance of a Modified Generalized Likelihood Ratio Processor for Random Signals of Unknown Location

Albert H. Nuttall
Surface ASW Directorate

DTIC

DEC 2 3 1993

Naval Undersea Warfare Center Detachment
New London, Connecticut

93-30841

93 12 21 181

PREFACE

The author of this report is located at the Naval Undersea Warfare Center Detachment, New London, CT 06320. The technical reviewer for this report was Erik B. Siborg, (Code 2111).

REVIEWED AND APPROVED: 23 November 1993

Donald W. Counsellor
Director, Surface Antisubmarine Warfare

REPORT DOCUMENTATION PAGE

Form Approved
OMB No. 0704-0188

1. AGENCY USE ONLY (Leave blank)	2. REPORT DATE 23 November 1993	3. REPORT TYPE AND DATES COVERED Progress

4. TITLE AND SUBTITLE
Detection Performance of a Modified Generalized Likelihood Ratio Processor for Random Signals of Unknown Location

5. FUNDING NUMBERS
PE 0601152N

6. AUTHOR(S)
Albert H. Nuttall

7. PERFORMING ORGANIZATION NAME(S) AND ADDRESS(ES)
Naval Undersea Warfare Center Detachment
New London, Connecticut 06320

8. PERFORMING ORGANIZATION REPORT NUMBER
NUWC-NPT TR 10,539

9. SPONSORING/MONITORING AGENCY NAME(S) AND ADDRESS(ES)
Office of Naval Research
800 North Quincy Street, BCT 1
Arlington, VA 22217-5000

10. SPONSORING/MONITORING AGENCY REPORT NUMBER

11. SUPPLEMENTARY NOTES

12a. DISTRIBUTION/AVAILABILITY STATEMENT
Approved for public release; distribution is unlimited.

12b. DISTRIBUTION CODE

13. ABSTRACT (Maximum 200 words)

A search region of N bins in time, frequency space contains either noise only, or noise plus a signal which occupies a subset of M bins of unknown location. The unknown signal strengths are estimated by means of a maximum likelihood procedure modified by a breakpoint x_o, in order to suppress the weaker estimates. The stronger signal estimates are then used to implement a modified form of generalized likelihood ratio processor.

The highly nonlinear character of this generalized likelihood ratio processor debilitates against an exact analysis of its performance. To circumvent this difficulty, all the nonlinear components are replaced by piecewise-linear devices which best match the given characteristics according to minimum mean square error. The false alarm and detection probabilities of this piecewise-linear processor are then derived exactly. These analytic results enable ready determination of threshold settings and receiver operating

14. SUBJECT TERMS
detection performance, generalized, random signals, modified processor, likelihood ratio, unknown location

15. NUMBER OF PAGES 146

16. PRICE CODE

17. SECURITY CLASSIFICATION OF REPORT	18. SECURITY CLASSIFICATION OF THIS PAGE	19. SECURITY CLASSIFICATION OF ABSTRACT	20. LIMITATION OF ABSTRACT
UNCLASSIFIED	UNCLASSIFIED	UNCLASSIFIED	SAR

NSN 7540-01-280-5500

Standard Form 298 (Rev 2-89)
Prescribed by ANSI Std 239-18
299-102

13. ABSTRACT (continued)

characteristics for a variety of values of N, M, xo, and the signal-to-noise ratio. However, for small breakpoint values xo, a fourth-order moment fit to the exact statistics of the nonlinear characteristics is required and used instead. Receiver operating characteristics for a general set of parameter values are presented and verified by means of simulations.

14. SUBJECT TERMS (continued)

maximum likelihood estimation
breakpoint
piecewise-linear fits
minimum mean-square error
false alarm probability
detection probability
receiver operating characteristics
fourth-order moment fit

Accesion For		
NTIS CRA&I		☒
DTIC TAB		☐
Unannounced		☐
Justification		
By		
Distribution /		
Availability Codes		
Dist	Avail and / or Special	
A-1		

DTIC QUALITY INSPECTED 3

TABLE OF CONTENTS

APPENDICES

LIST OF FIGURES

LIST OF TABLES

LIST OF SYMBOLS

MGLR	modified generalized likelihood ratio
N	total number of search bins, (1)
x_n	n-th bin measurement or observation, (1)
bold	random variable
H_0	noise-only hypothesis, (1)
q_0	probability density function of x_n under H_0, (1)
$E\{x_n\}$	ensemble average of x_n, (1)
overbar	ensemble average, (1), (44)
M	number of bins occupied by signal (when present), (2)
H_1	signal-plus-noise hypothesis, (2)
q_1	probability density function of x_n under H_1, (2)
$\underline{S}_n$	average signal power in n-th bin, (2)
$\underline{a}_n$	signal power parameter $(1 + \underline{S}_n)^{-1}$, (2)
S_o	minimum acceptable signal power level estimate, (3)
x_o	breakpoint $1 + S_o$, (3)
$g(x)$	nonlinear function, (3)
y_n	n-th distorted random variable $g(x_n)$, (4)
z	decision variable, processor output, (4)
v	threshold, (4)
$h(x)$	approximating nonlinearity, (5)
c,b	constants in device $h(x)$, (5)
η_n	output of device, $h(x_n)$, (7)
ζ	output of summer, approximation to z, (8)
P_f	false alarm probability
P_d	detection probability

c_o, b_o	parameters of device $h(x)$ for noise only, (10)
E_η	exceedance distribution function of η_n, (10)
$Pr(E)$	probability of event E, (10)
B	$\exp(-x_o)$, (11)
p_η	probability density function of η_n, (12)
$U(x)$	unit step: 1 for $x > 0$, 0 otherwise, (12)
ξ	argument of characteristic function
f_η	characteristic function of device output η_n, (13)
f_ζ	characteristic function of summer output ζ, (14)
p_n	normalized probability density function, (15)
f_n	normalized characteristic function, (16)
E_n	normalized exceedance distribution function, (17)
C_n	normalized cumulative distribution function, (18)
p_ζ	probability density function of ζ, (19)
E_ζ	exceedance distribution function of ζ, (20)
C_ζ	cumulative distribution function of ζ, (21)
Q_1	exceedance distribution function of x_n under H_1, (22)
$\underline{S}$	equal signal power level, (22)
$\underline{a}$	signal power parameter, $1/(1 + \underline{S})$, (22)
A	$\exp(-\underline{a}x_o)$, (24)
K	$N - M$, (27)
f_a, f_b	component characteristic functions, (27)
U_m	expansion coefficients, (29)
T_k	expansion coefficients, (31)
μ_{kn}	expansion coefficients, (33), (37)
ν_{mn}	expansion coefficients, (33), (37)

$X_y(k)$ k-th cumulant of y_n, (43)

$X_z(k)$ k-th cumulant of z, (43)

$\mu_y(k)$ k-th moment of y_n, (44)

$f_4(\xi)$ candidate characteristic function, FIT-4, (46)

b', c' numerator constants in $f_4(\xi)$, (46)

w', M' denominator constants in $f_4(\xi)$, (46)

X_k auxiliary constants, (47)

w energy detector output, (52)

f_w characteristic function of w, (53)

ROC   receiver operating characteristic, figure 8

P_{fm} maximum false alarm probability, (59)

ED   energy detector, table 1

$\mu(\underline{S}, x_o)$ mean output of $g(x)$, (63)

$E_1(z)$ exponential integral, (63)

μ_z mean of summer output z, (65)

$\underline{S}_e$ effective signal power, (66), (67)

M_e effective number of signal bins, (68)

$\underline{S}_p$ peak signal power, $\max\{\underline{S}_m\}$, (68)

$\sigma^2(\underline{S}, x_o)$ variance of output of $g(x)$, (69)

$R(\underline{S}, x_o)$ ratio of functions, (70)

σ_z^2 variance of summer output z, (74)

FIT-2   fitting procedure, (B-3)

FIT-1   fitting procedure, (B-9)

$f_z(\xi)$ characteristic function of z, (G-2)

DETECTION PERFORMANCE OF A MODIFIED GENERALIZED LIKELIHOOD RATIO PROCESSOR FOR RANDOM SIGNALS OF UNKNOWN LOCATION

INTRODUCTION

The detection of weak signals of unknown strength and location, in the presence of noise, is a common requirement in many applications. One method of trying to restore information about the unknown parameters of the signal is to estimate them from the received data and to substitute these estimates into the likelihood ratio. When this is done, the resulting generalized likelihood ratio is compared with a threshold for a decision about signal presence or absence.

Here, we will consider a modification of the generalized likelihood ratio procedure, to be called the MGLR processor, where only those signal strength estimates above a minimum acceptable level are utilized [1]. This results in a processor with nonlinearities in each channel which have breakpoints in their characteristics. This, in turn, leads to channel outputs and a processor output which are distinctly non-Gaussian in many cases, thereby making the analysis of performance a rather difficult task. In fact, use of the Gaussian approximation and the central limit theorem can yield very misleading values for the threshold settings and signal-to-noise ratios that are required in order to achieve specified false alarm and detection probabilities.

The specific problem of interest is as follows. A total number, N, of search bins contains independent noises of uniform power distribution; this can be accomplished by a normalization procedure. When signal is present, it occupies a subset of M of these bins, whose locations are unknown. Each of the N channel outputs are subjected to a common nonlinearity and then summed; this sum is then compared with a threshold. We will derive the false alarm and detection probabilities of this MGLR processor and verify the results by simulation over a wide variety of parameter values.

Some related results on a processor with a dead zone are available in [2]; however, the work here is a generalization in several respects. The number of signal bins, M, can be less than the total number of search bins, N, and the approximating nonlinearity is more general, being characterized by two parameters rather than one. In fact, in the following analysis for the detection probability, we will utilize a different pair of parameter values for the signal-plus-noise bins, compared with the pair for the noise-only bins. The fact that M is less than N significantly complicates the detection probability analysis relative to that in [2].

PROBLEM DEFINITION

A search space consisting of N bins contains a noise background which has a uniform power distribution over all the bins; this situation is achieved in practice by the use of normalization, which could be based upon neighboring bins or past behavior. In addition, when signal is present, M of these bins contain random signal components of unknown locations and strengths. We will presume that the number of occupied bins, M, is also unknown; this will lead to a processor that must make some assumption about M in order to achieve decent levels of performance in terms of the false alarm and detection probabilities. Other approaches, which estimate M, or which can function without knowledge of M, are the subject of a future report [3].

Under the noise-only hypothesis H_0, the N bin outputs, $\{x_n\}$, are statistically independent and identically-distributed random variables with exponential probability density function

$$q_0(u_n) = \exp(-u_n) \quad \text{for } u_n > 0 \quad \text{for } 1 \leq n \leq N . \tag{1}$$

For example, these random variables, $\{x_n\}$, could be the envelope-squared outputs of a bank of disjoint narrowband filters (or FFT outputs) for a Gaussian noise input with a flat spectrum over the total search band. The assumption of a unit average power level, $E\{x_n\} = \overline{x_n} = \int du \, q_0(u) \, u = 1$ in (1), is a matter of convenience and is considered to have been achieved in practice through the use of normalization.

Under the signal-plus-noise hypothesis H_1, M of the bins also contain signal, with average power $\underline{S}_n$ in the n-th bin. These constants, $\{\underline{S}_n\}$, are unknown. The governing probability density function for the bin output random variables $\{x_n\}$ in this case is

$$q_1(u_n) = \underline{a}_n \exp(-\underline{a}_n u_n) \quad \text{for } u_n > 0 \ , \quad \underline{a}_n = \frac{1}{1 + \underline{S}_n} \ , \tag{2}$$

for n corresponding to the M occupied signal bins; otherwise, density (1) holds true. Since the actual n-th signal power level $\underline{S}_n$ is unknown, it must be estimated from the available data measurements or observations, $\{x_n\}$, of the N bin outputs.

The derivation of the MGLR (modified generalized likelihood ratio) processor [1] for this environment is accomplished in appendix A. In order to introduce it, we first define S_o as the minimum acceptable signal power level that will be tolerated as an estimate of the signal strength. Also, we define breakpoint $x_o = 1 + S_o$, and nonlinear function

$$g(x) = \begin{cases} x - 1 - \ln(x) & \text{for } x \geq x_o \\ 0 & \text{otherwise} \end{cases} \ . \tag{3}$$

We require level $S_o \geq 0$, thereby making $x_o \geq 1$. Then, the MGLR test for deciding on presence or absence of a signal in observation, $\{x_n\}$, depends on decision variable z, which is given by

$$z = \sum_{n=1}^{N} Y_n = \sum_{n=1}^{N} g(x_n) \underset{<}{\overset{>}{\gtrless}} v \ . \tag{4}$$

We are interested in determining the false alarm and detection probabilities of this MGLR test, where v is the threshold.

DERIVATION OF FALSE ALARM PROBABILITY

APPROACH

An exact derivation of the false alarm and detection probabilities of the precise MGLR processor in (3) and (4) would be extremely difficult and time-consuming. Instead, we will determine the performance by combining two different approximation techniques. In the first technique, the breakpoint nonlinearity, $g(x)$, in (3) is replaced by the best fitting piecewise-linear device, which is then analyzed exactly. On the other hand, in the second technique, the exact device, $g(x)$, is retained, but, instead, the probability analysis is approximate, relying on a fourth-order fit to the exact first four moments or cumulants of decision variable z. This two-pronged approach has been found adequate to cover the range of values of N, M, x_o, and signal-to-noise ratio that are of major interest. Simulations verify the accuracy and viability of this approach.

PIECEWISE-LINEAR APPROXIMATION

The specified nonlinearity $g(x)$ of interest is given by (3). However, the approximating nonlinearity that we adopt in its stead is the piecewise-linear function

$$h(x) = \begin{cases} c + b(x - x_o) & \text{for } x \geq x_o \\ 0 & \text{for } x < x_o \end{cases} , \tag{5}$$

where constants c and b depend on breakpoint x_o, nonlinearity $g(x)$, and the probability density functions $q_k(u)$ of input random variables $\{x_n\}$, as given in (1) and (2) for k = 0 and 1, respectively. For example, we could choose the tangent line at breakpoint x_o (independent of $q_k(u)$); then, we would have

$$c = g(x_o) = x_o - 1 - \ln(x_o) \,, \quad b = g'(x_o) = 1 - \frac{1}{x_o} \,. \quad (6)$$

Other choices for c and b, which minimize a mean square error criterion, are derived and tabulated in appendix B. Additional viewpoints and interpretations are presented there and should be examined for a complete explanation of the approach.

The approximating-nonlinearity output is no longer the random variable $y_n = g(x_n)$ introduced in (4), but is instead the random variable

$$\eta_n = h(x_n) \quad \text{for } 1 \leq n \leq N \,. \quad (7)$$

The approximation to the original summer output z in (4) is

$$\zeta = \sum_{n=1}^{N} \eta_n = \sum_{n=1}^{N} h(x_n) \,. \quad (8)$$

We will evaluate the exceedance distribution functions of this new random variable, ζ, exactly for both hypotheses H_0 and H_1. Hopefully, the piecewise-linear fit utilized in (5) will be adequate to accurately determine false alarm probability P_f in the 10^{-6} range and detection probability P_d in the .99 range. Simulation results will bear out this approach.

EXCEEDANCE PROBABILITY FOR NOISE ALONE

For noise alone, the probability density function and exceedance distribution function of input random variables $\{x_n\}$ to device $h(x)$ are, from (1), respectively,

$$q_0(u) = \exp(-u) \quad \text{for } u > 0 \ ,$$

$$Q_0(v) = \int_v^\infty du \ q_0(u) = \exp(-v) \quad \text{for } v > 0 \ . \tag{9}$$

Parameters c and b of the approximating nonlinearity $h(x)$ are positive constants; in particular, in the case H_0 of noise-alone inputs $\{x_n\}$, they will be denoted by c_o and b_o, respectively. This reflects and accents the fact that, during analysis, the approximating nonlinearity $h(x)$ should be chosen differently for the noise-only bins versus the signal-plus-noise bins in case H_1.

If $v > c_o > 0$, the exceedance distribution function of device output $\eta_n = h(x_n)$ in (7) is (for $b_o > 0$)

$$E_\eta(v) = \Pr(\eta_n > v) = \Pr(c_o + b_o(x_n - x_o) > v) = \tag{10}$$

$$= \Pr\left(x_n > x_o + \frac{v - c_o}{b_o}\right) = \exp\left(-x_o - \frac{v - c_o}{b_o}\right) = B \exp\left(-\frac{v - c_o}{b_o}\right) \ ,$$

where we used (5) and (9), and where

$$B = \exp(-x_o) \ , \quad B_1 = 1 - B \ . \tag{11}$$

The probability density function of device output η_n follows as

$$p_\eta(u) = -\frac{d}{du} E_\eta(u) = B_1 \, \delta(u) + \frac{B}{b_o} \exp\left(-\frac{u - c_o}{b_o}\right) U(u - c_o) \quad (12)$$

for all u, where U is the unit step function. The characteristic function of η_n is therefore the Fourier transform

$$f_\eta(\xi) = B_1 + B \frac{\exp(i\xi c_o)}{1 - i\xi b_o} \quad \text{for all } \xi . \quad (13)$$

The approximation ζ (to the original summer output z) is given by (8) as a sum of N independent terms $\{\eta_n\}$. Therefore, its characteristic function is closed form

$$f_\zeta(\xi) = f_\eta^N(\xi) = \left(B_1 + B \frac{\exp(i\xi c_o)}{1 - i\xi b_o}\right)^N =$$

$$= B_1^N + \sum_{n=1}^{N} \binom{N}{n} B_1^{N-n} B^n \frac{\exp(i\xi n c_o)}{(1 - i\xi b_o)^n} . \quad (14)$$

At this point, it is convenient to define several sets of functions which will help to minimize notation in the sequel. The first is the set of normalized probability density functions

$$p_n(u) = \begin{cases} \dfrac{u^{n-1} \exp(-u)}{(n-1)!} & \text{for } u > 0 \\ \\ 0 & \text{for } u \leq 0 \end{cases} \quad \text{for } n = 1,2,\ldots \quad (15)$$

with their corresponding characteristic functions

$$f_n(\xi) = \int_{-\infty}^{\infty} du \, \exp(i\xi u) \, p_n(u) = \frac{1}{(1 - i\xi)^n} \quad \text{for } n = 1,2,\ldots \quad (16)$$

Also, define the corresponding exceedance distribution functions

$$E_n(v) = \int_v^\infty du\; p_n(u) = \left\{ \begin{array}{ll} \exp(-v) \sum_{k=0}^{n-1} \dfrac{v^k}{k!} & \text{for } v > 0 \\[2mm] 1 & \text{for } v \leq 0 \end{array} \right\} \quad \text{for } n = 1,2,\ldots \tag{17}$$

Finally, define the corresponding cumulative distribution functions

$$C_n(v) = 1 - E_n(v) \text{ for all } v \;, \quad \text{for } n = 1,2,\ldots \tag{18}$$

Then, the probability density function of ζ, corresponding to characteristic function (14), is

$$p_\zeta(u) = B_1^N\, \delta(u) + \sum_{n=1}^{N} \binom{N}{n} B_1^{N-n}\, B^n\, \frac{1}{b_0}\, p_n\!\left(\frac{u - nc_0}{b_0}\right) \quad \text{for all } u, \tag{19}$$

where we used (15) and (16). The corresponding exceedance distribution function of ζ is, from (17),

$$E_\zeta(v) = \int_v^\infty du\; p_\zeta(u) = \sum_{n=1}^{N} \binom{N}{n} B_1^{N-n}\, B^n\, E_n\!\left(\frac{v - nc_0}{b_0}\right) \quad \text{for } v > 0. \tag{20}$$

Finally, the cumulative distribution function of ζ is, from (18) and (19),

$$C_\zeta(v) = B_1^N + \sum_{n=1}^{N} \binom{N}{n} B_1^{N-n}\, B^n\, C_n\!\left(\frac{v - nc_0}{b_0}\right) \quad \text{for } v > 0 \;. \tag{21}$$

It is very important to observe in (21) that as soon as summation index n exceeds v/c_0, this sum can be terminated, because cumulative distribution function C_n in (18) is zero for

negative arguments. This is a very advantageous property, especially for large values of breakpoint x_o, because parameter c_o is large then. That is, the upper limit N in (21) can be replaced by the integer N' = INT(v/c_o), which can be considerably less than N.

This result in (21) for cumulative distribution function $C_\zeta(v)$ pertains to hypothesis H_0, noise-only present in all N search bins. Parameters c_o and b_o used in device $h(x)$ in (5) are chosen for a good fit to $g(x)$ in (3) for $x > x_o$ for the case of noise-only inputs. See appendix B for more details on the fitting procedure and numerical results.

DERIVATION OF DETECTION PROBABILITY

STATISTICS OF BIN OUTPUTS WITH SIGNAL

For the signal-present bins, the probability density function of inputs $\{x_n\}$ is given by (2). The corresponding exceedance distribution function for these particular bins is

$$Q_1(v) = \exp(-\underline{a}v) \quad \text{for } v > 0 . \tag{22}$$

Here, for the analysis of performance of summer output ζ in (8), we presume that the signal power levels $\underline{S}_n$ in all M occupied bins are equal, with value $\underline{S}$; then $\underline{a}_n = \underline{a} = (1 + \underline{S})^{-1}$ for these M bins, while $\underline{a} = 1$ for the remaining N - M noise-only bins.

For the signal-plus-noise bins, we allow the piecewise-linear approximation $h(x)$ in (5) (to the given nonlinearity $g(x)$) to have different values for the parameters, c and b, which depend on $\underline{S}$, x_o, and $g(x)$. The values c_o and b_o for the N - M noise-only bins are kept the same as in the false alarm analysis above.

If $v > c > 0$, the exceedance distribution function of a signal-present bin output η_n is (for b > 0)

$$E_\eta(v) = \Pr(\eta_n > v) = \Pr(c + b(x_n - x_o) > v) = \tag{23}$$

$$= \Pr\left(x_n > x_o + \frac{v - c}{b}\right) = \exp\left(-\underline{a}x_o - \underline{a}\frac{v - c}{b}\right) = A \exp\left(-\underline{a}\frac{v - c}{b}\right),$$

where we used (22) and defined

$$A = \exp(-\underline{a}x_o) , \quad A_1 = 1 - A . \tag{24}$$

The probability density function of device output η_n is

$$p_\eta(u) = A_1 \, \delta(u) + \underline{a} \frac{A}{b} \exp\left(- \underline{a}\frac{u - c}{b}\right) U(u - c) \quad \text{for all } u , \quad (25)$$

while the corresponding characteristic function is

$$f_\eta(\xi) = A_1 + A \frac{\exp(i\xi c)}{1 - i\xi b/\underline{a}} \quad \text{for all } \xi . \quad (26)$$

These functions in (25) and (26) pertain only to the signal-plus-noise bins.

STATISTICS OF SUMMER OUTPUT ζ

Since summer output ζ is composed of M (≥ 1) signal bins and $K = N - M$ noise-only bins, its characteristic function is

$$f_\zeta(\xi) = \left(A_1 + A \frac{\exp(i\xi c)}{1 - i\xi b/\underline{a}}\right)^M \left(B_1 + B \frac{\exp(i\xi c_o)}{1 - i\xi b_o}\right)^K \equiv f_a(\xi) f_b(\xi) \quad (27)$$

where we used (26) and (13). If $\underline{S} = 0$, then $\underline{a} = 1$, $A = B$, $A_1 = B_1$, $c = c_o$, $b = b_o$, and $f_\zeta(\xi)$ reduces to the earlier result in (14) for noise only.

For $M \geq 1$, we use the binomial expansion on (27) to get

$$f_a(\xi) = \left(A_1 + A \frac{\exp(i\xi c)}{1 - i\xi b/\underline{a}}\right)^M = U_0 + \sum_{m=1}^{M} U_m \frac{\exp(i\xi mc)}{(1 - i\xi b/\underline{a})^m} , \quad (28)$$

where

$$U_m = U_m(M, \underline{a}x_o) \equiv \binom{M}{m} A_1^{M-m} A^m \quad \text{for } 0 \leq m \leq M . \quad (29)$$

For $K \geq 1$, that is, $M < N$, (the case of $M = N$ is much simpler), the noise-only characteristic function term is

$$f_b(\xi) = \left(B_1 + B \frac{\exp(i\xi c_o)}{1 - i\xi b_o}\right)^K = T_0 + \sum_{k=1}^{K} T_k \frac{\exp(i\xi k c_o)}{(1 - i\xi b_o)^k} , \qquad (30)$$

where

$$T_k = T_k(K, x_o) = \binom{K}{k} B_1^{K-k} B^k \quad \text{for } 0 \leq k \leq K . \qquad (31)$$

Therefore, the characteristic function of summer output ζ, for signal present in M out of N bins, is

$$f_\zeta(\xi) = f_a(\xi) \, f_b(\xi) =$$

$$= U_0 \, T_0 + U_0 \sum_{k=1}^{K} T_k \frac{\exp(i\xi k c_o)}{(1 - i\xi b_o)^k} + T_0 \sum_{m=1}^{M} U_m \frac{\exp(i\xi m c)}{(1 - i\xi b/\underline{a})^m} +$$

$$+ \sum_{m=1}^{M} \sum_{k=1}^{K} U_m \, T_k \frac{\exp(i\xi(mc + k c_o))}{(1 - i\xi b/\underline{a})^m (1 - i\xi b_o)^k} . \qquad (32)$$

At this point, we utilize the results in appendix C (by identifying $\alpha \to b/\underline{a}$, $\beta \to b_o$, $z \to -i\xi$ in (C-9)) to obtain the partial fraction expansion of the last term in (32):

$$\frac{1}{(1 - i\xi b/\underline{a})^m (1 - i\xi b_o)^k} = \sum_{n=0}^{m-1} \frac{\mu_{kn}(b/\underline{a}, b_o)}{(1 - i\xi b/\underline{a})^{m-n}} + \sum_{n=0}^{k-1} \frac{\nu_{mn}(b/\underline{a}, b_o)}{(1 - i\xi b_o)^{k-n}}$$

$$(33)$$

Substitution in (32) then yields the characteristic function of summer output ζ in the form

$$f_\zeta(\xi) = U_0 \, T_0 + U_0 \sum_{k=1}^{K} T_k \frac{\exp(i\xi k c_0)}{(1 - i\xi b_0)^k} + T_0 \sum_{m=1}^{M} U_m \frac{\exp(i\xi m c)}{(1 - i\xi b/\underline{a})^m} +$$

$$+ \sum_{m=1}^{M} \sum_{k=1}^{K} U_m \, T_k \, \exp(i\xi(mc + kc_0)) \times$$

$$\times \left\{ \sum_{n=0}^{m-1} \frac{\mu_{kn}(b/\underline{a}, b_0)}{(1 - i\xi b/\underline{a})^{m-n}} + \sum_{n=0}^{k-1} \frac{\nu_{mn}(b/\underline{a}, b_0)}{(1 - i\xi b_0)^{k-n}} \right\} . \tag{34}$$

We now use the following connection between a corresponding characteristic function, its probability density function, and its cumulative distribution function; referring to (15) - (18), we have, for k integer,

$$\frac{\exp(i\xi d)}{(1 - i\xi r)^k} \longleftrightarrow \frac{1}{r} p_k\left(\frac{u - d}{r}\right) \longleftrightarrow C_k\left(\frac{v - d}{r}\right) \quad \text{for } k \geq 1 . \tag{35}$$

The cumulative distribution function of ζ corresponding to characteristic function (34) then follows immediately in the form

$$C_\zeta(v) = U_0 \, T_0 \, C_0(v) + U_0 \sum_{k=1}^{K} T_k \, C_k\left(\frac{v - kc_0}{b_0}\right) + T_0 \sum_{m=1}^{M} U_m \, C_m\left(\frac{v - mc}{b/\underline{a}}\right) +$$

$$+ \sum_{m=1}^{M} \sum_{k=1}^{K} U_m \, T_k \left\{ \sum_{n=0}^{m-1} \mu_{kn}(b/\underline{a}, b_0) \, C_{m-n}\left(\frac{v - mc - kc_0}{b/\underline{a}}\right) + \right.$$

$$\left. + \sum_{n=0}^{k-1} \nu_{mn}(b/\underline{a}, b_0) \, C_{k-n}\left(\frac{v - mc - kc_0}{b_0}\right) \right\} , \tag{36}$$

where $C_0(v) = 0$ for $v < 0$, and is 1 otherwise. One of the attractive features of this expression is that when $mc + kc_0$

exceeds threshold v, normalized cumulative distribution functions C_{m-n} and C_{k-n} are zero, allowing the summations on m and k to be terminated.

Coefficients μ_{kn} and ν_{mn} in (34) and (36) are immediately available from appendix C by identifying $\alpha \rightarrow b/\underline{a}$, $\beta \rightarrow b_0$ in (C-1) and (C-2) to get

$$\mu_{kn}\left(\frac{b}{\underline{a}}, b_0\right) = \frac{b^k \, (-\underline{a}b_0)^n}{(b-\underline{a}b_0)^{k+n}} \frac{(k)_n}{n!} \quad \text{for } k \geq 1 \text{ , } n \geq 0 \text{ ,} \qquad (37)$$

$$\nu_{mn}\left(\frac{b}{\underline{a}}, b_0\right) = \frac{(\underline{a}b_0)^m \, (-b)^n}{(\underline{a}b_0-b)^{m+n}} \frac{(m)_n}{n!} \quad \text{for } m \geq 1 \text{ , } n \geq 0 \text{ .} \qquad (38)$$

These quantities can be rapidly evaluated by recursions; dropping the arguments for the time being, we have

$$\mu_{k0} = \left(\frac{b}{b-\underline{a}b_0}\right)^k \quad \text{for } k \geq 1 \text{ ,} \qquad (39)$$

$$\mu_{kn} = \mu_{k,n-1} \frac{\underline{a}b_0}{\underline{a}b_0-b} \frac{k-1+n}{n} \quad \text{for } n \geq 1 \text{ , } k \geq 1 \text{ ;} \qquad (40)$$

along with

$$\nu_{m0} = \left(\frac{\underline{a}b_0}{\underline{a}b_0-b}\right)^m \quad \text{for } m \geq 1 \text{ ,} \qquad (41)$$

$$\nu_{mn} = \nu_{m,n-1} \frac{b}{b-\underline{a}b_0} \frac{m-1+n}{n} \quad \text{for } n \geq 1 \text{ , } m \geq 1 \text{ .} \qquad (42)$$

The desired result for the cumulative distribution function of summer output ζ is given by (36). The detection probability for this processor is $1 - C_\zeta(v)$, for threshold v.

FOURTH-ORDER MOMENT APPROACH

When breakpoint x_o in nonlinear device $g(x)$ in (3) is large, the techniques in the previous two sections work well enough to yield useful results for both the false alarm and detection probabilities. However, as x_o decreases, the series expansions require progressively more terms, and the execution time becomes excessive for large values of N, like 1024. In addition, the alternating series in (36) for the cumulative distribution function loses all its significance, eventually giving negative values as well as values larger than 1.

Another approach that has worked well in the past is to use a large number of moments or cumulants of the decision variable of interest, if they can be calculated accurately to high order [4]. Additional elaboration on this approach is given in appendix D. Here, however, we will limit consideration to the first four moments of the <u>exact</u> decision variable z in (4) and fit a fourth-order candidate characteristic function; this procedure has been used successfully in a previous detectability study [5]. We label this procedure FIT-4 here.

Let the k-th cumulant of random variable $y_n = g(x_n)$ in (4) be denoted by $\chi_y(k, x_o, \underline{S})$, where it is presumed that the signal powers in the occupied bins are all equal to $\underline{S}$. (The dependence of the cumulants on breakpoint x_o is indicated explicitly.) For the noise-only bins, the pertinent cumulant is $\chi_y(k, x_o, 0)$.

When signal is present in M bins out of the total of N search bins, the k-th cumulant of summer output z in (4) is given by

$$X_z(k) = M \, X_y(k, x_o, \underline{S}) + (N - M) \, X_y(k, x_o, 0) \quad \text{for } k \geq 1 . \quad (43)$$

In order to find the cumulants $\{X_y(k, x_o, \underline{S})\}$, we first numerically evaluate the corresponding moments $\{\mu_y(k, x_o, \underline{S})\}$ exactly by means of the integral expression

$$\mu_y(k, x_o, \underline{S}) = \overline{y_n^k} = \overline{g(x_n)^k} = \int du \, q_1(u) \, g(u)^k =$$

$$= \int_{x_o}^{\infty} du \, \underline{a} \, \exp(-\underline{a}u) \, [u - 1 - \ln(u)]^k \quad \text{for } k \geq 1 , \quad (44)$$

along with $\mu_y(0, x_o, \underline{S}) = 1$. In particular, we evaluate (44) for $k = 1, 2, 3, 4$. The desired cumulants of y_n then follow according to

$$X_y(1, x_o, \underline{S}) = \mu_y(1, x_o, \underline{S}) ,$$

$$X_y(2, x_o, \underline{S}) = \mu_y(2, x_o, \underline{S}) - \mu_y^2(1, x_o, \underline{S}) ,$$

$$X_y(3) = \mu_y(3) - 3 \, \mu_y(2) \, \mu_y(1) + 2 \, \mu_y^3(1) , \quad (45)$$

$$X_y(4) = \mu_y(4) - 4 \, \mu_y(3) \, \mu_y(1) - 3 \, \mu_y^2(2) + 12 \, \mu_y(2) \, \mu_y^2(1) - 6\mu_y^4(1)$$

where we have adopted an abbreviated notation in the last two lines. Tables of the first four cumulants $\{X_y(k, x_o, \underline{S})\}$ are given in appendix E.

The candidate characteristic function, FIT-4, that will be fit to the first four cumulants $\{X_z(k)\}$ in (43) is [5; page 59]

$$f_4(\xi) = \frac{\exp(i\xi b' - \xi^2 c'/2)}{(1 - i\xi w')^{M'}} = \exp\left[i\xi b' - \xi^2 c'/2 - M' \ln(1 - i\xi w')\right]$$

(46)

which is a product of Gaussian and chi-squared characteristic functions; this guarantees that $f_4(\xi)$ is a legal characteristic function, although its corresponding probability density function can be nonzero for negative arguments. For notational shorthand, let

$$X_1 = \chi_z(1) , \quad X_2 = \chi_z(2) , \quad X_3 = \chi_z(3)/2 , \quad X_4 = \chi_z(4)/6 .$$ (47)

Then, in order for characteristic function (46) to have cumulants $\{\chi_z(k)\}$ for $k = 1,2,3,4$, we must take its constants as

$$b' = X_1 - \frac{X_3^3}{X_4^2} , \quad c' = X_2 - \frac{X_3^2}{X_4} , \quad w' = \frac{X_4}{X_3} , \quad M' = \frac{X_3^4}{X_4^3} .$$ (48)

If $X_2 < X_3^2/X_4$, then $c' < 0$; in this case, an alternative is to set $c' = 0$, getting instead the constants

$$b' = X_1 - \frac{X_2^2}{X_3} , \quad w' = \frac{X_3}{X_2} , \quad M' = \frac{X_2^3}{X_3^2} .$$ (49)

This is, in fact, the third-order fit utilized in [5; page 43]. However, even if $c' < 0$ in (48), candidate characteristic function (46) can still be useful; namely, the magnitude $|f_4(\xi)|$ has a minimum at

$$\xi_m = \left(\frac{M'}{|c'|} - \frac{1}{w'^2}\right)^{\frac{1}{2}} ,$$ (50)

with minimum value

$$|f_4(\xi_m)| = \exp\left(\frac{M'}{2} - \frac{|c'|}{2w'^2}\right) \left(\frac{M'w'^2}{|c'|}\right)^{-M'/2} . \tag{51}$$

If $|f_4(\xi_m)| <<< f_4(0) = 1$, namely rapid decay of $f_4(\xi)$, we can still use approximation $f_4(\xi)$ in (46) to get useful results for the corresponding exceedance distribution function, by utilizing only those values $|\xi| < \xi_m$.

ENERGY DETECTOR PERFORMANCE

This section is not concerned with performance of the MGLR processor or its nonlinearity $g(x)$ given by (3). Rather, we derive the exact performance of a processor employing a completely _linear_ summation of the same N search bin outputs $\{x_n\}$, looking for a signal in M bins of unknown location. This system will serve as a worthwhile basis for comparison with the MGLR processor and will indicate quantitatively when we should prefer one processor over the other. Some related results for weighted energy detectors operating under mismatches in frequency and time locations are available in [6].

The energy detector sums over all N bin outputs according to the linear sum

$$w = \sum_{n=1}^{N} x_n .$$

(52)

It is called an energy detector because bin outputs, $\{x_n\}$, are themselves envelope-squared quantities. By reference to (1) and (2), it is immediately seen that the characteristic function of w under hypothesis H_1 is

$$f_w(\xi) = \frac{1}{(1 - i\xi/\underline{a})^M (1 - i\xi)^{N-M}} , \qquad \underline{a} = \frac{1}{1 + \underline{S}} ,$$

(53)

where we presume equal signal power, $\underline{S}$, in all M occupied bins. At this point, we could directly use the partial fraction expansion presented in appendix C; however, we would again

21

encounter an alternating series and loss of significance. Instead, we have resorted to the accurate numerical FFT procedure presented in [7] in order to determine the receiver operating characteristics exactly.

Some special cases of (53) are worth noting. For signal power $\underline{S} = 0$, the characteristic function reduces to

$$f_w(\xi) = \frac{1}{(1 - i\xi)^N} , \tag{54}$$

for which the false alarm probability is

$$P_f = \Pr(w > v | H_0) = \exp(-v) \sum_{n=0}^{N-1} \frac{v^n}{n!} \quad \text{for } v > 0 . \tag{55}$$

Another special case occurs for $M = N$, namely signal in every bin, when present. The energy detector is then the optimum (likelihood ratio) processor. The characteristic function in (53) reduces to

$$f_w(\xi) = \frac{1}{(1 - i\xi/\underline{a})^N} , \qquad \underline{a} = \frac{1}{1 + \underline{S}} , \tag{56}$$

for which the detection probability is

$$P_d = \Pr(w > v | H_1) = \exp(-\underline{a}v) \sum_{n=0}^{N-1} \frac{1}{n!}(\underline{a}v)^n \quad \text{for } v > 0 , \tag{57}$$

while the false alarm probability is (55) again.

GRAPHICAL RESULTS

PIECEWISE-LINEAR FIT h(x)

An example of the ability of piecewise-linear fit h(x) in (5), to approximate the actual nonlinearity g(x) in (3), is given in figure 1 for signal absent, $\underline{S} = 0$, and for breakpoint values $x_o = 1,3,5,7,9,11$. As expected, the approximations for the larger x_o values are on top of their corresponding portions of the dashed curve, which is $x - 1 - \ln(x)$. However, for the smaller values of breakpoint x_o, like 1, the best linear fit cuts across the dashed curve, and for large x values, considerably underestimates the desired values. This is unavoidable because of the considerable curvature of g(x) near $x = 1$ when $x_o = 1$. The fit is significantly improved for $x_o = 3$ and larger values.

The example in figure 2 holds the breakpoint fixed at value $x_o = 5$ while the signal power, $\underline{S}$, is varied over the values 0 dB, 5 dB, 10 dB. The fit for $\underline{S} = 5$ dB lies on top of the dashed curve, while the fit for $\underline{S} = 10$ dB overestimates g(x) in the plotted region displayed. However, for argument values x larger than 18, the two curves will eventually cross.

These results in figures 1 and 2 indicate that we can expect the piecewise-linear fitting procedure to yield useful performance prediction results for the larger values of breakpoint x_o. On the other hand, they also indicate that some problems can be expected for the smaller values of x_o, and that an alternative procedure will be necessary for those cases.
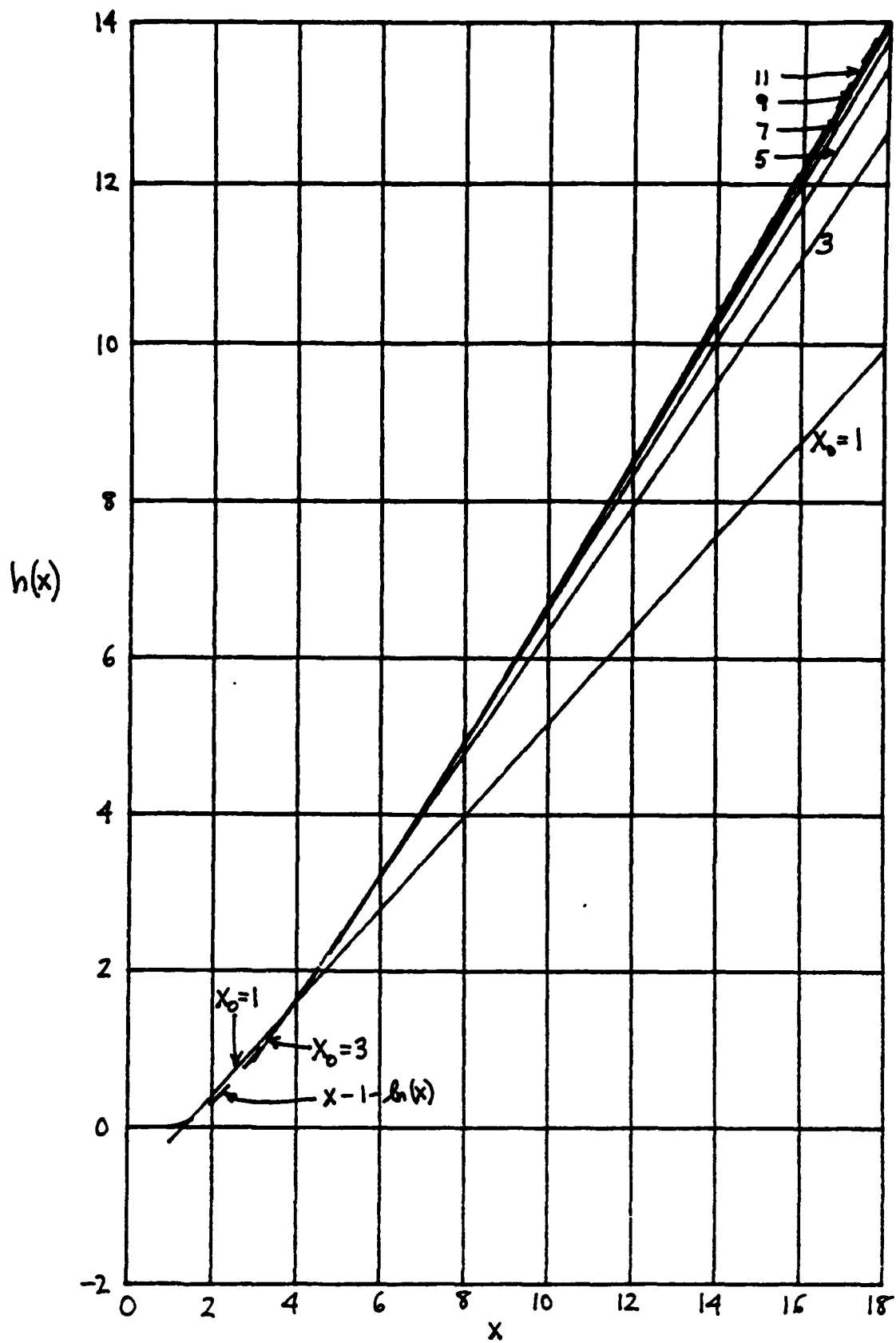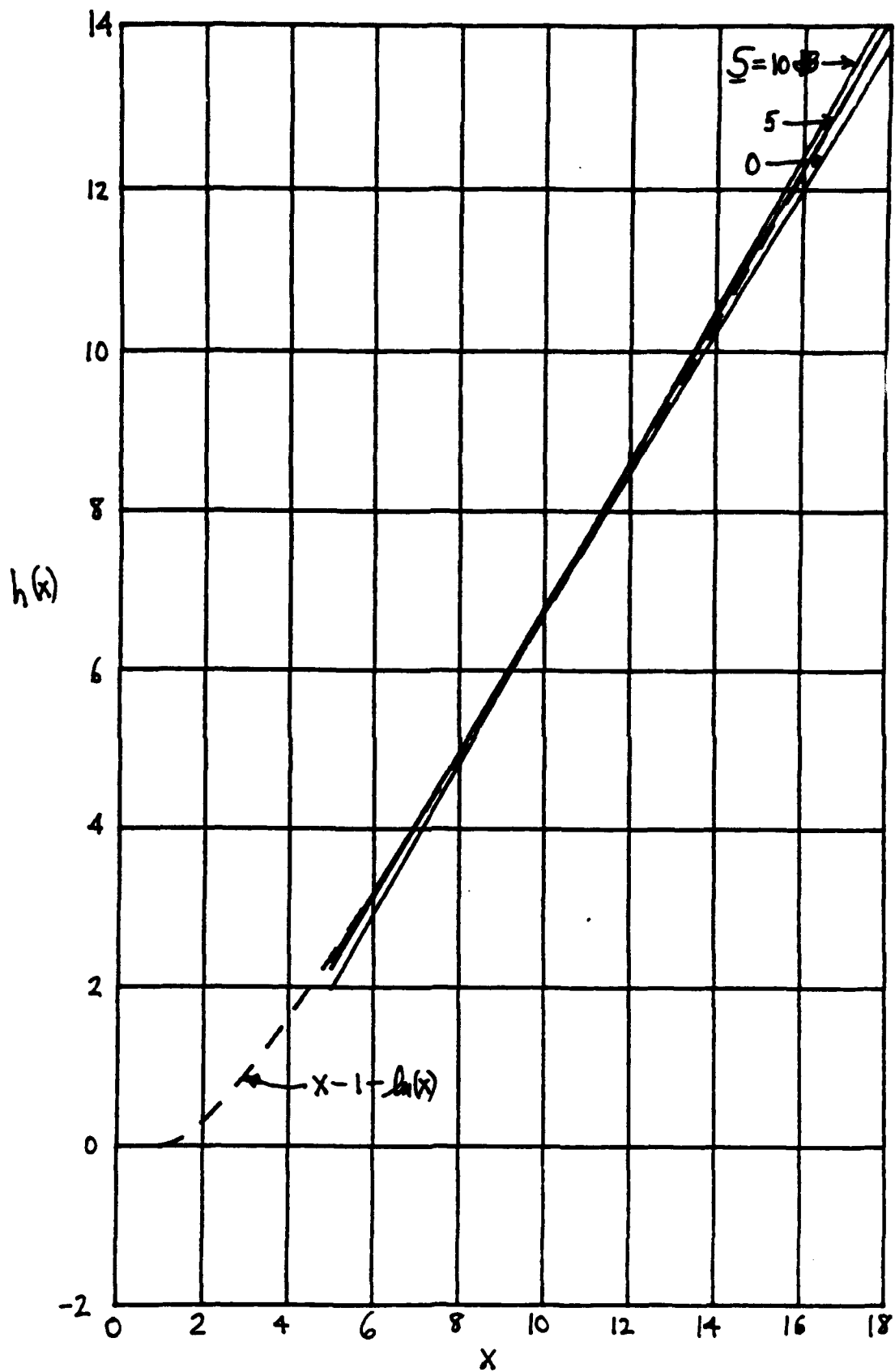
Figure 1.   FIT-2 for $\underline{S} = 0 = -\infty$ dB

Figure 2. FIT-2 for $x_0 = 5$

FALSE ALARM PROBABILITY

The false alarm probability P_f for the MGLR processor was evaluated numerically from the cumulative distribution function in (21), namely as $1 - C_\zeta(v)$, for various values of search size N and breakpoint x_o, versus threshold v. These results are presented in figures 3 - 7 for N = 1024, 512, 256, 128, 64, respectively. For example, in figure 3 for N = 1024, breakpoint x_o is varied from 1 to 11 in increments of 1. Superposed on these smooth curves in figure 3 are a set of jagged curves corresponding to a simulation utilizing 700,000 trials of processor output z using the exact nonlinear device g(x) in (4). This simulation verifies the accuracy of (21) over the complete range of values in figure 3, including the low threshold values, v, in the range (0,10), where the exceedance distribution function has abrupt changes in its character.

Similar confirmation is indicated in the remaining figures 4 - 7, where simulations of various sizes (at least 1,000,000 trials) have been employed for comparison. The only case of significant departure between theory and simulation is in figure 7 for small N (64), small x_o (< 3), and large v (> 20). The systematic deviation between the two curves for x_o = 2 (at small P_f values) illustrates that the piecewise-linear fit described in appendix B is unable to accurately represent device g(x) in this particular region.

The particular results in figures 3 - 7 were obtained by means of FIT-2, which is derived and tabulated in appendix B. That is, both constants c and b in linear fit (5) were optimized for minimum mean squared error. Other fits fared poorer than FIT-2 in the problem region of figure 7. For example, FIT-1 was never better than FIT-2 and was sometimes poorer in predicting P_f values. Attempts to utilize a Gaussian approximation for decision variable z were much poorer, often leading to gross underestimates of the actual false alarm probabilities. Finally, when FIT-4 in (46) was tried, it failed because the fitting constants b' and c' in (48) were negative, and remedy (51) was not small enough to warrant its use.

In order to rectify the shortcoming in the bottom-right portion of figure 7, it would be necessary to employ a two-piece linear fit to g(x). Nevertheless, as it is, the combination of the two types of results available in figures 3 - 7 enable accurate selection of threshold values, v, in order to realize specified false alarm probabilities $P_f > 1E-6$ for various breakpoint values x_0 and search sizes N.
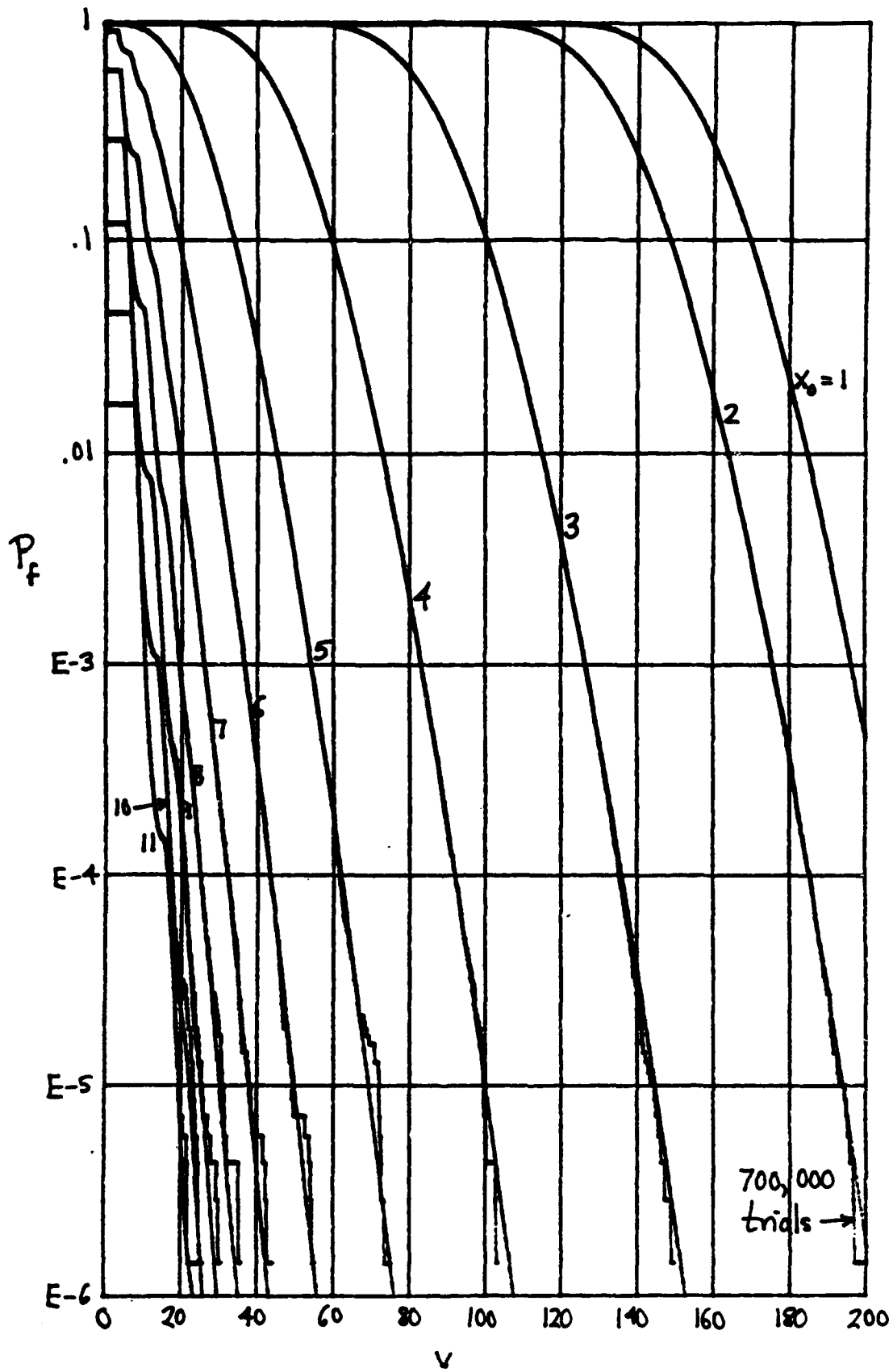
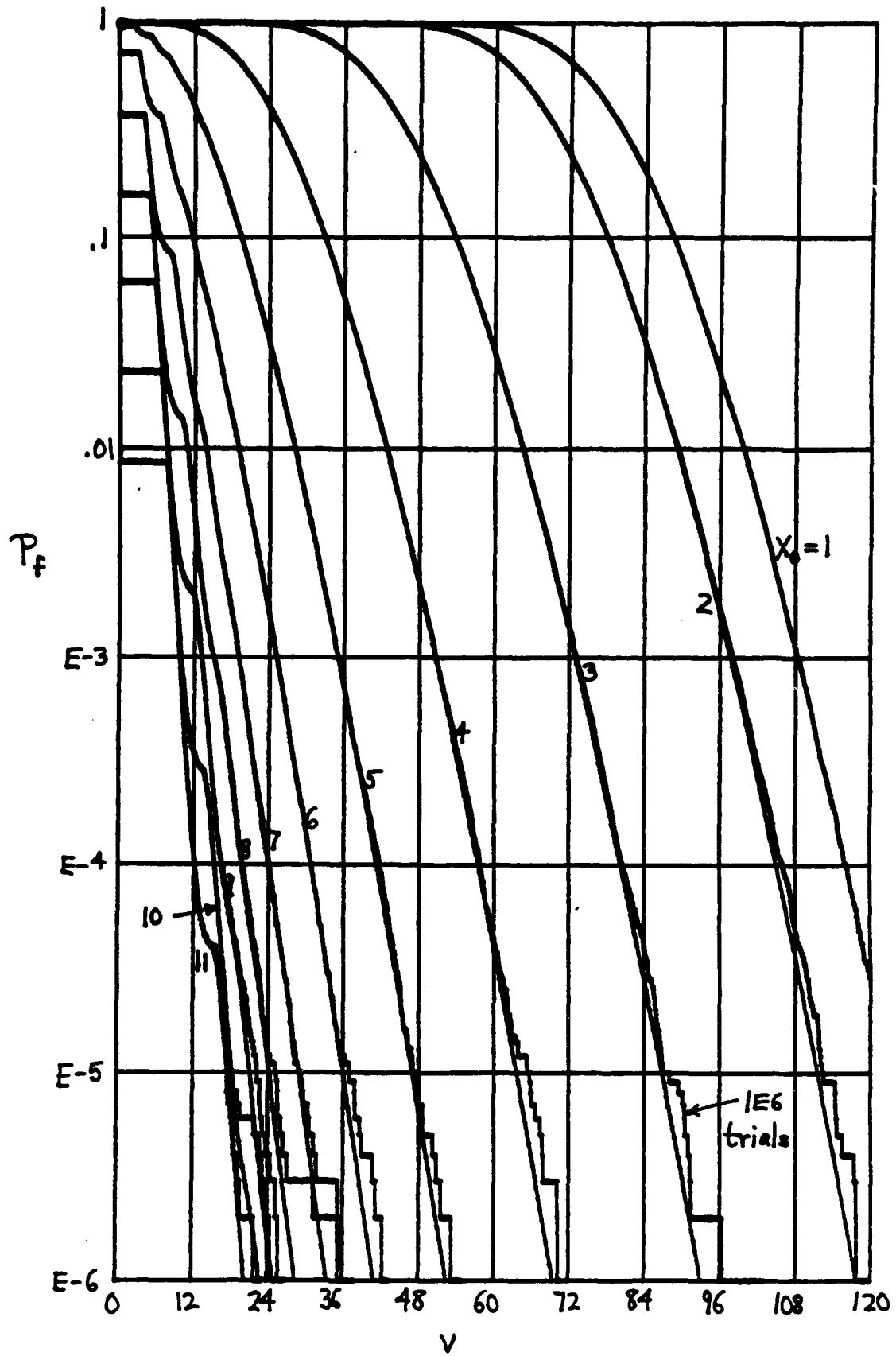Figure 3. P_f versus v for N = 1024, FIT-2

Figure 4. P_f versus v for N = 512, FIT-2
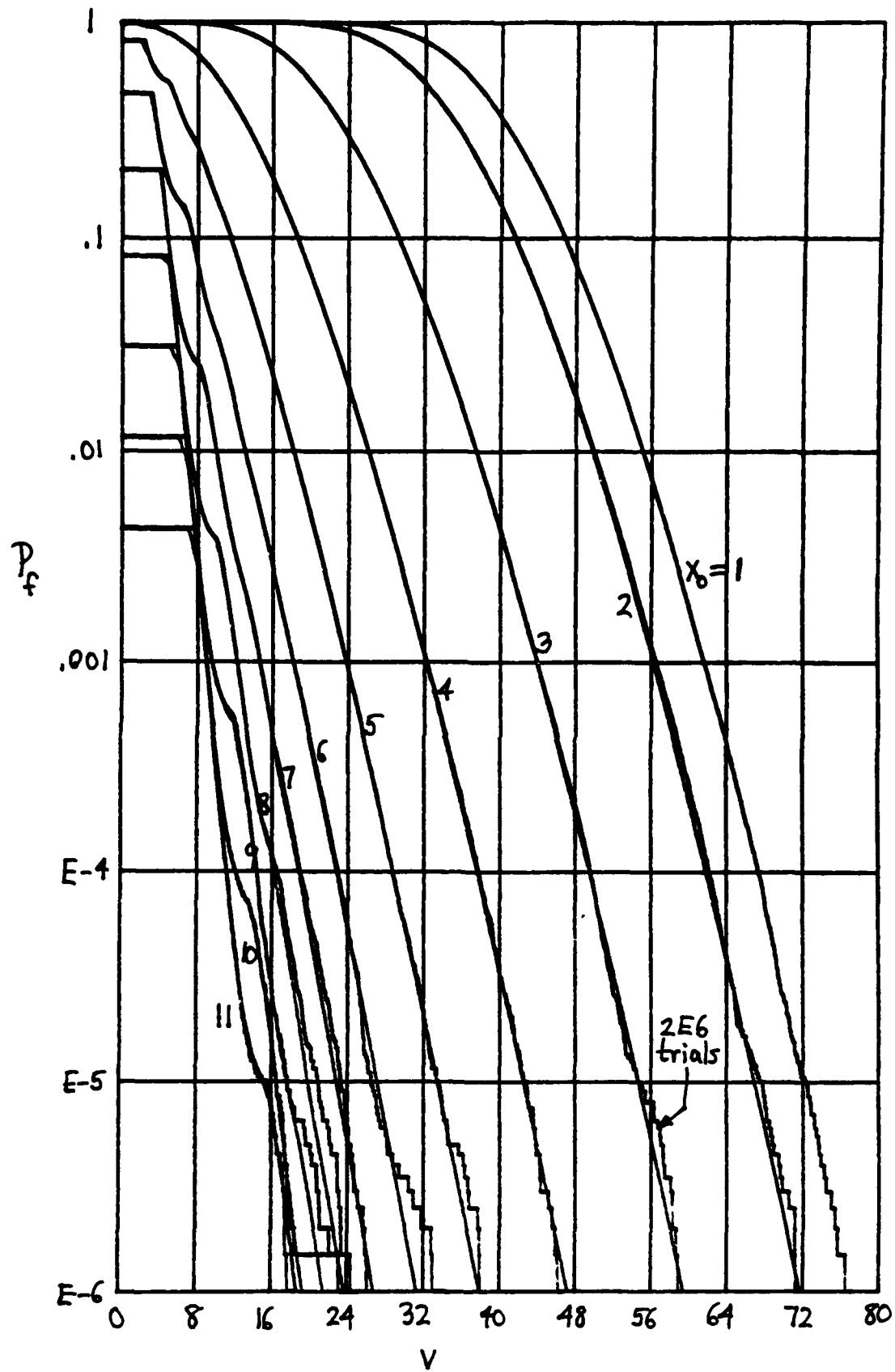
Figure 5. P_f versus v for N = 256, FIT-2
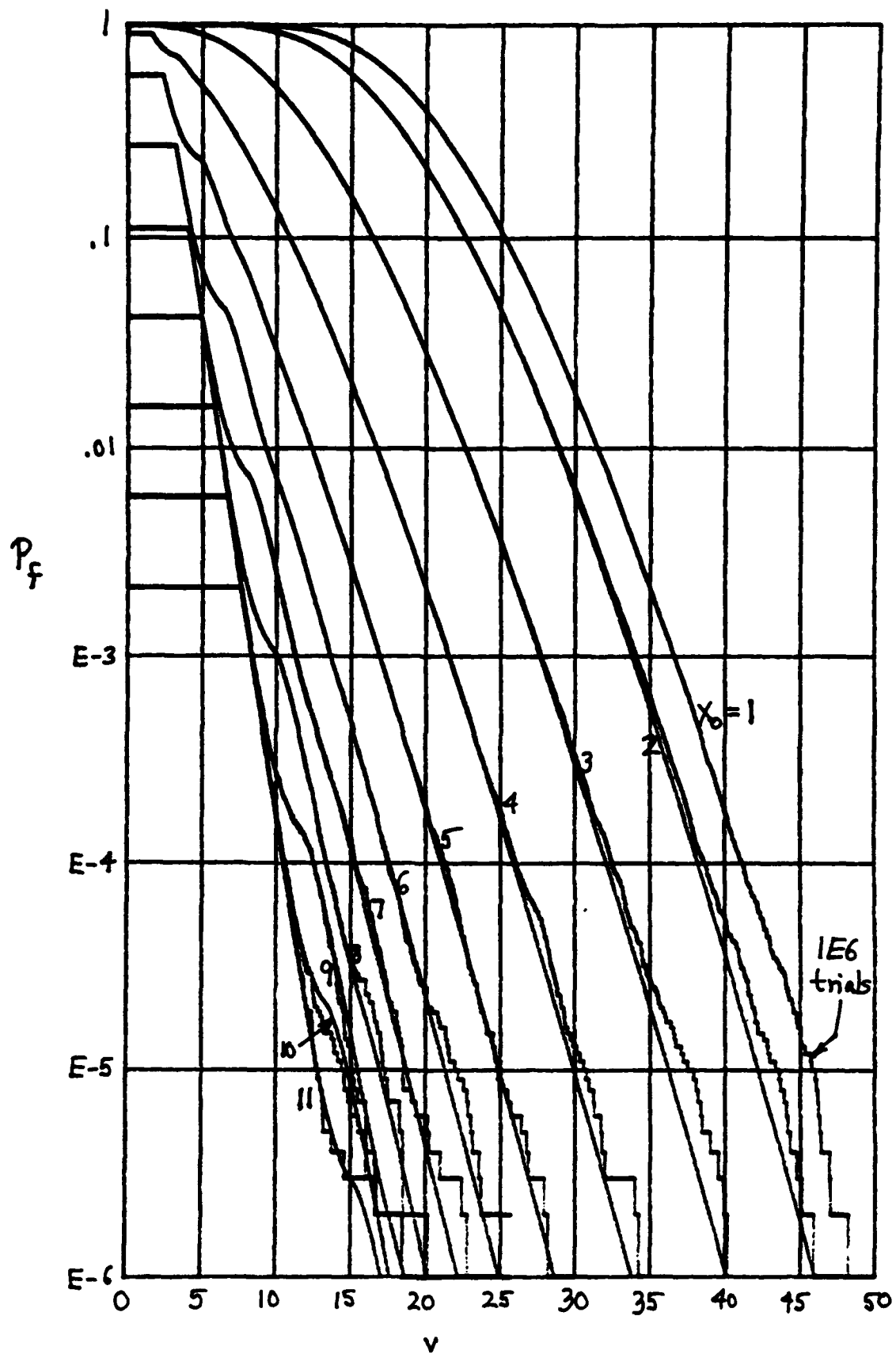
Figure 6. P_f versus v for N = 128, FIT-2
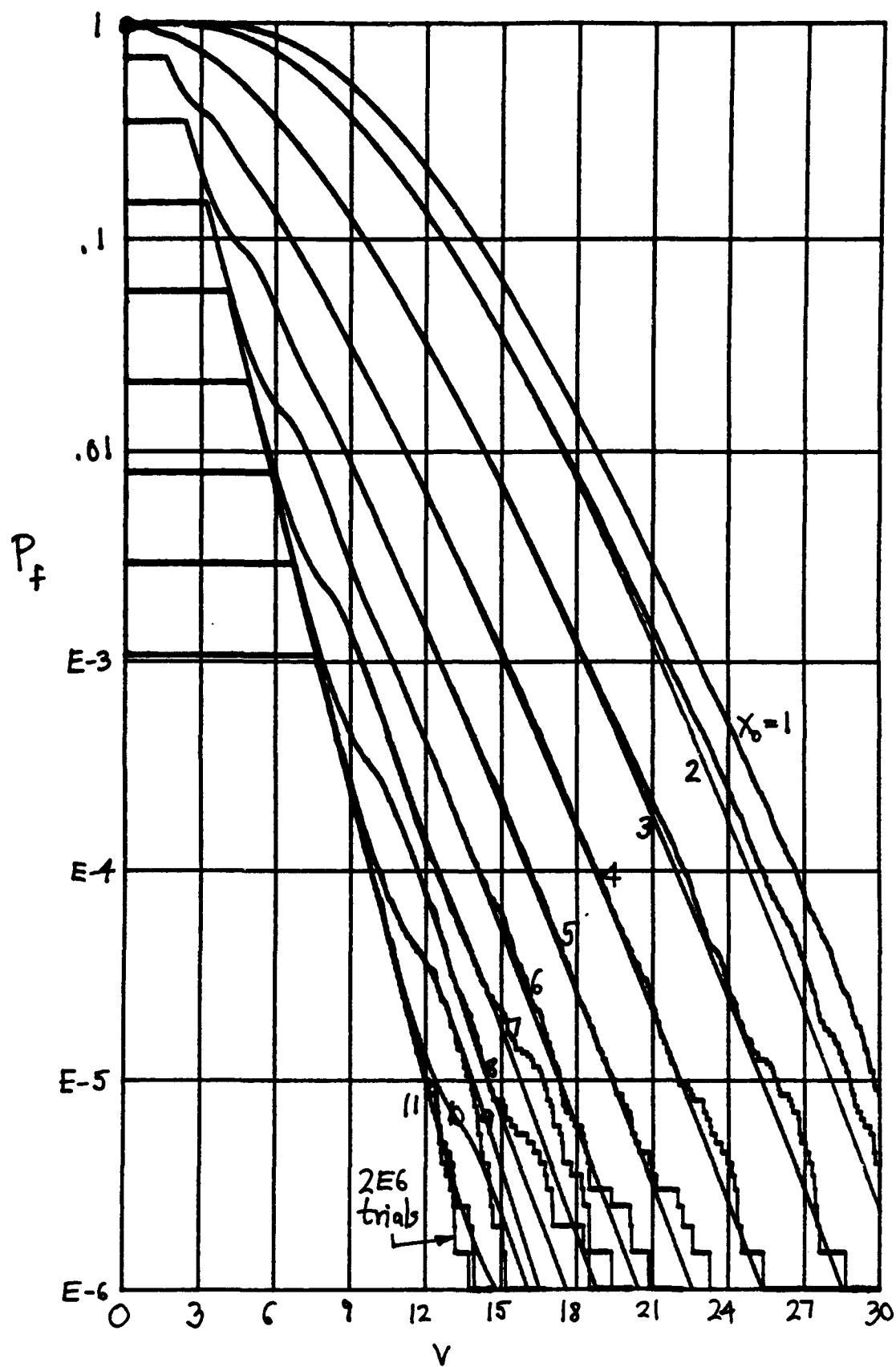
Figure 7. P_f versus v for N = 64, FIT-2

DETECTION PROBABILITY

A number of receiver operating characteristics (ROCs) for the MGLR processor are presented in figures 8 - 43. They have all been evaluated for search size N - 1024. The values of the number, M, of bins occupied by signal and the breakpoint, x_o, cover all 36 combinations f the following numbers:

$$M = 8, 16, 32, 64, 128, 256,$$
$$x_o = 1, 3, 5, 7, 9, 11. \tag{58}$$

A detailed explanation of the ROC, receiver operating characteristic, in figure 8 for N - 1024, M - 8, x_o - 1, and FIT-4 follows. The solid smooth curves were evaluated by means of the candidate characteristic function in (46), for both the false alarm probability as well as the detection probability. The jagged curve, labeled A, is a simulation result, using 10,000 trials with the exact nonlinear device, g(x), with no approximations, for $\underline{S}$ - 9 dB. The simulation result is seen to overlay and verify the theoretical curve within random errors inherent with a limited number of trials. The dashed curve, labeled B, is what the Gaussian approximation predicts for the performance capability, again for $\underline{S}$ - 9 dB. For this particular example of small x_o, namely 1, the Gaussian result is optimistic by only .6 dB at the left edge of the curve.

When breakpoint x_o is increased, the behavior of the receiver operating characteristics for the MGLR processor changes significantly, and it is necessary to switch to procedure FIT-2,

which utilizes piecewise-linear function h(x) in (5); this switch occurs in figure 10 for $x_o \geq 5$ when M = 8. For still larger breakpoint values, such as $x_o = 11$ in figure 13, there are pronounced bumps in the characteristics, in addition to an unachievable region. That is, the only value of false alarm probability, P_f, larger than

$$P_{fm} = 1 - \left(1 - \exp(-x_o)\right)^N = .0170 \qquad (59)$$

that can be realized is 1, due to the dead zone character of nonlinearity g(x). This is due to the impulse of area B_1 at the origin of probability density function $p_\eta(u)$ in (12).

The simulation result A for 10,000 trials and $\underline{S} = 8$ dB in figure 13 confirms the theoretical approach, FIT-2, to performance prediction. Another point to observe is the poor quality of the Gaussian approximation B, which cuts across the plot with virtually zero slope. Curve B bears no resemblance to the actual characteristics, although it does cross the correct curve just below $P_f = .001$.

Most of the theoretical receiver operating characteristics in figures 8 - 43 have been verified by simulations, each using 10,000 trials. In no case is the discrepancy greater than .1 dB. One case was pursued further; namely, figure 17 used 200,000 trials at $\underline{S} = 5$ dB, thereby allowing a check down to $P_f = 1E-5$. The two results for $\underline{S} = 5$ dB in figure 17 are overlays, including the bumps near P_f equal .25 and .07.

From figures 8 - 43, it is now possible to determine the signal power per bin, $\underline{S}$, required for the MGLR processor, in order to realize a specified operating point in terms of the false alarm and detection probability pair P_f, P_d. We denote the pair $10^{-3}, .5$ as a low-quality operating point, and the pair $10^{-6}, .9$ as a high-quality operating point.

In table 1, the required signal powers per bin, $\underline{S}$, for the low-quality point are presented for all 36 combinations of M and x_0 in (58) and for $N = 1024$. (The column headed ED is for the energy detector, (52); its receiver operating characteristics will be presented in a later subsection.) It is immediately observed that for each choice of M, there is a best breakpoint value x_0 to use in the MGLR processor, in order to operate with minimum signal power $\underline{S}$. For example, for $M = 8$, the best x_0 is 11, and the minimum signal power is $\underline{S} = 6.3$ dB. This is 2.5 dB better than the signal power required for $x_0 = 1$, namely 8.8 dB. It is also 4.9 dB better than the energy detector, which requires 11.2 dB for $M = 8$.

As M increases, the best breakpoint x_0 decreases, eventually reaching its minimum value of 1 for $M = 128$. For $M = 256$, the MGLR and energy detector require the same signal power level of -4.0 dB. As M tends closer to N, the energy detector will outperform the MGLR; in fact, the energy detector is the optimum processor for $M = N$.

The corresponding results for the high-quality operating point are given in table 2. Basically the same conclusions follow, although all the signal powers are necessarily larger

than in table 1. The only real difference is that the best MGLR processor still outperforms the energy detector at M = 256, requiring .3 dB less signal power. This trend is expected to be reversed for M somewhat larger than 256.

Table 1. $\underline{S}$(dB) Required for N = 1024, $P_f = 10^{-3}$, $P_d = .5$

x_o M	1	3	5	7	9	11	ED
8	8.8	8.7	7.8	7.0	6.4	6.3	11.2
16	6.2	6.1	5.4	5.0	4.8	5.0	8.1
32	3.7	3.6	3.3	3.2	3.3	3.7	5.0
64	1.2	1.2	1.3	1.6	2.0	2.6	2.0
128	-1.3	-1.1	-0.6	0.0	0.7	1.5	-1.0
256	-4.0	-3.6	-2.6	-1.5	-0.5	0.4	-4.0
512							-7.0
1024							-10.0

Table 2. $\underline{S}$(dB) Required for N = 1024, $P_f = 10^{-6}$, $P_d = .9$

x_o M	1	3	5	7	9	11	ED
8	13.0	12.9	12.0	11.2	10.7	10.6	15.6
16	9.7	9.6	9.0	8.3	8.2	8.3	11.9
32	6.8	6.7	6.3	6.1	6.3	6.6	8.5
64	4.2	4.2	4.1	4.2	4.6	5.1	5.3
128	1.5	1.6	2.0	2.4	3.1	3.7	2.2
256	-1.1	-0.7	0.0	0.8	1.7	2.5	-0.8
512							-3.9
1024							-6.9
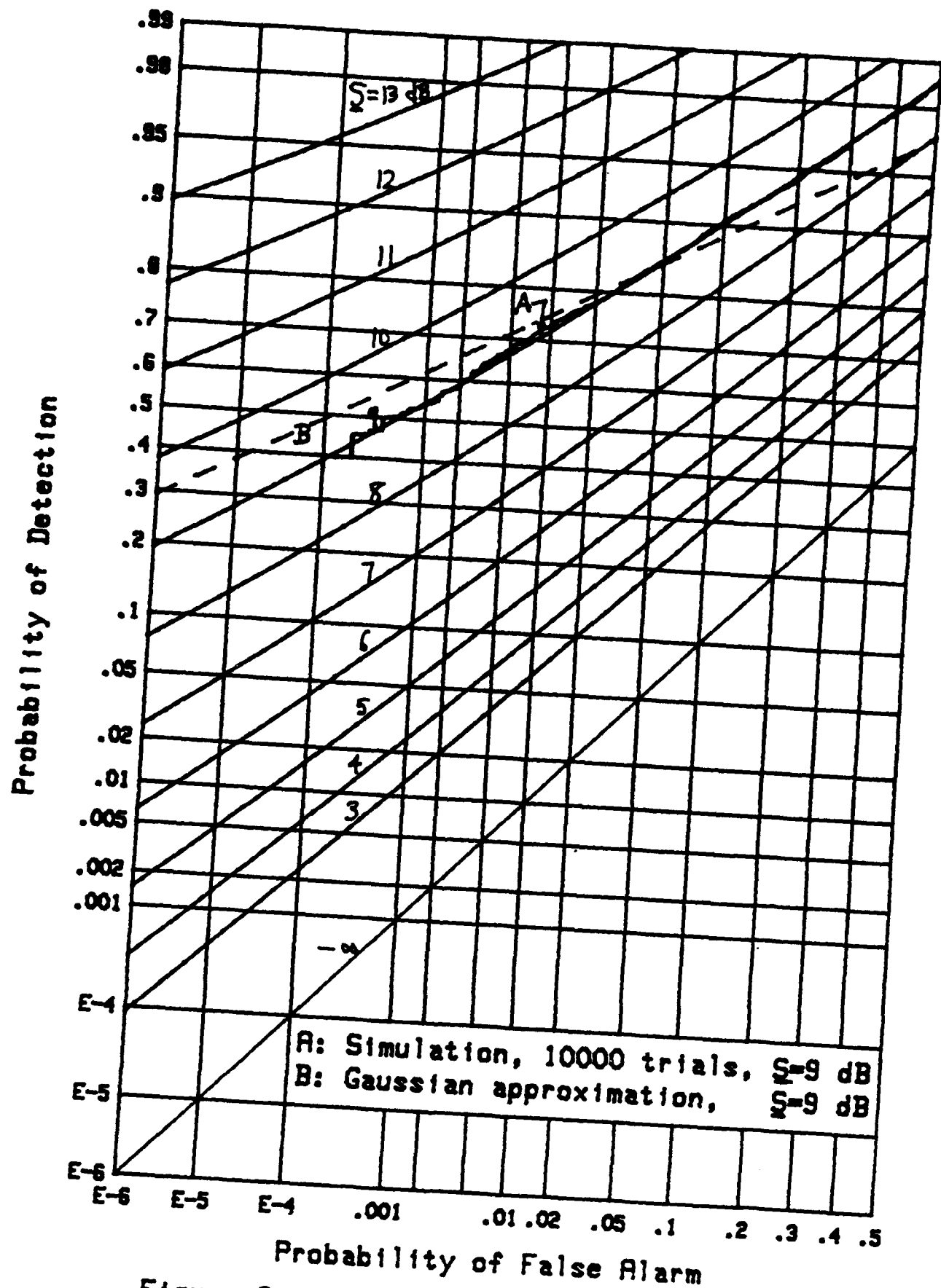
Figure 8. ROC for N=1024, M=8, Xo=1, FIT-4
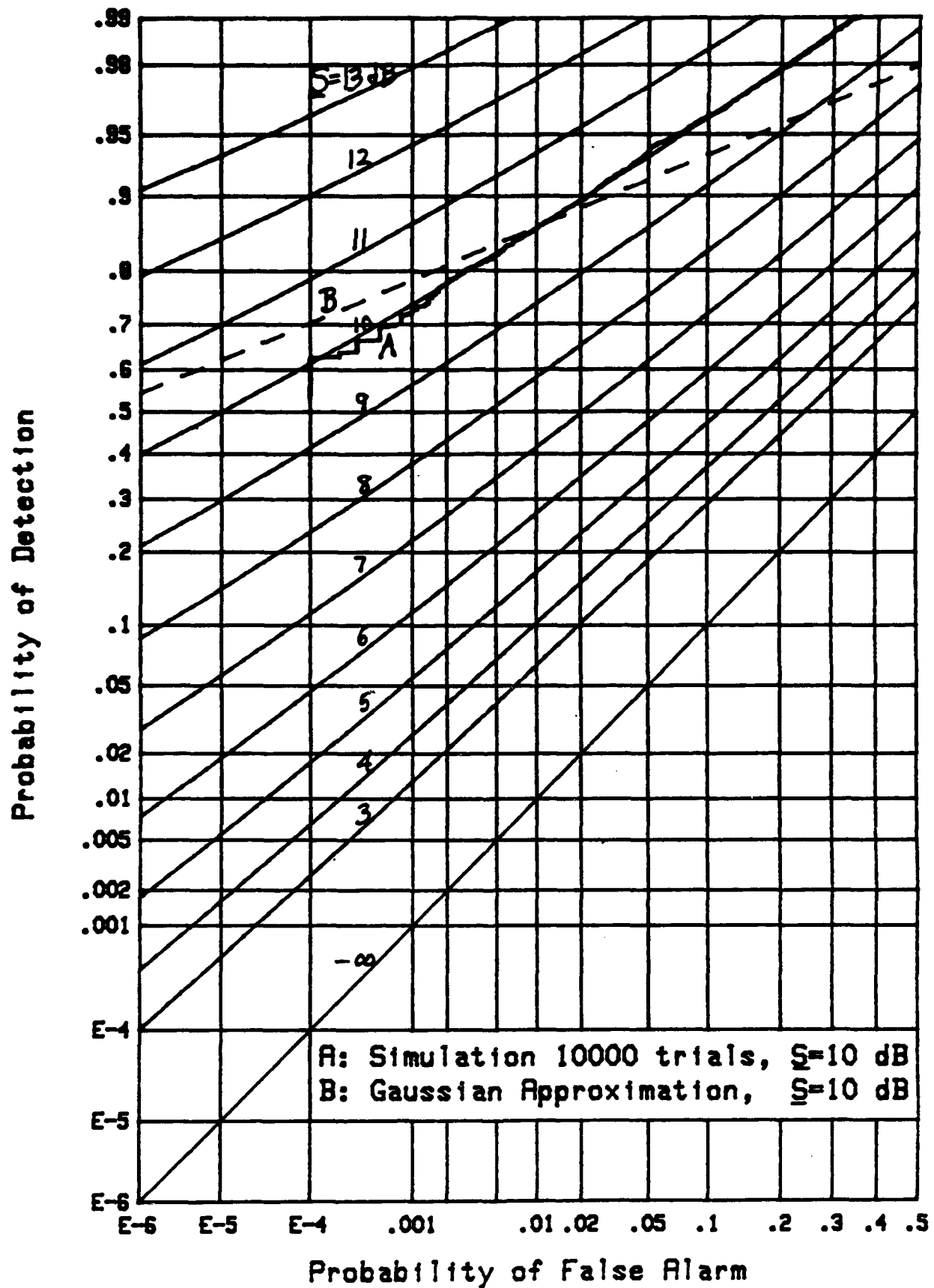
Figure 9. ROC for N=1024, M=8, Xo=3, FIT-4
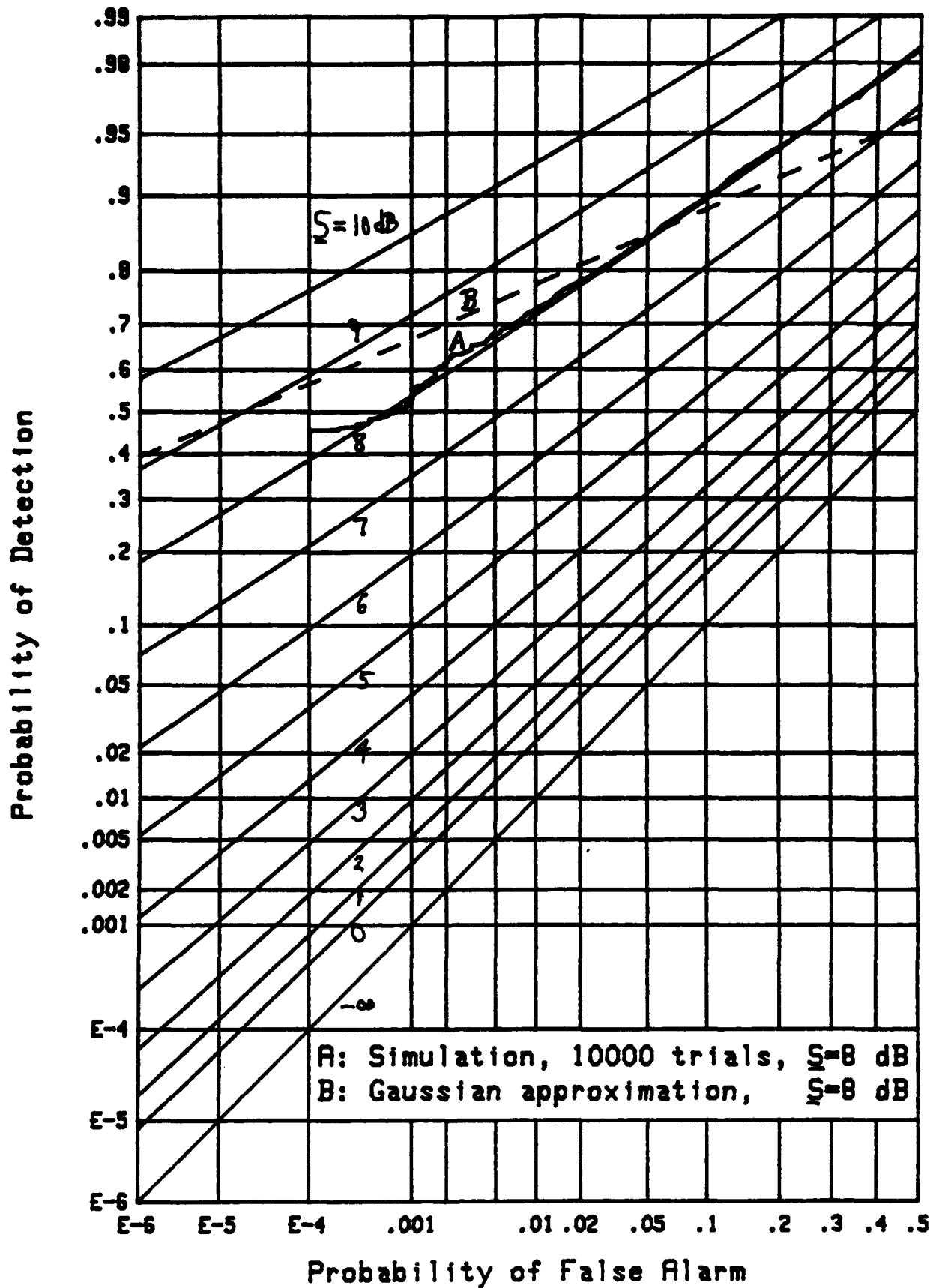
Figure 10. ROC for N=1024, M=8, Xo=5, FIT-2
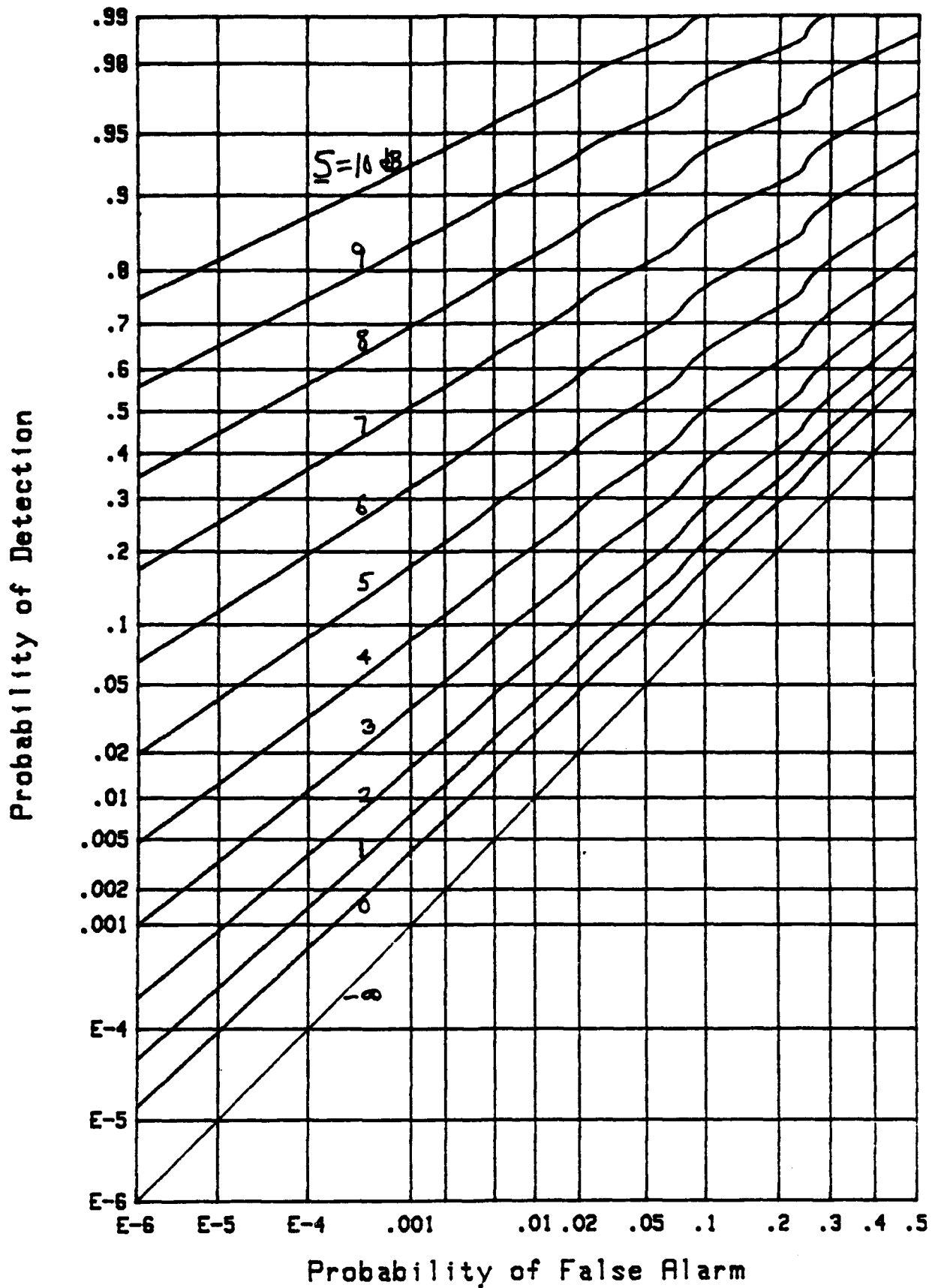
Figure 11. ROC for N=1024, M=8, Xo=7, FIT-2
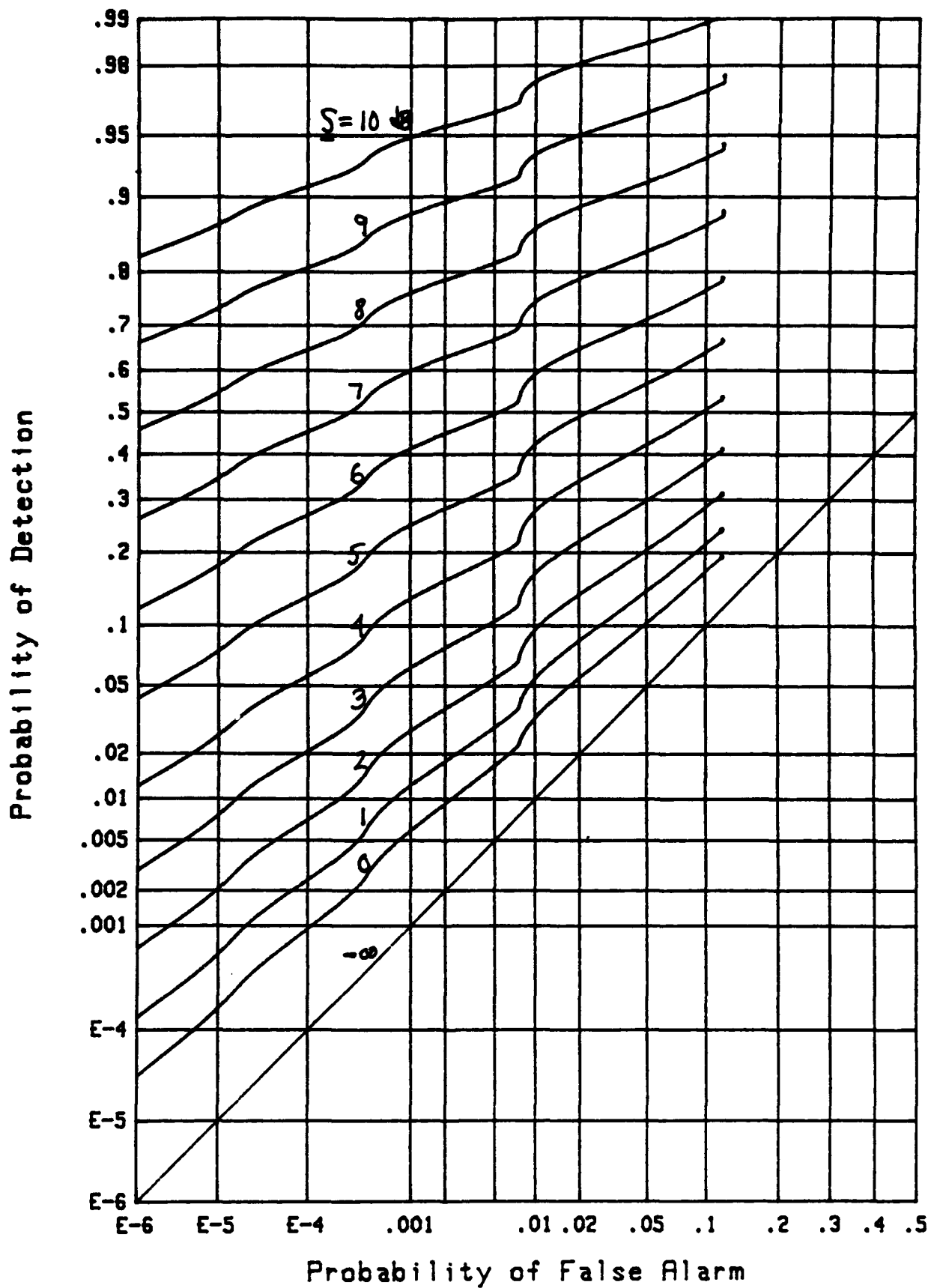
Figure 12. ROC for N=1024, M=8, Xo=9, FIT-2
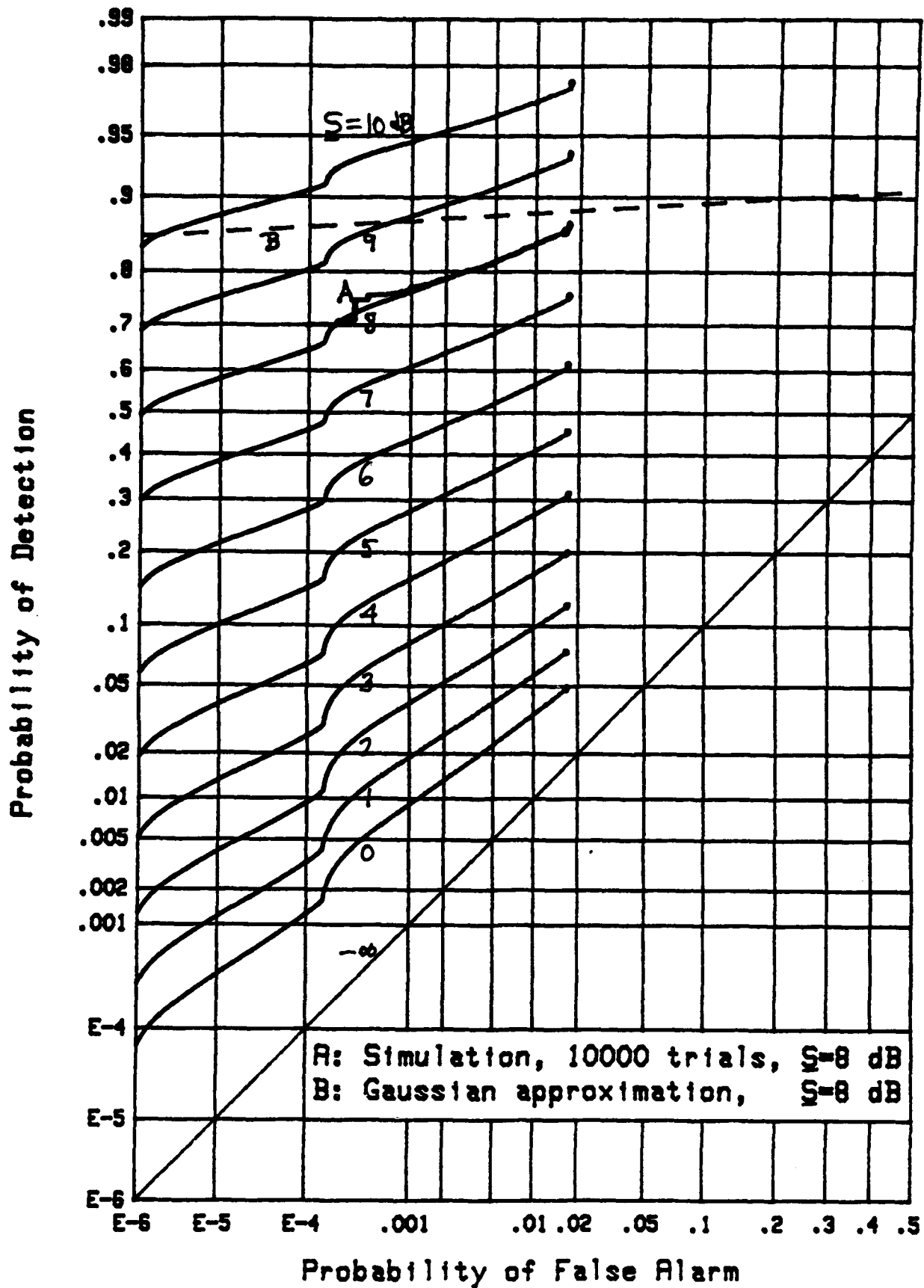
Figure 13. ROC for N=1024, M=8, Xo=11, FIT-2
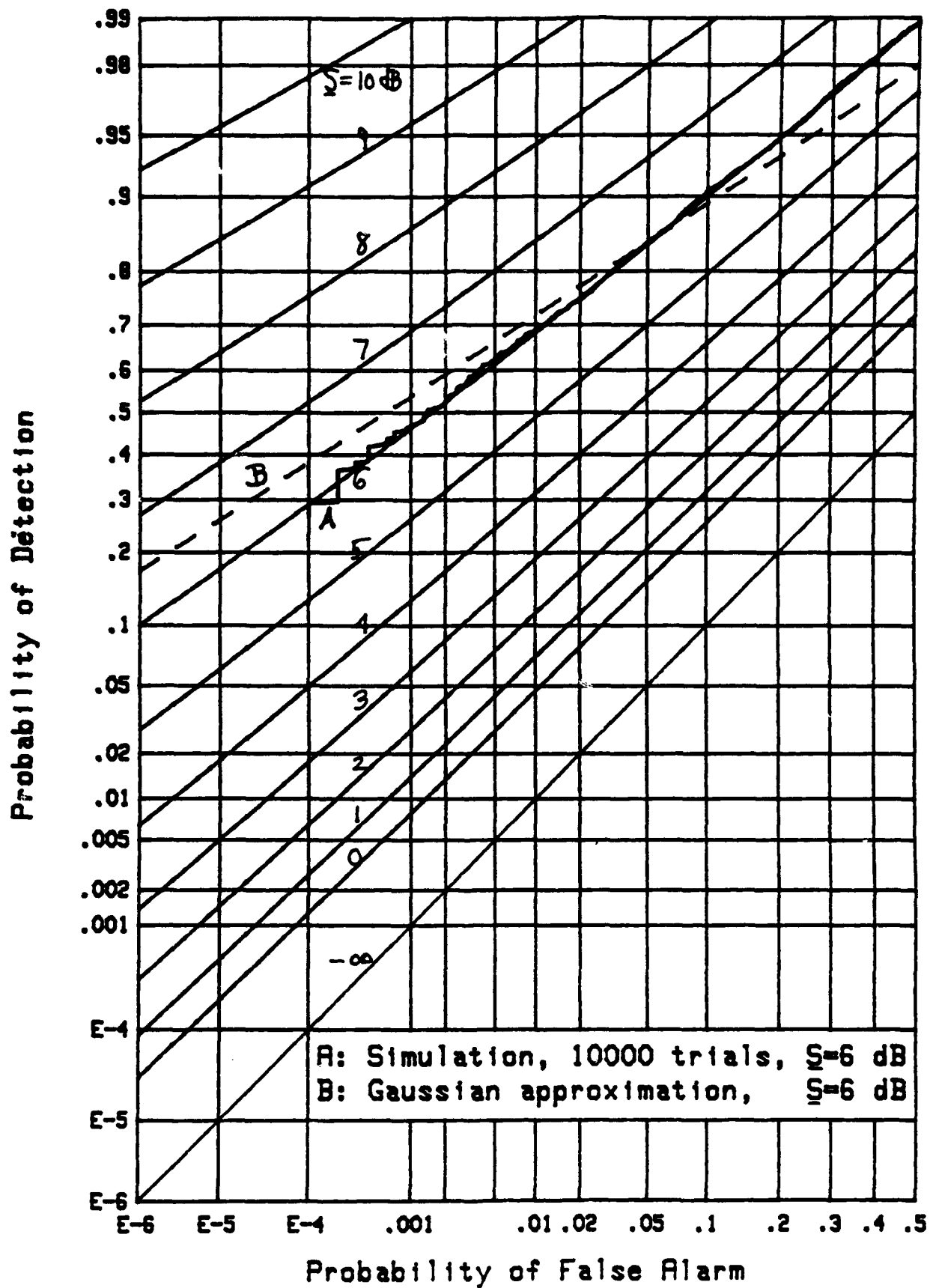
Figure 14. ROC for N=1024, M=16, Xo=1, FIT-4
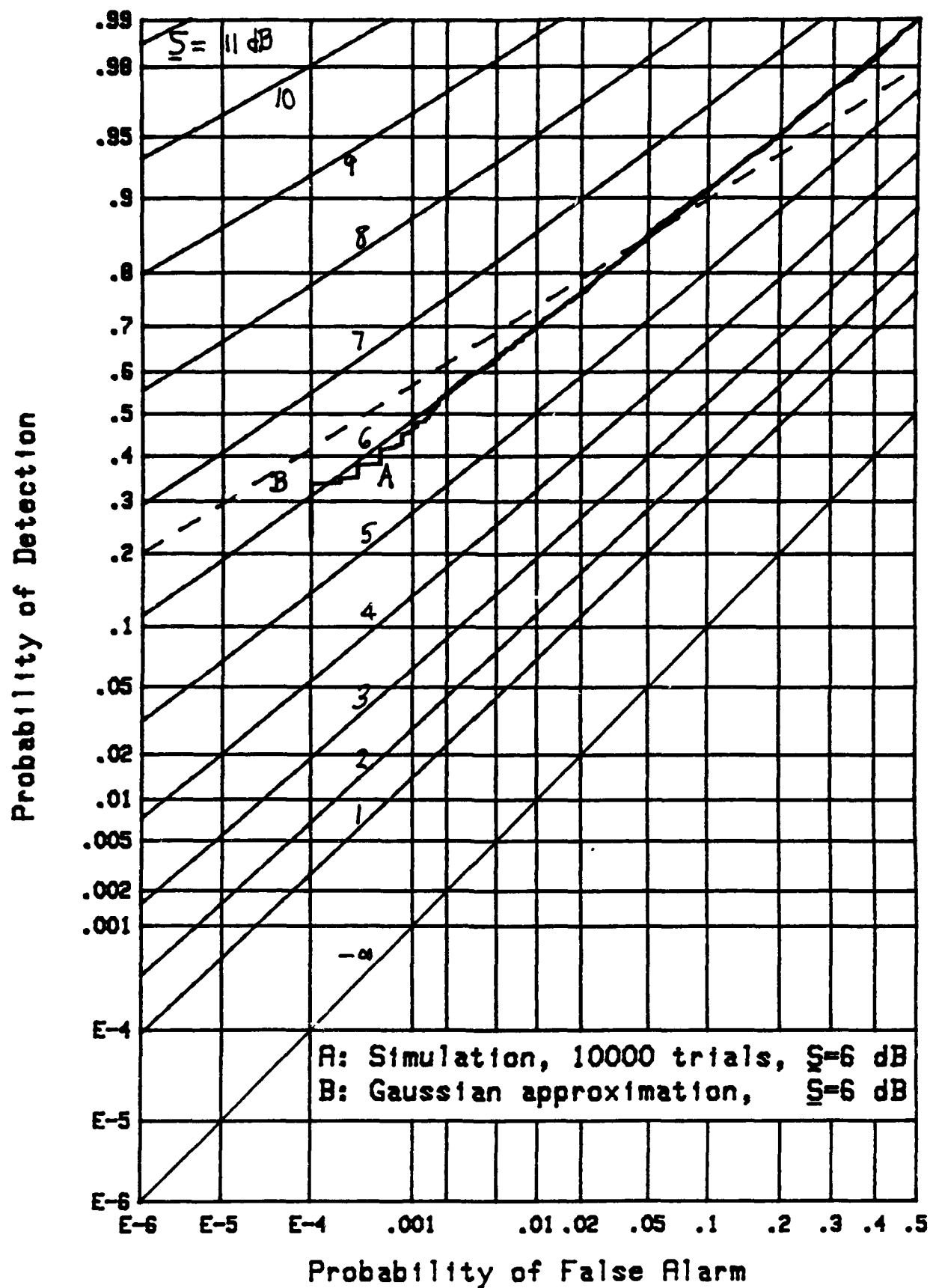
Figure 15. ROC for N=1024, M=16, Xo=3, FIT-4
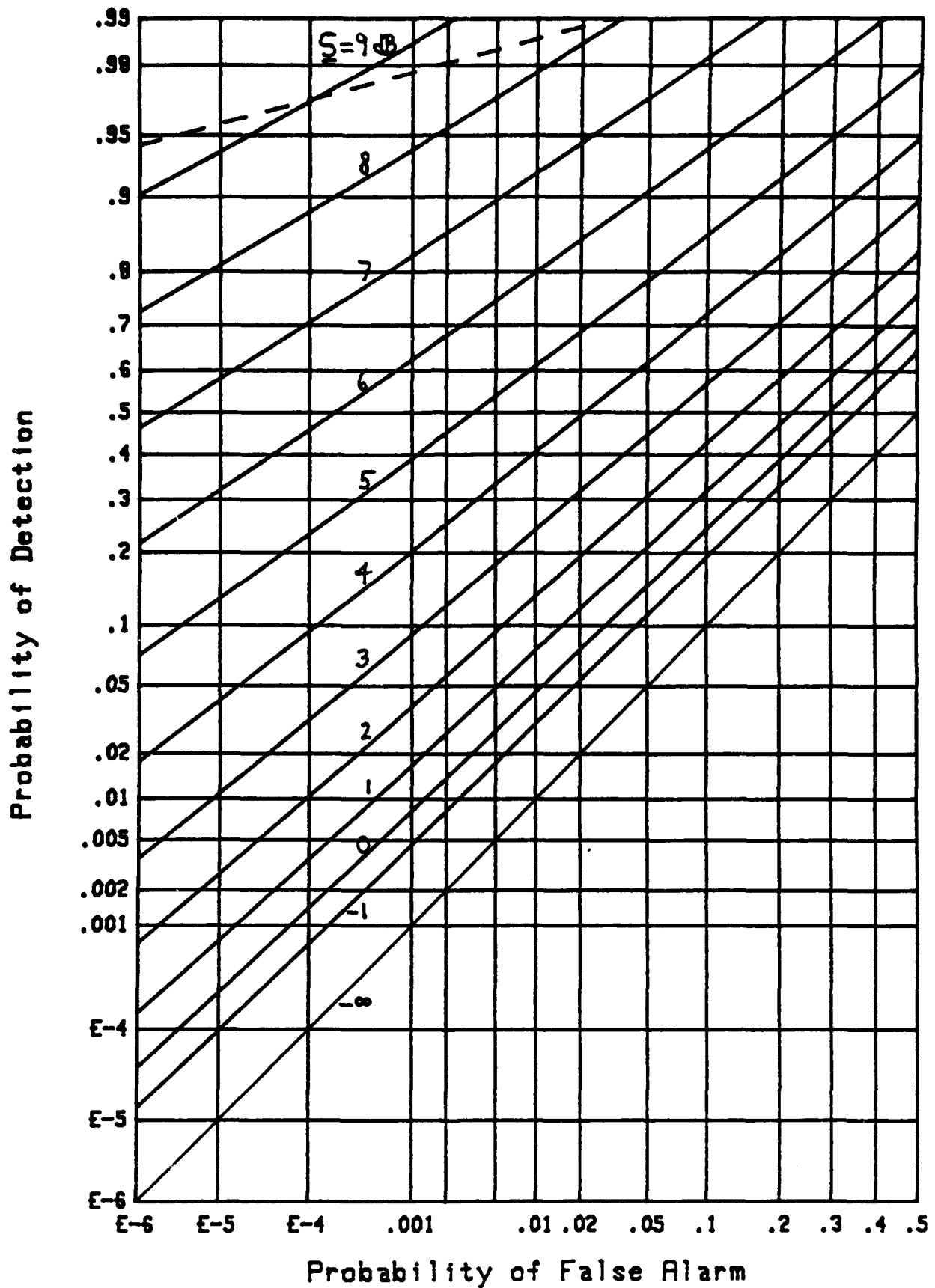
Figure 16. ROC for N=1024, M=16, Xo=5, FIT-2
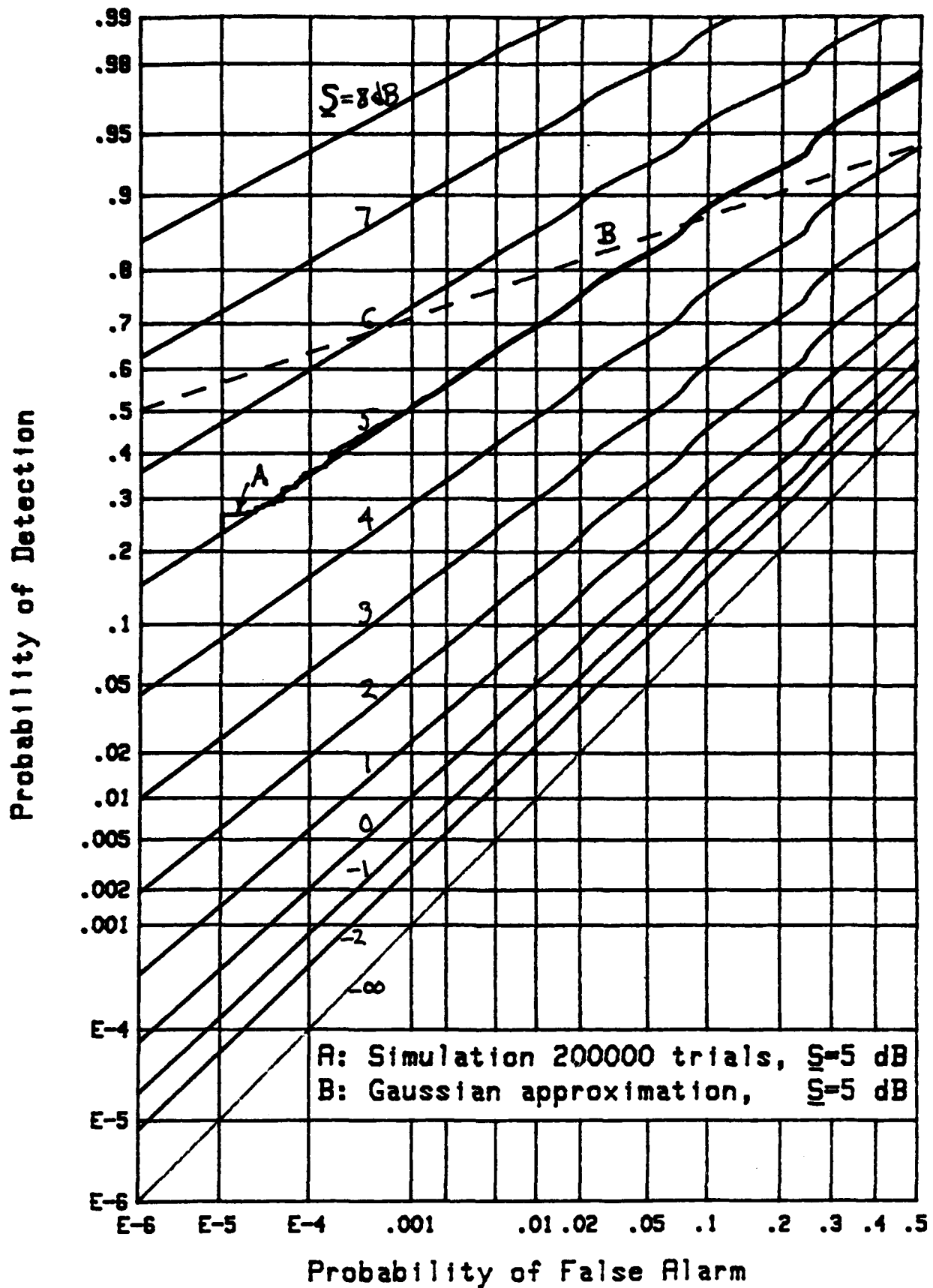
Figure 17. ROC for N=1024, M=16, Xo=7, FIT-2
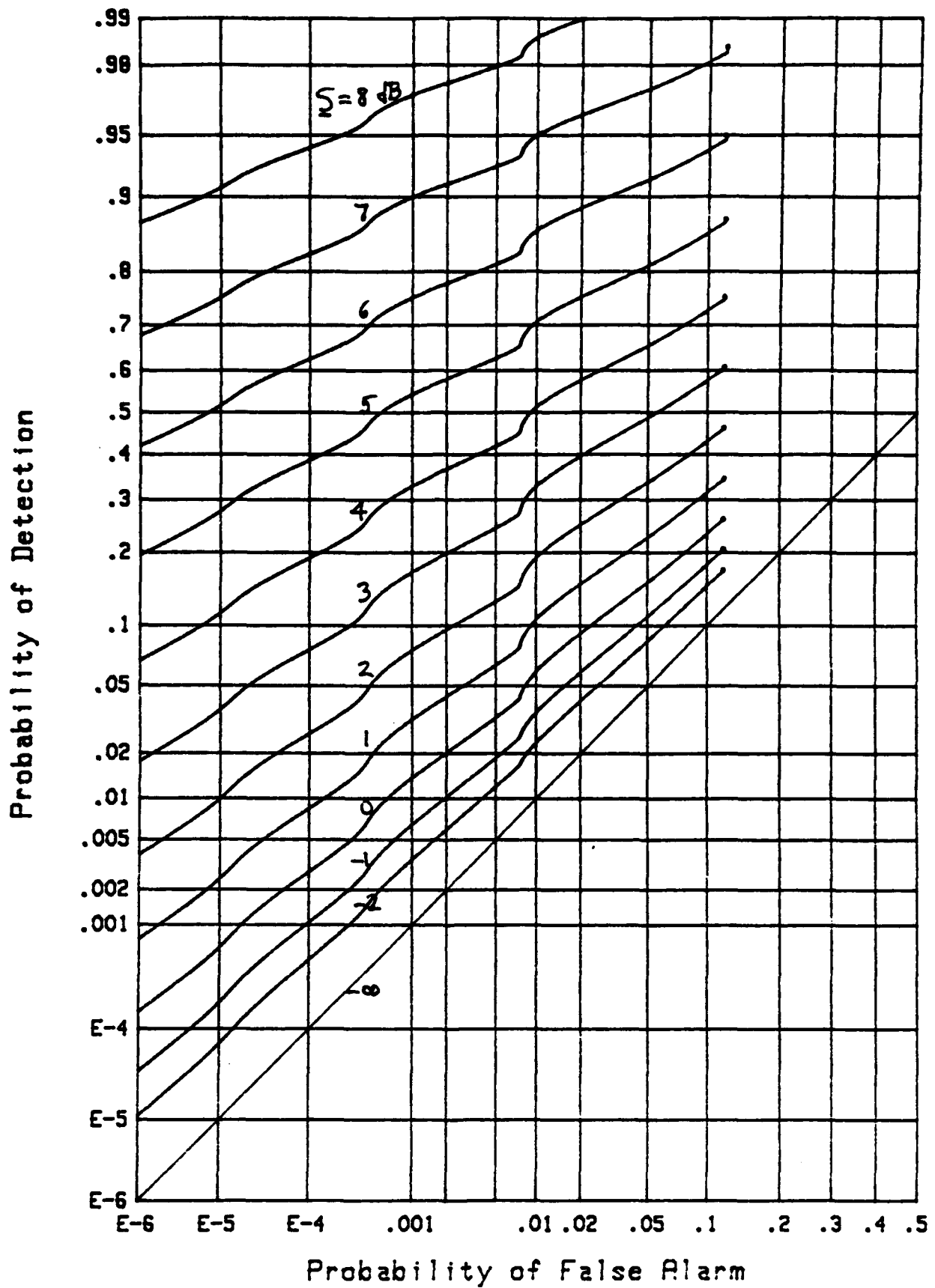
Figure 18. ROC for N=1024, M=16, Xo=9, FIT-2
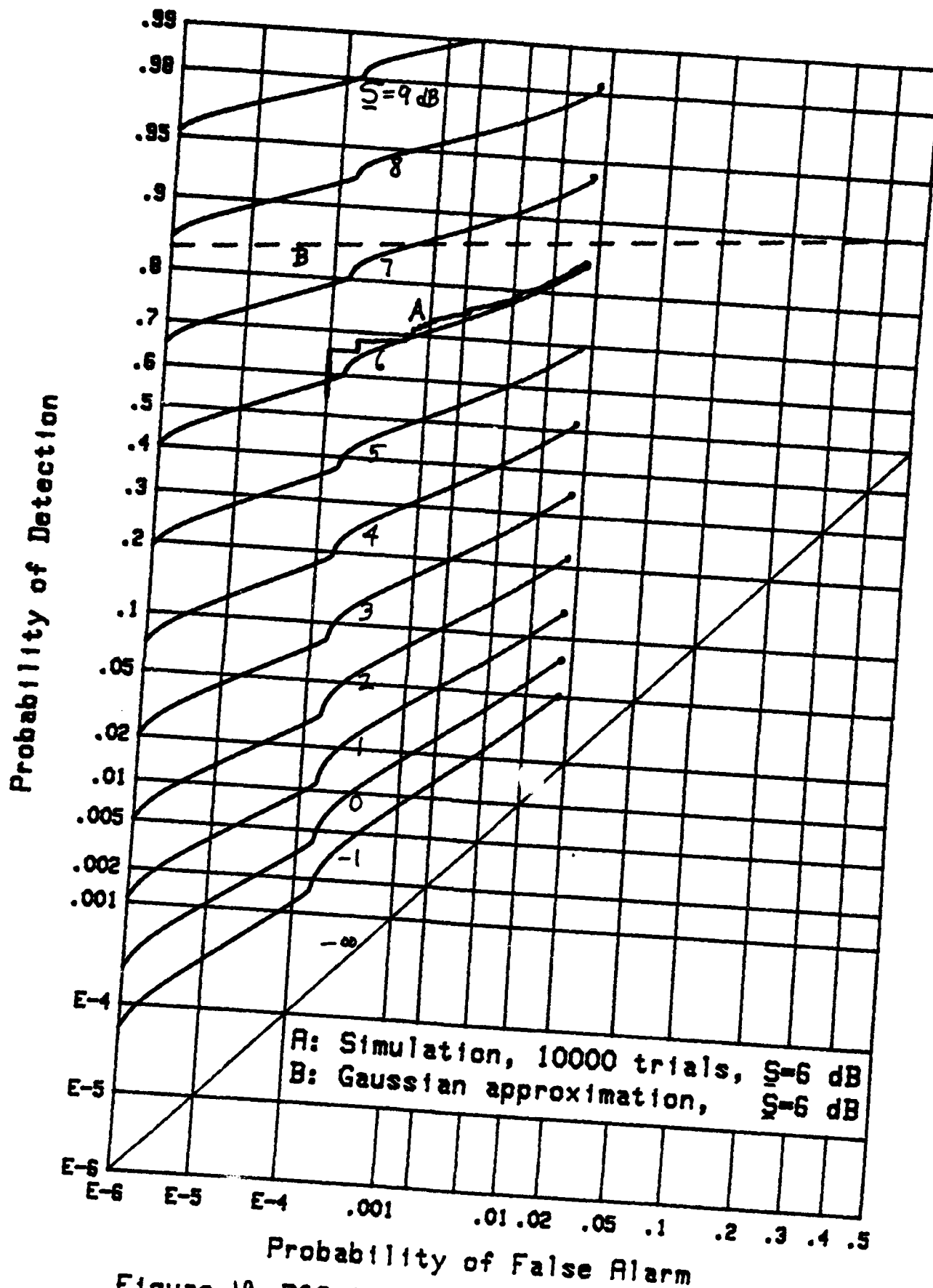
Figure 19. ROC for N=1024, M=16, Xo=11, FIT-2
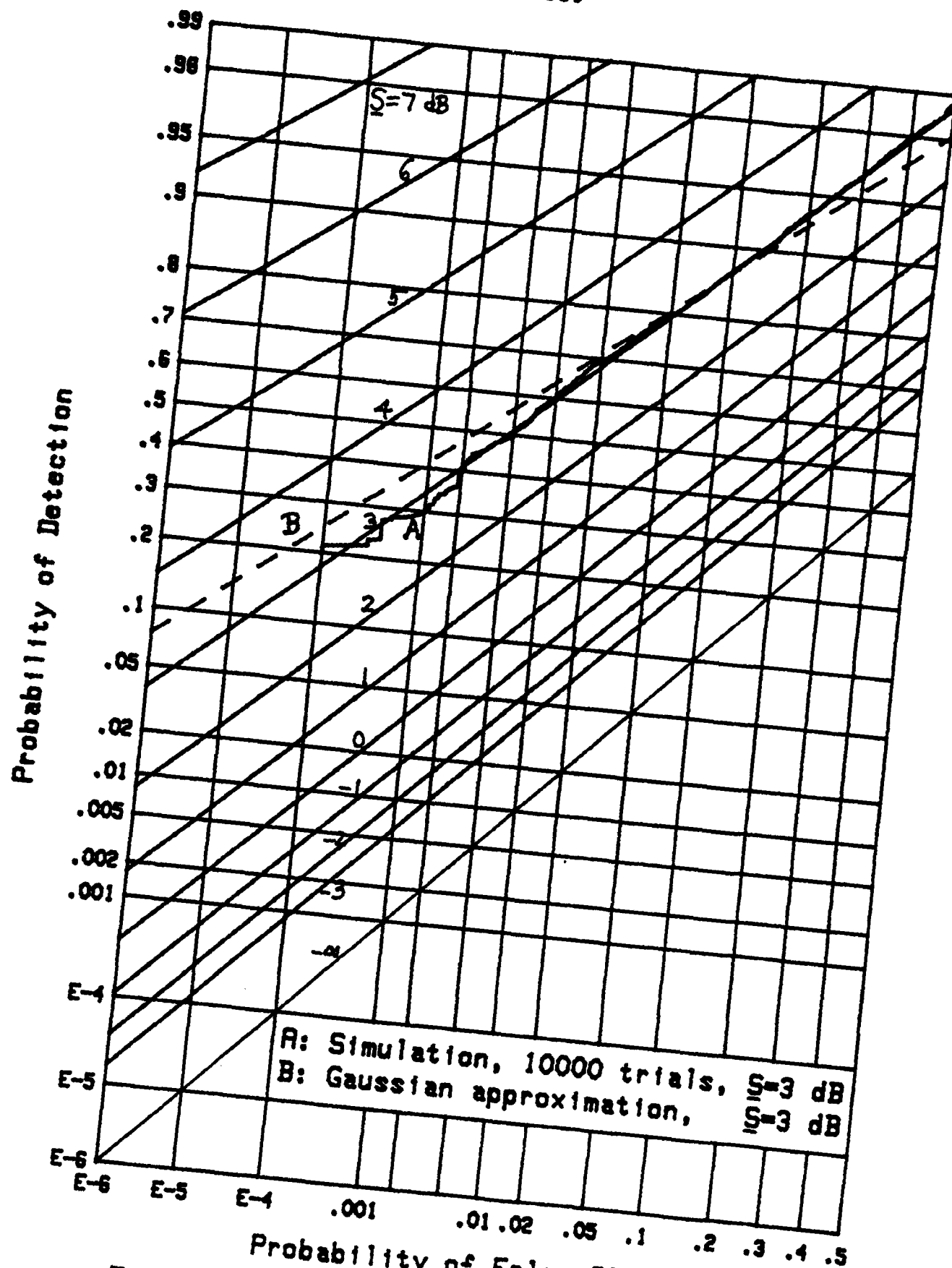
Figure 20. ROC for N=1024, M=32, Xo=1, FIT-4
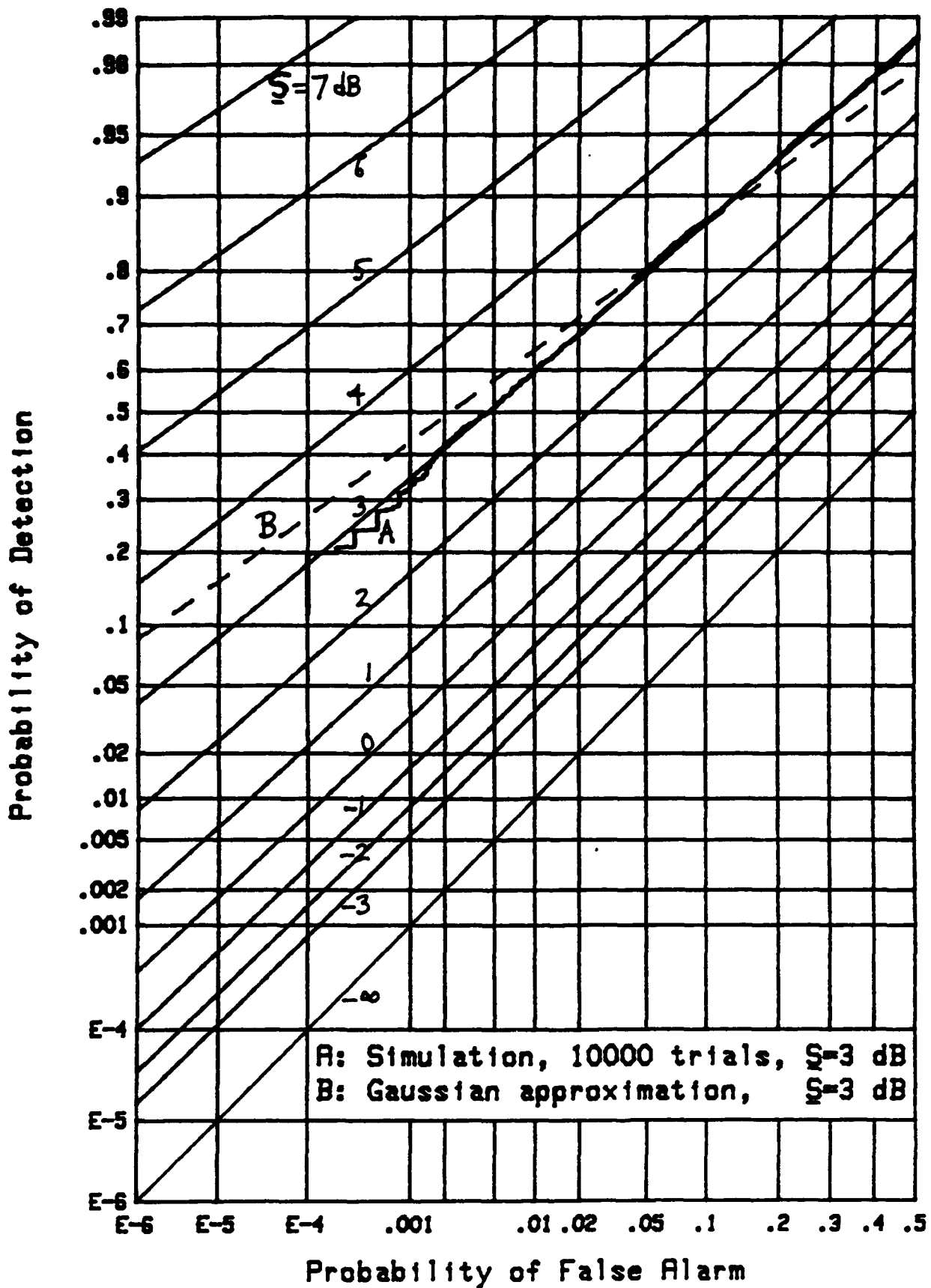
Figure 21. ROC for N=1024, M=32, Xo=3, FIT-4
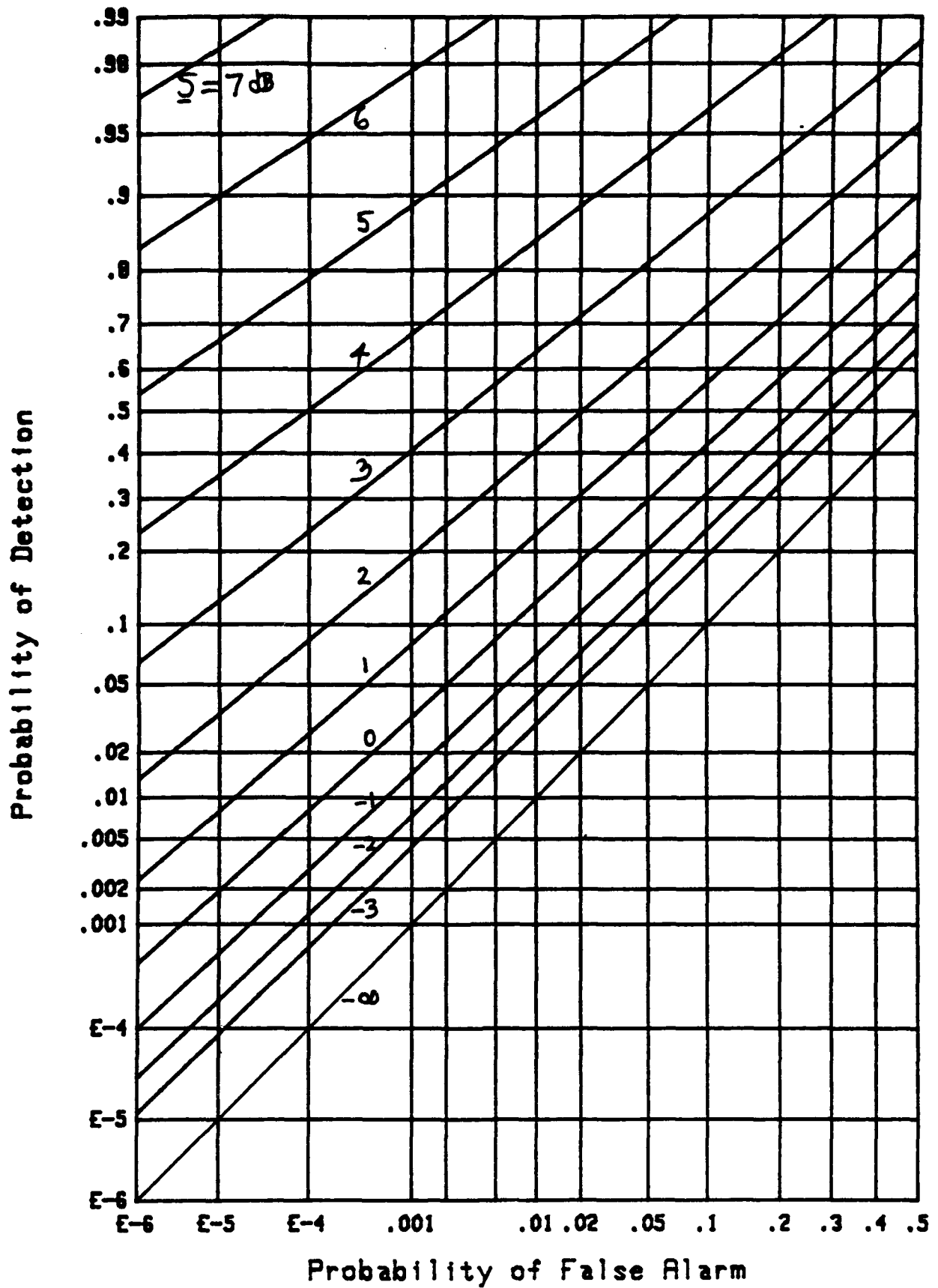
Figure 22. ROC for N=1024, M=32, Xo=5, FIT-2
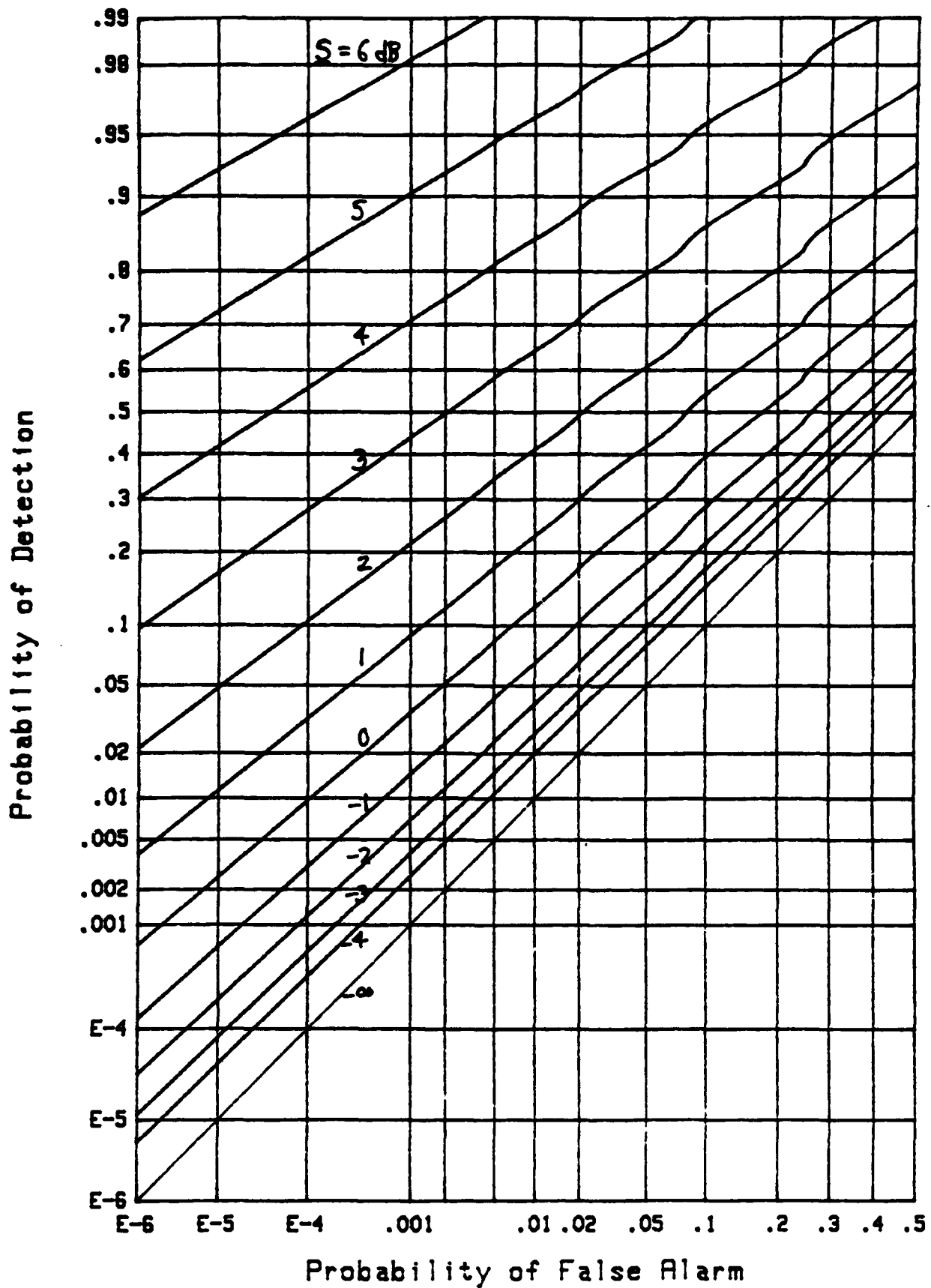
Figure 23. ROC for N=1024, M=32, Xo=7, FIT-2
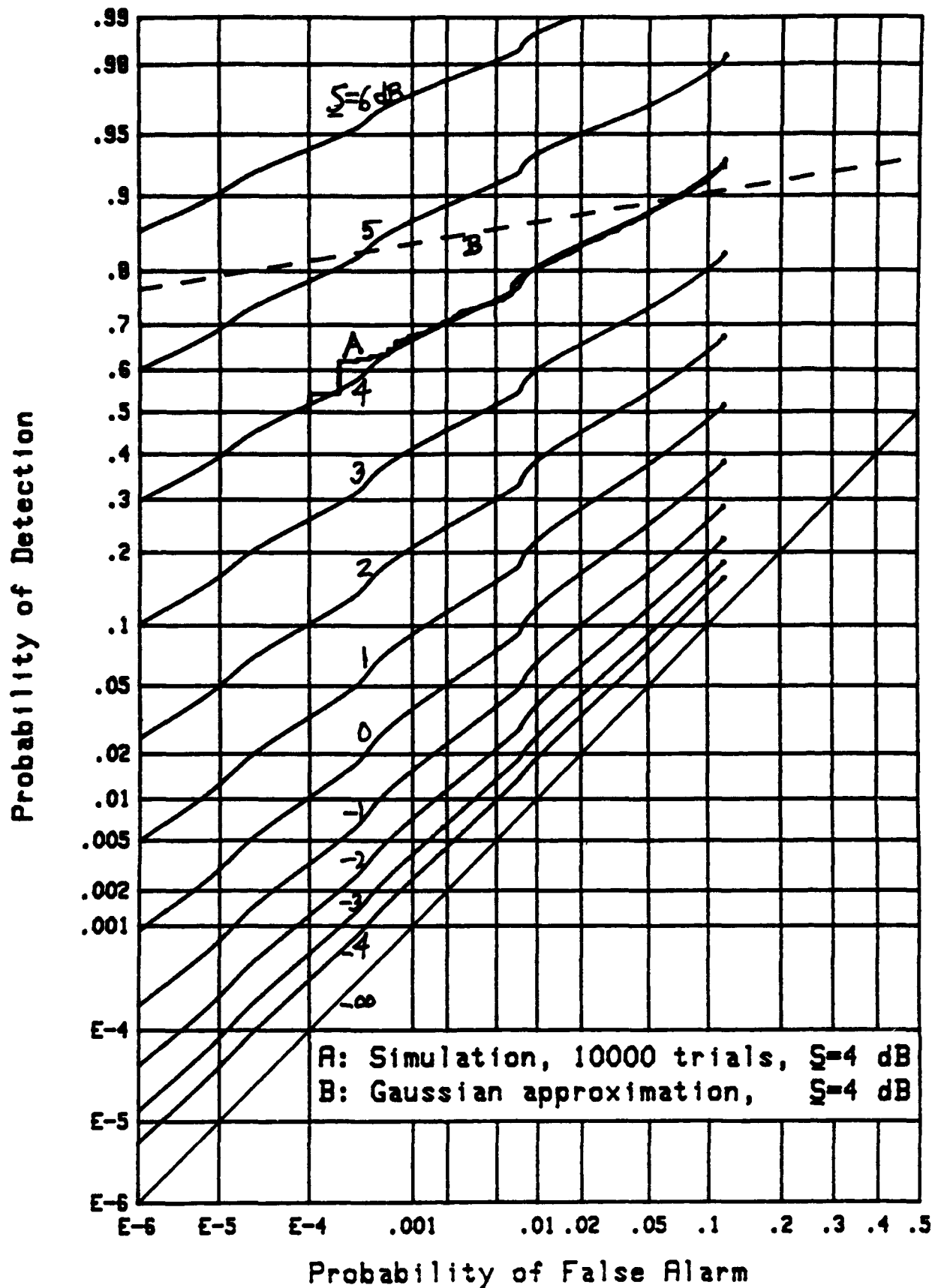
Figure 24. ROC for N=1024, M=32, Xo=9, FIT-2
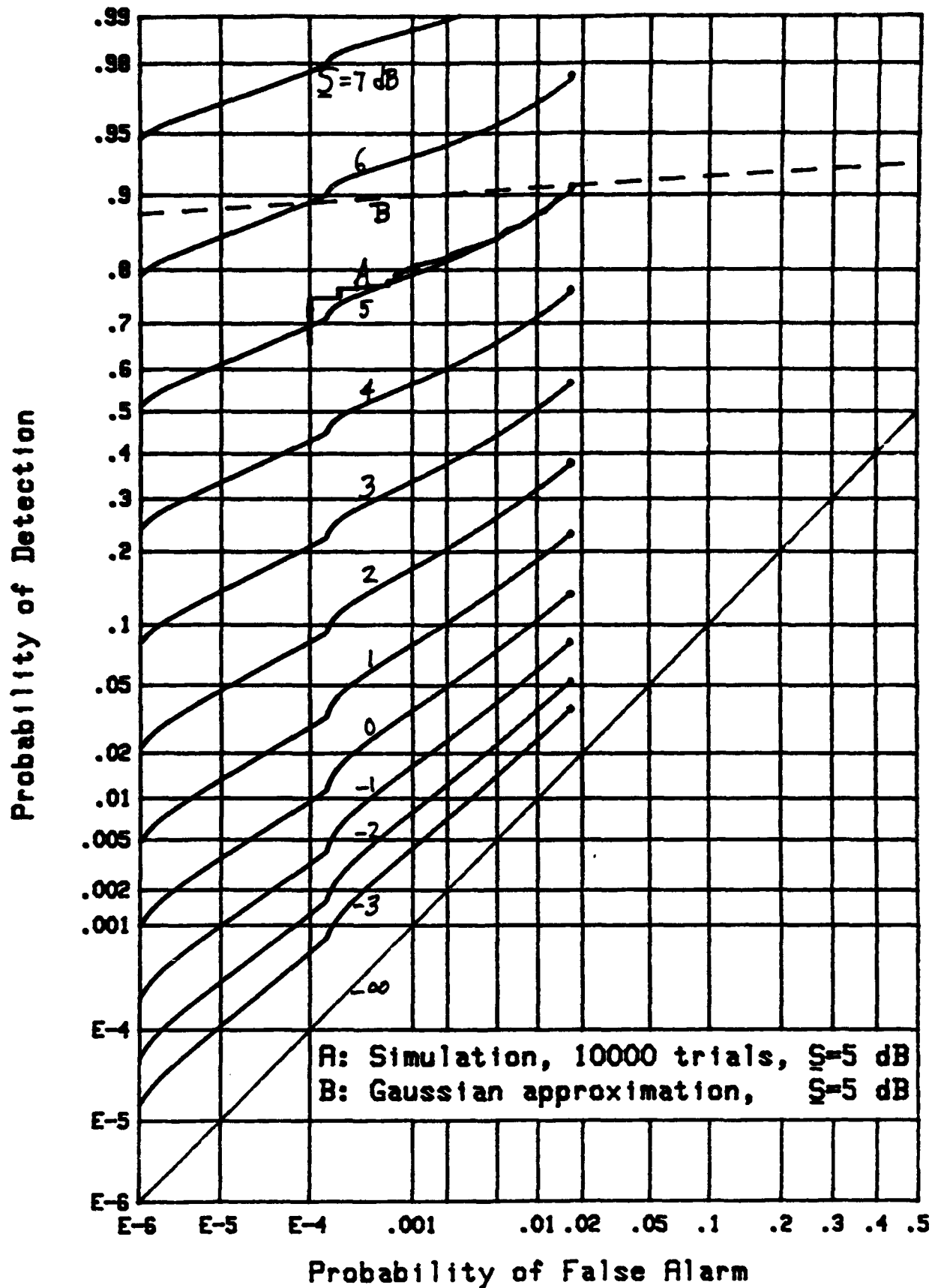
Figure 25. ROC for N=1024, M=32, Xo=11, FIT-2
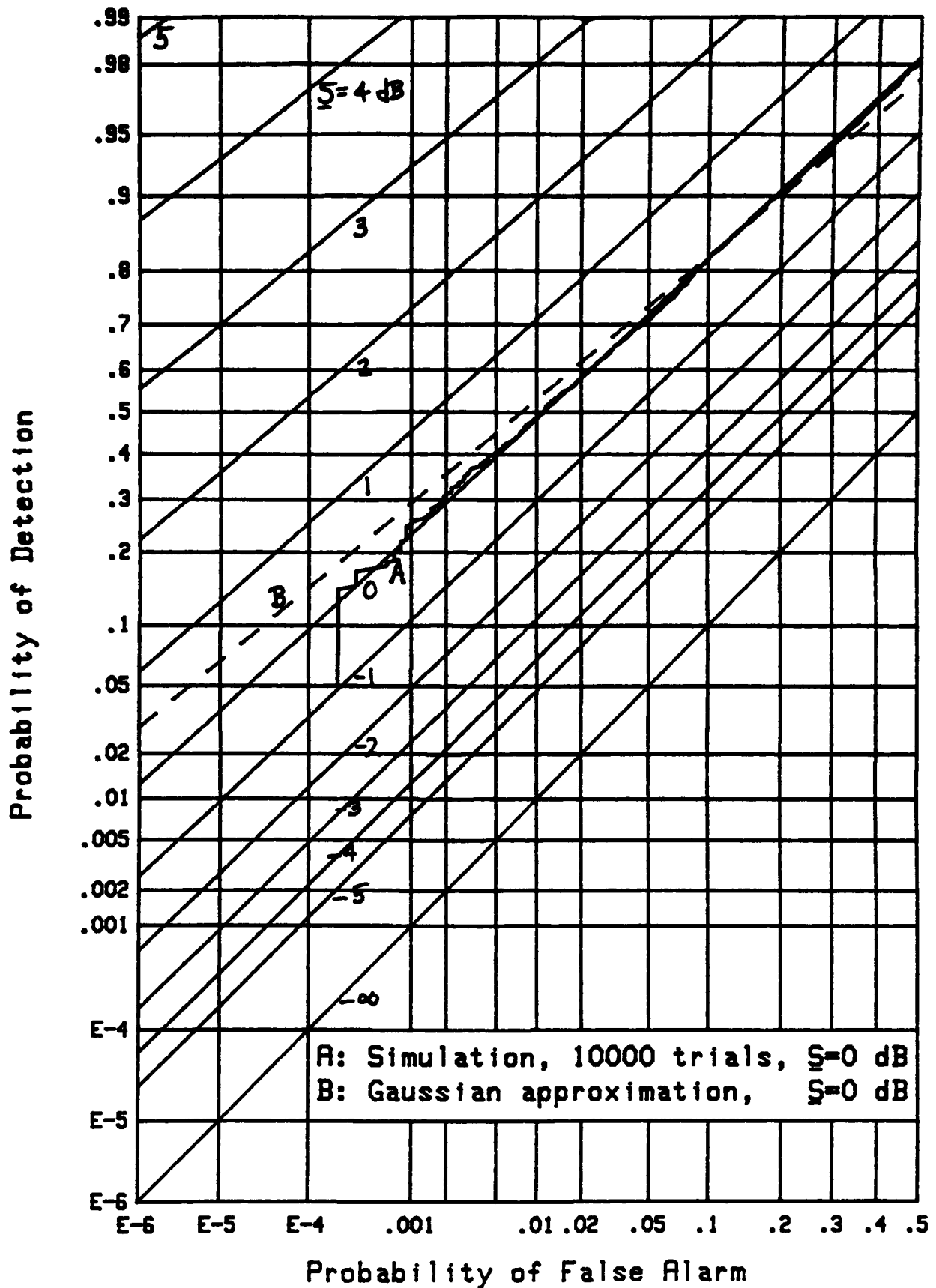
Figure 26. ROC for N=1024, M=64, Xo=1, FIT-4
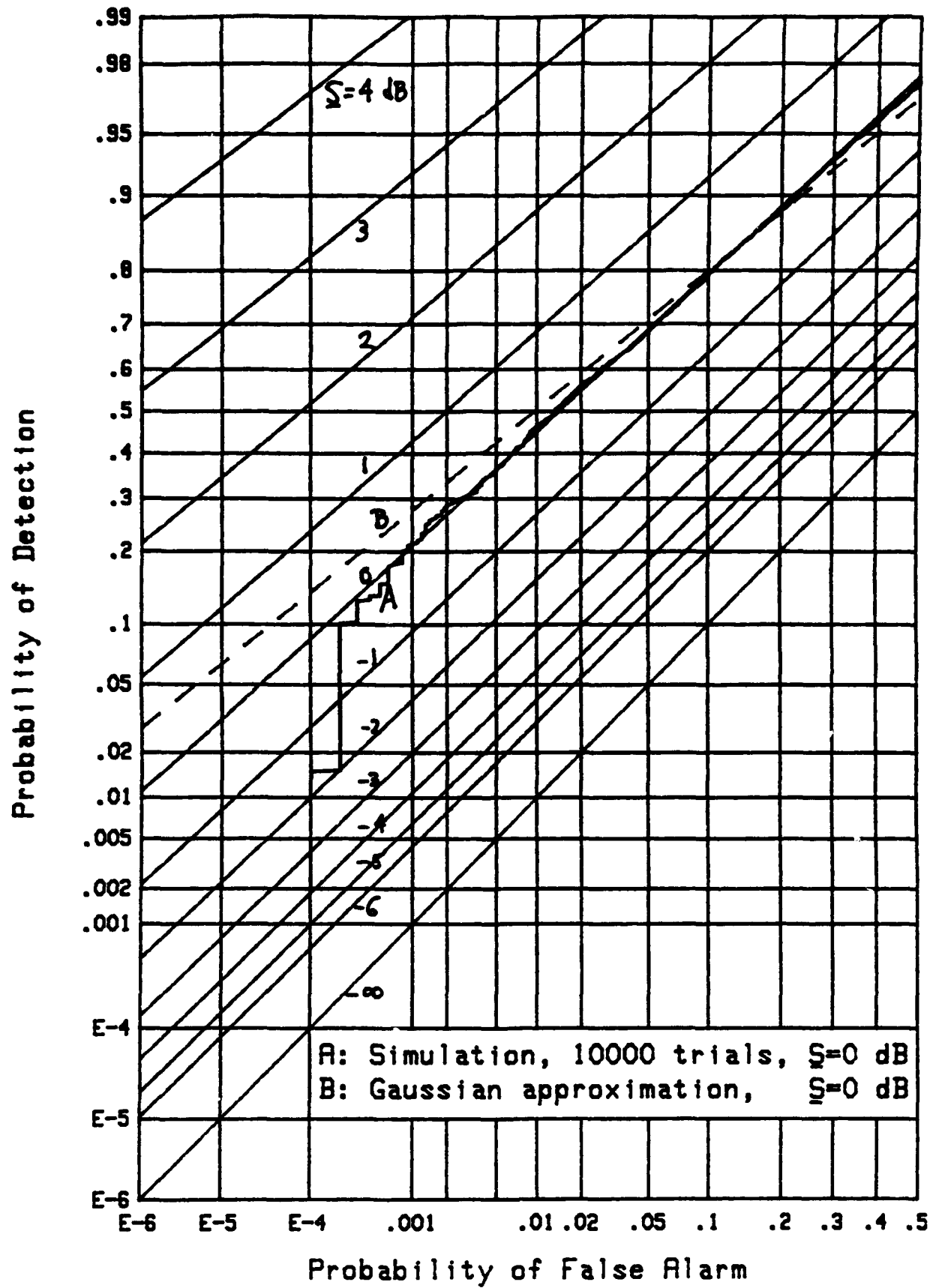
Figure 27. ROC for N=1024, M=64, Xo=3, FIT-4
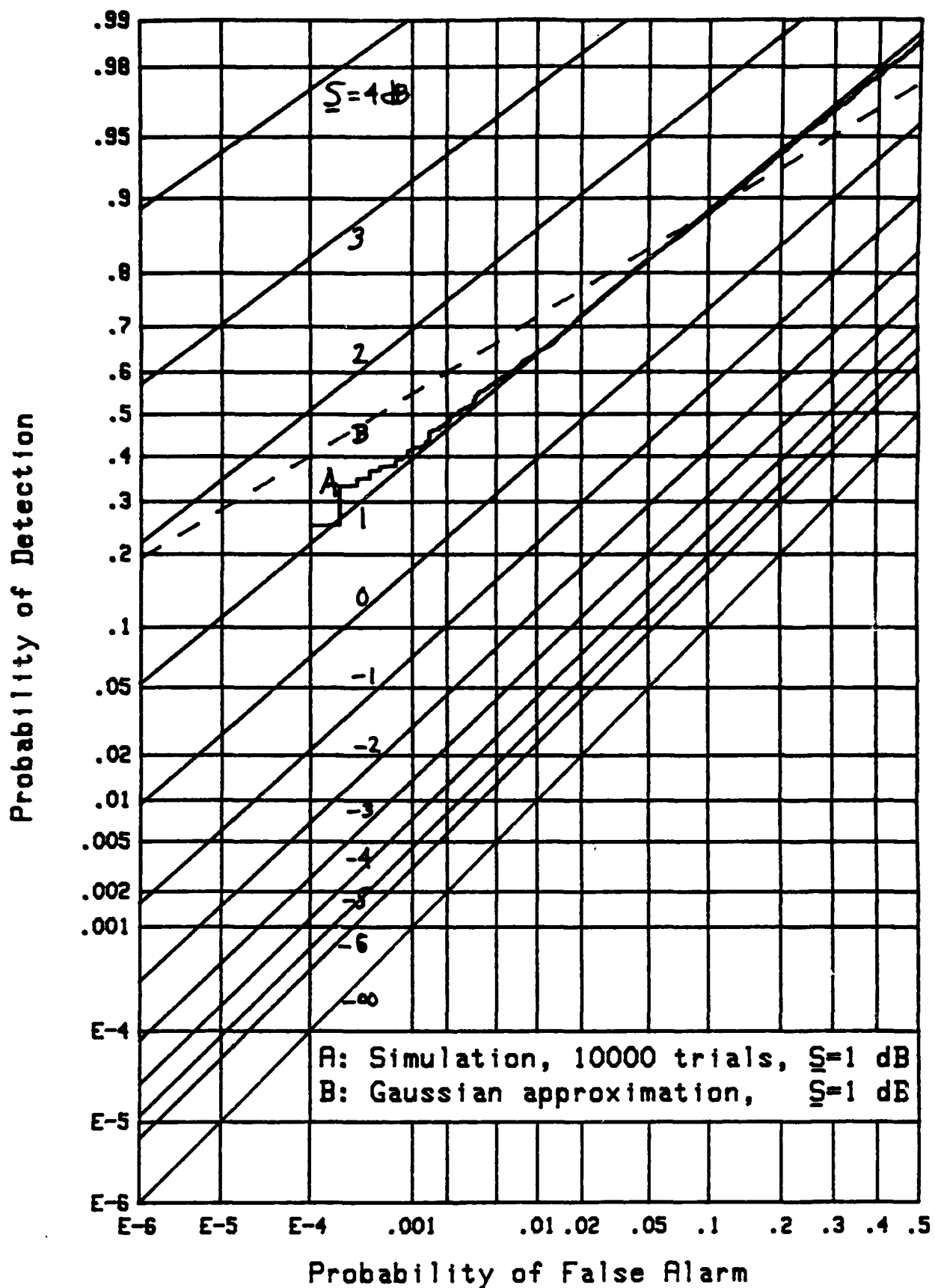
Figure 28. ROC for N=1024, M=64, Xo=5, FIT-4
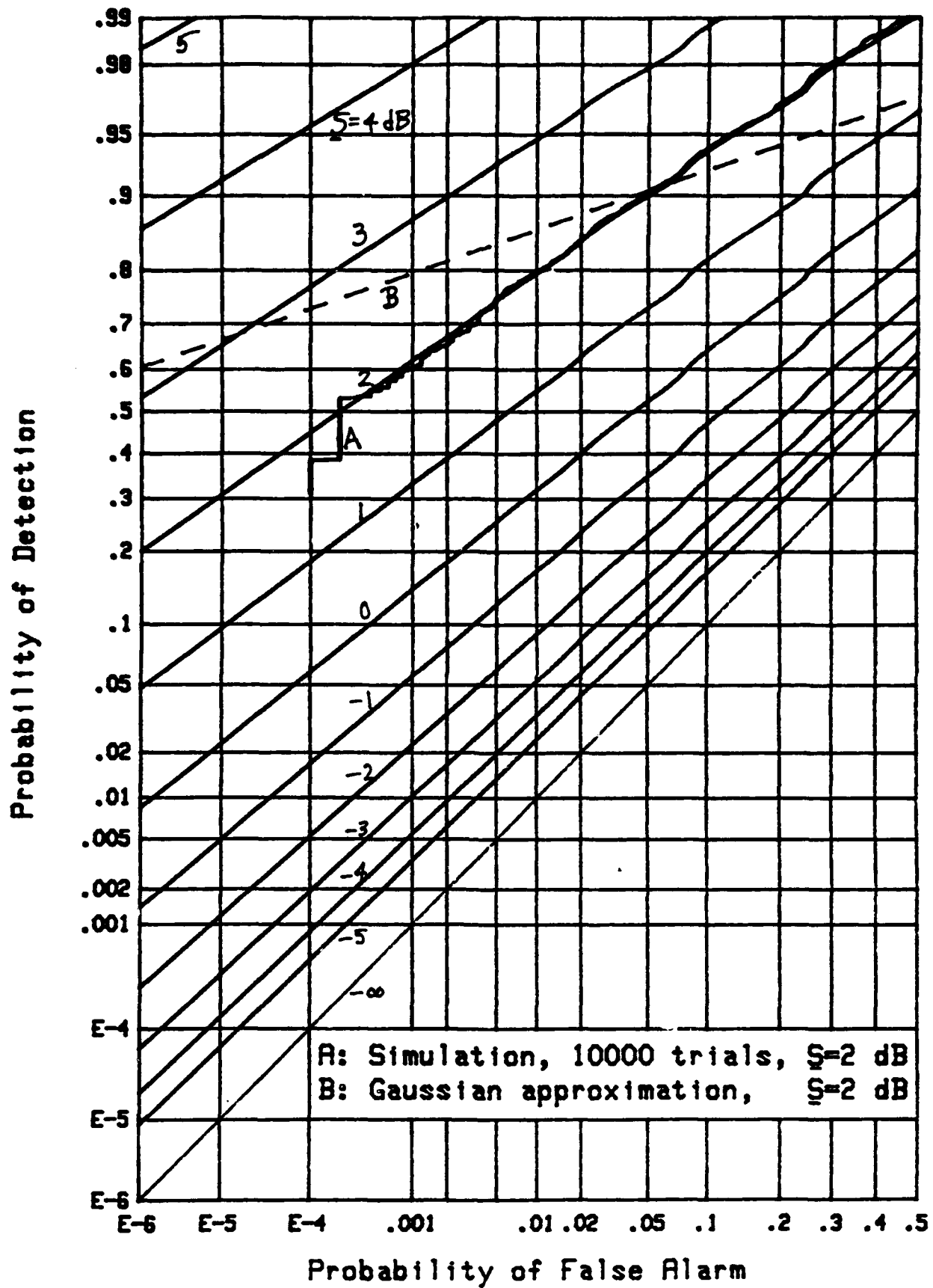
Figure 29. ROC for N=1024, M=64, Xo=7, FIT-2
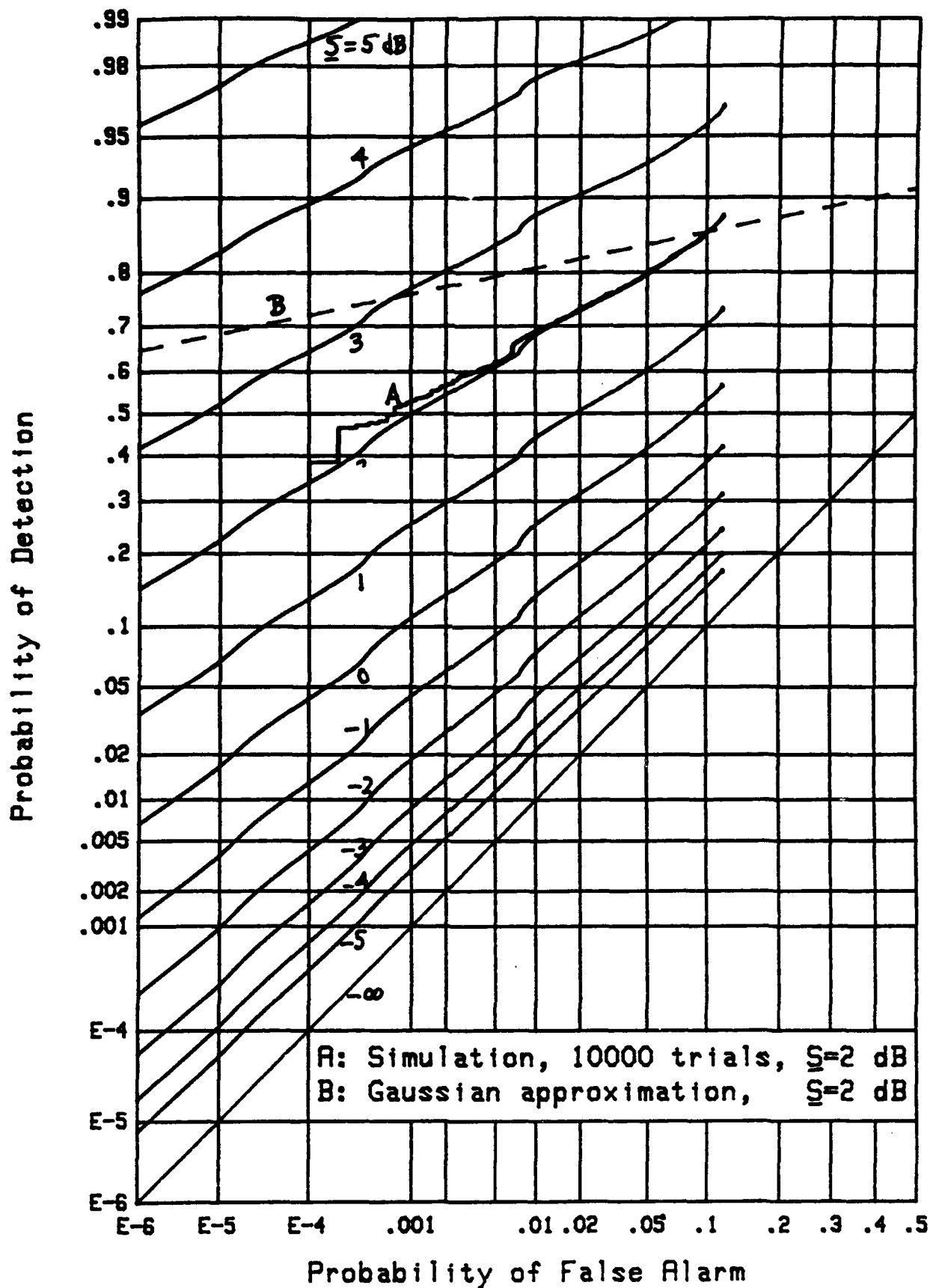
Figure 30. ROC for N=1024, M=64, Xo=9, FIT-2
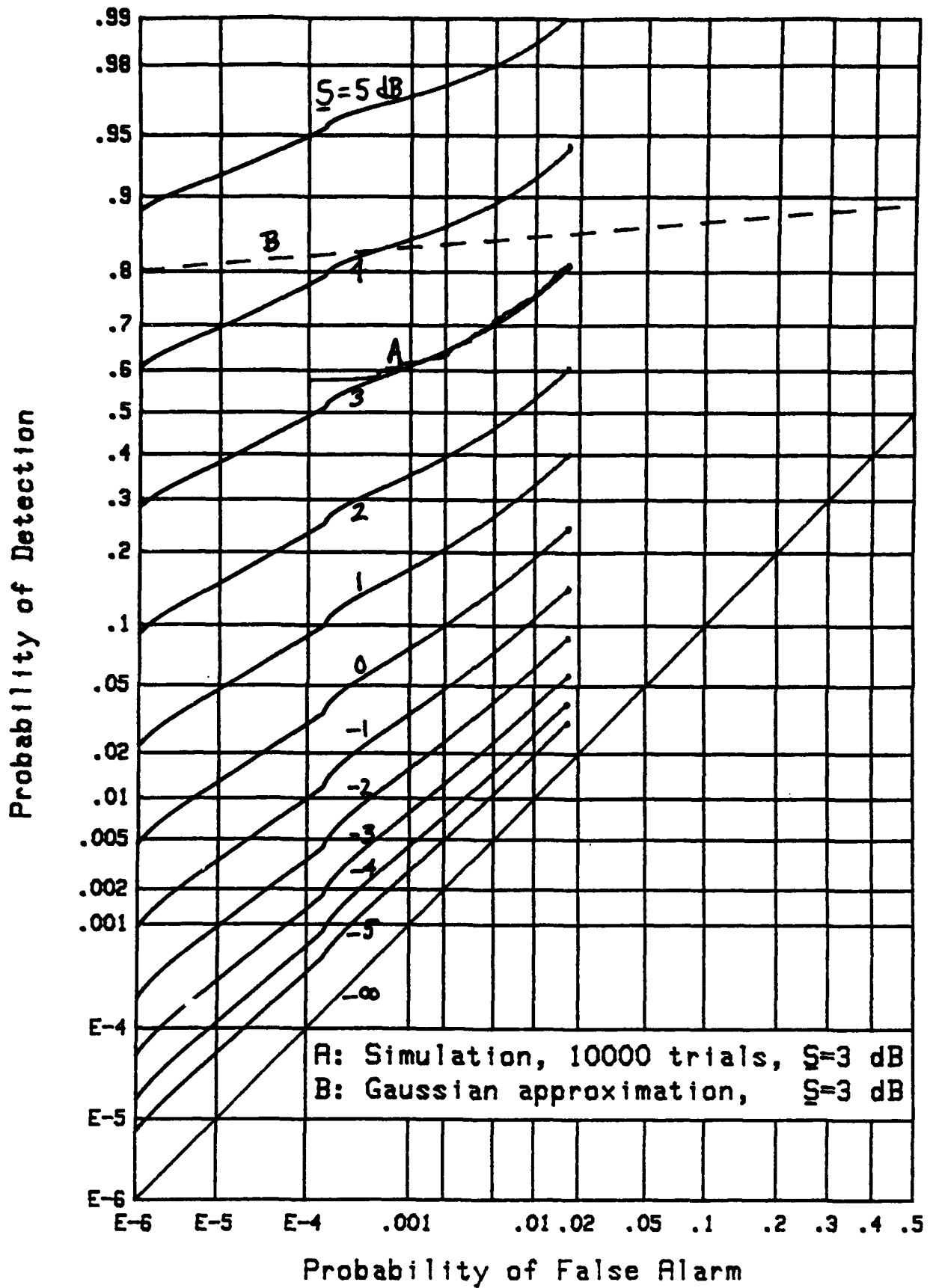
Figure 31. ROC for N=1024, M=64, Xo=11, FIT-2
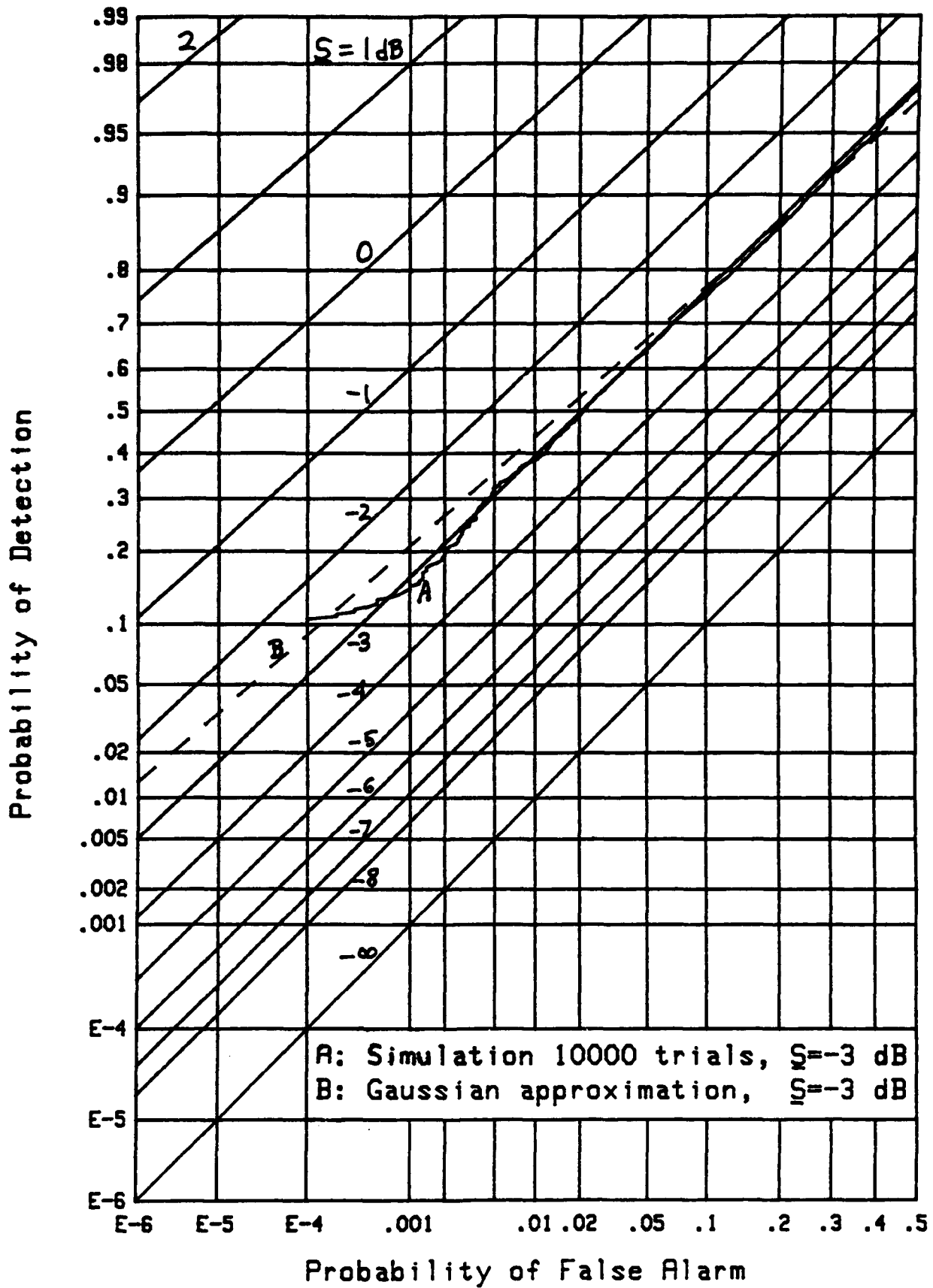
Figure 32. ROC for N=1024, M=128, Xo=1, FIT-4
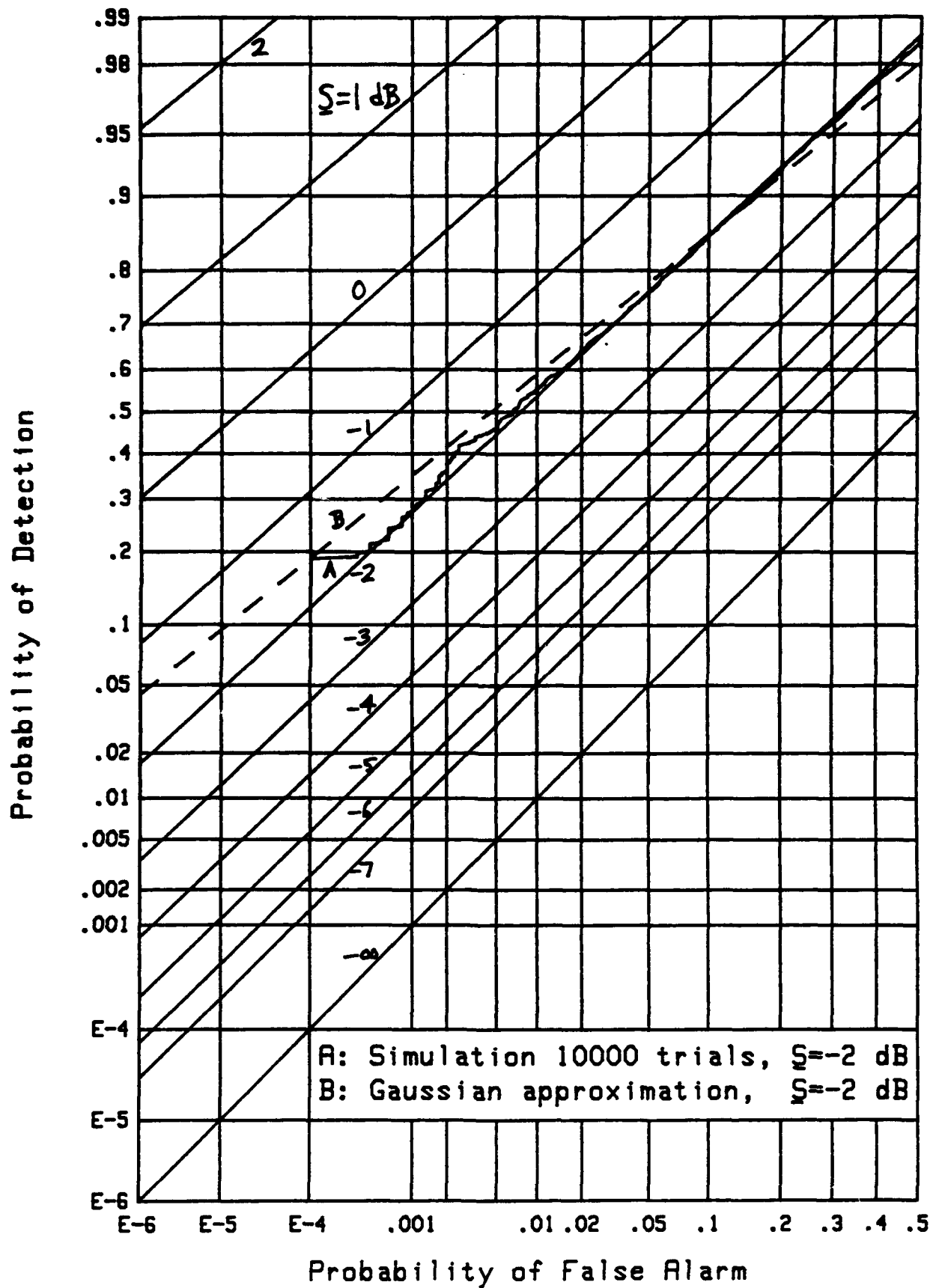
Figure 33. ROC for N=1024, M=128, Xo=3, FIT-4
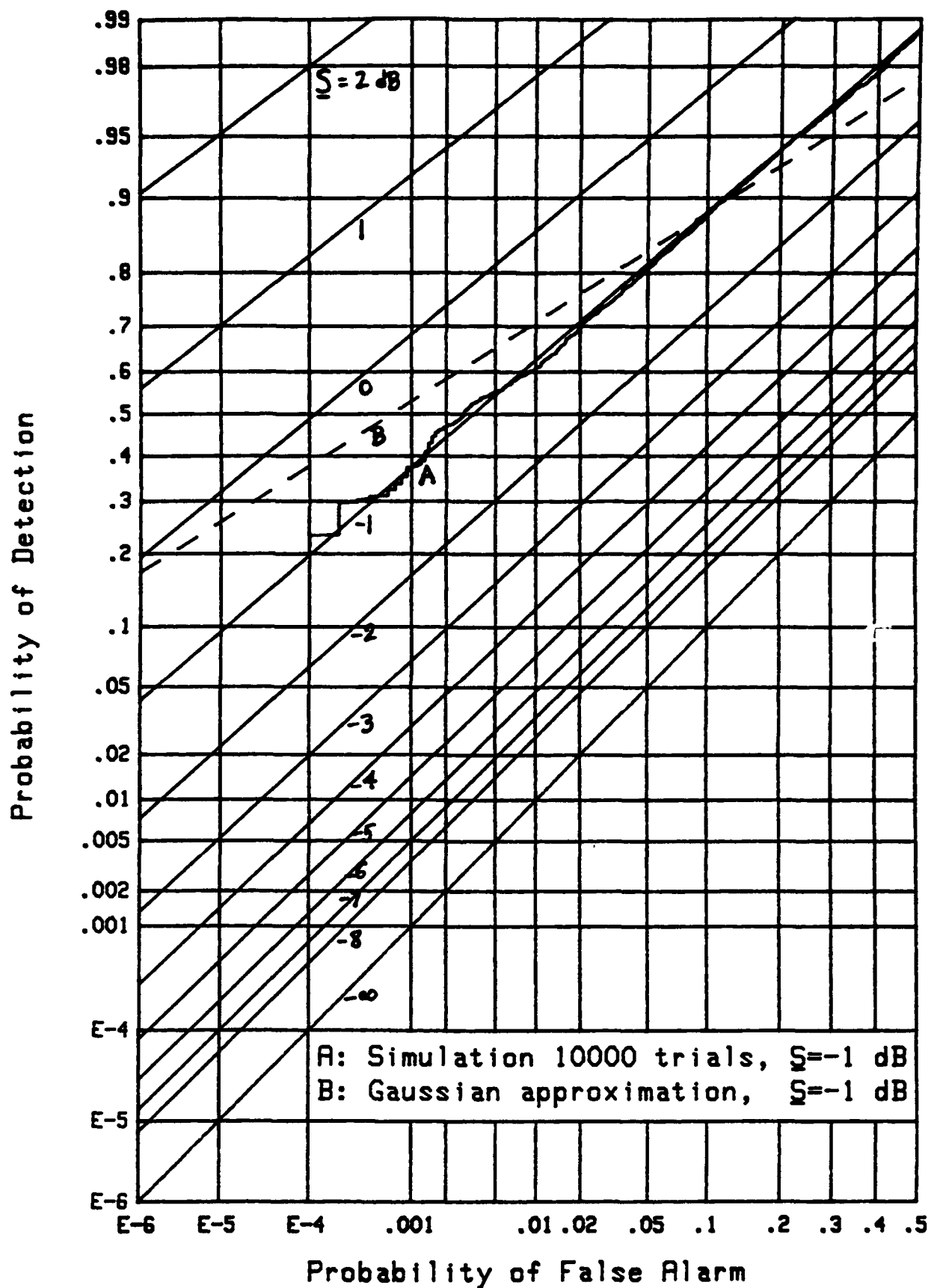
Figure 34. ROC for N=1024, M=128, Xo=5, FIT-4
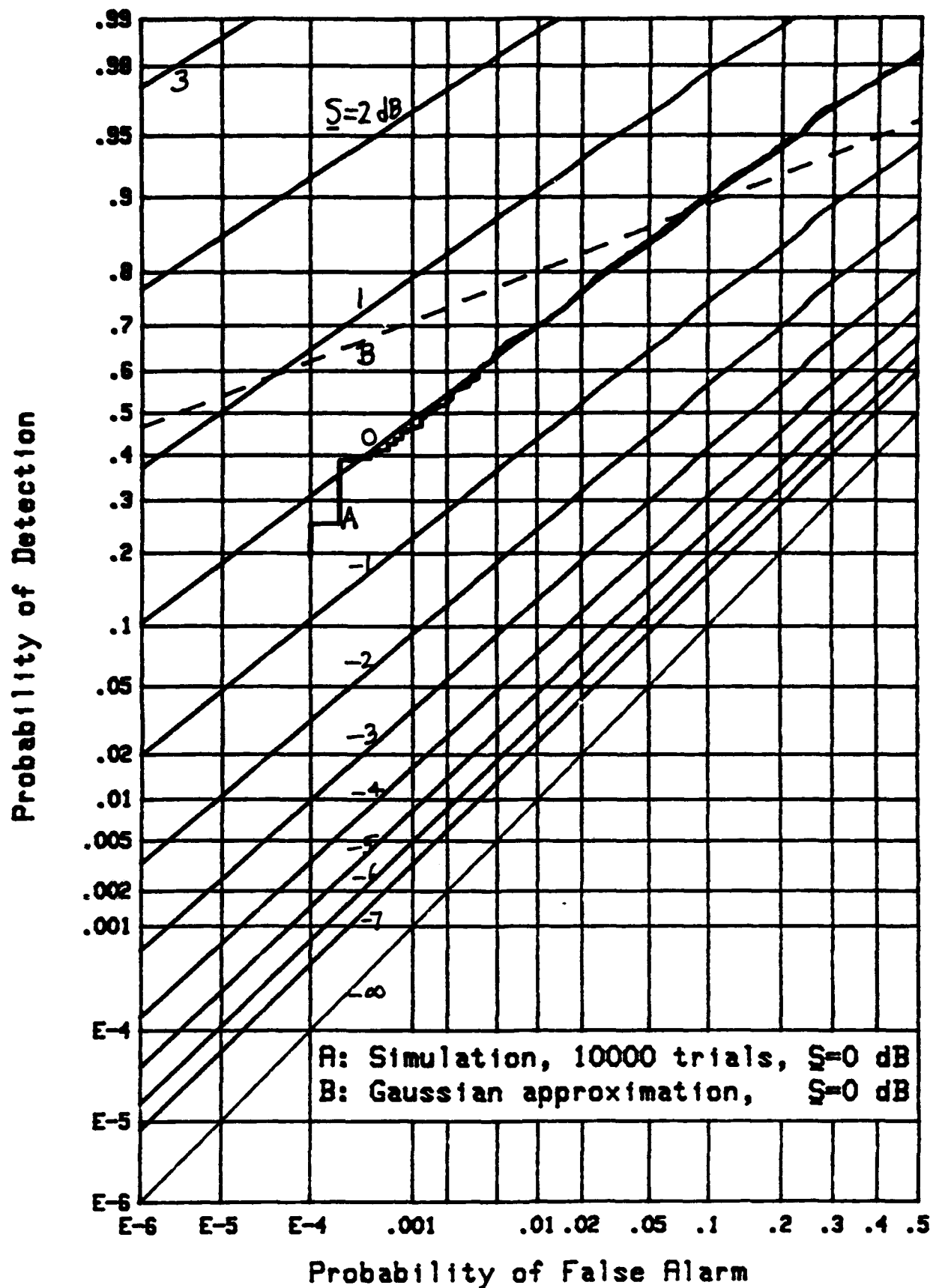
Figure 35. ROC for N=1024, M=128, Xo=7, FIT-2
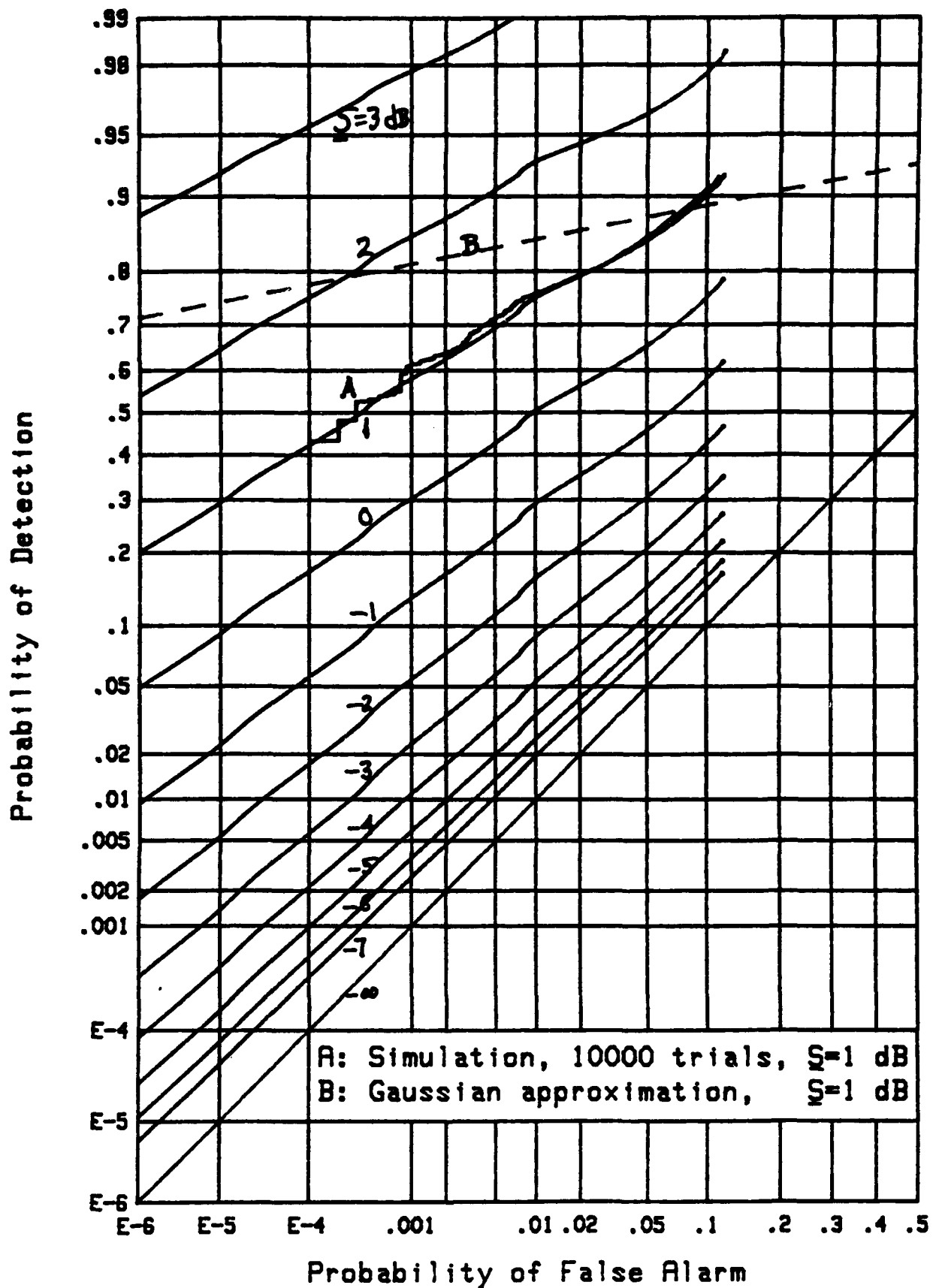
Figure 36. ROC for N=1024, M=128, Xo=9, FIT-2
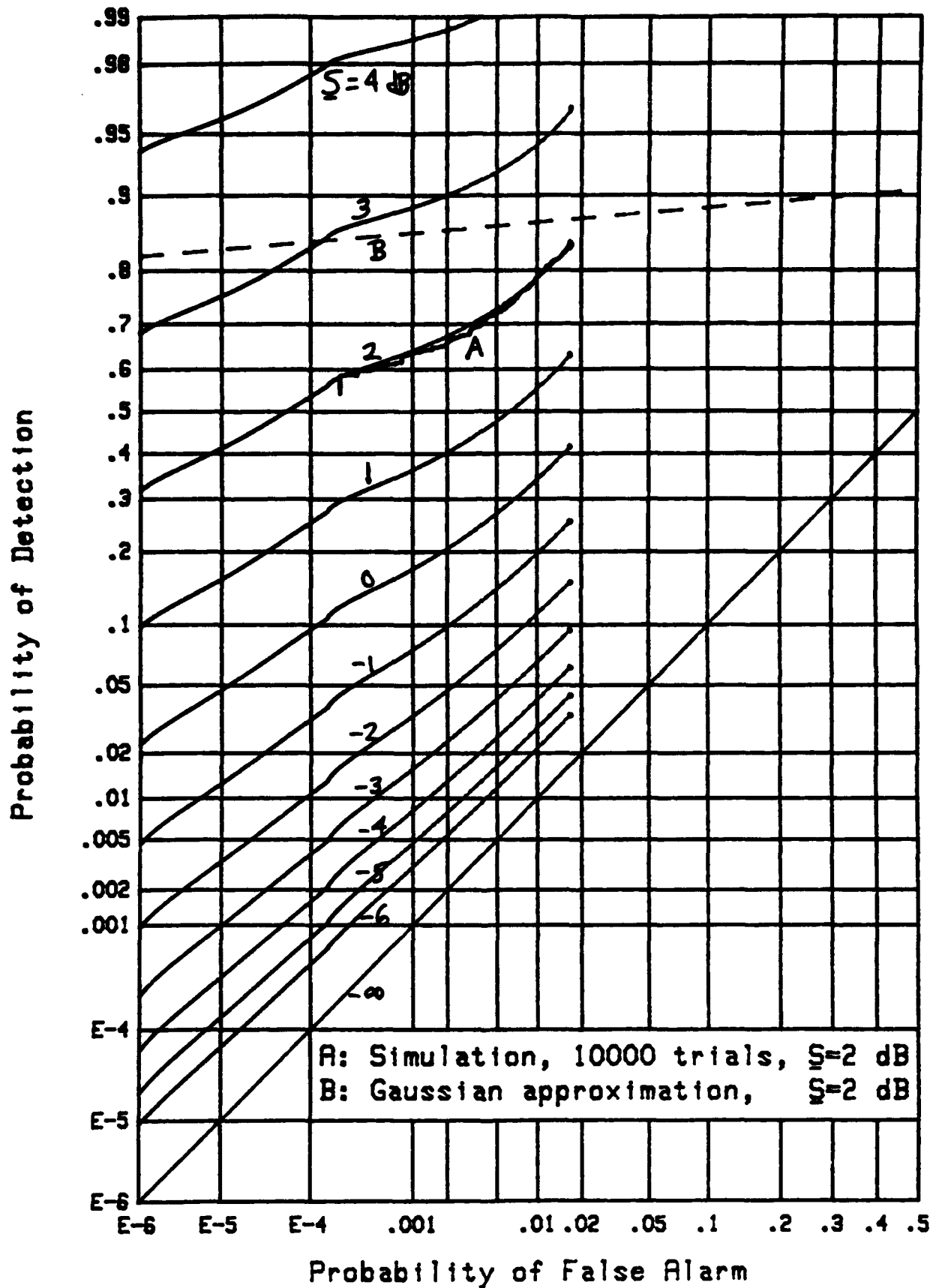
Figure 37. ROC for N=1024, M=128, Xo=11, FIT-2
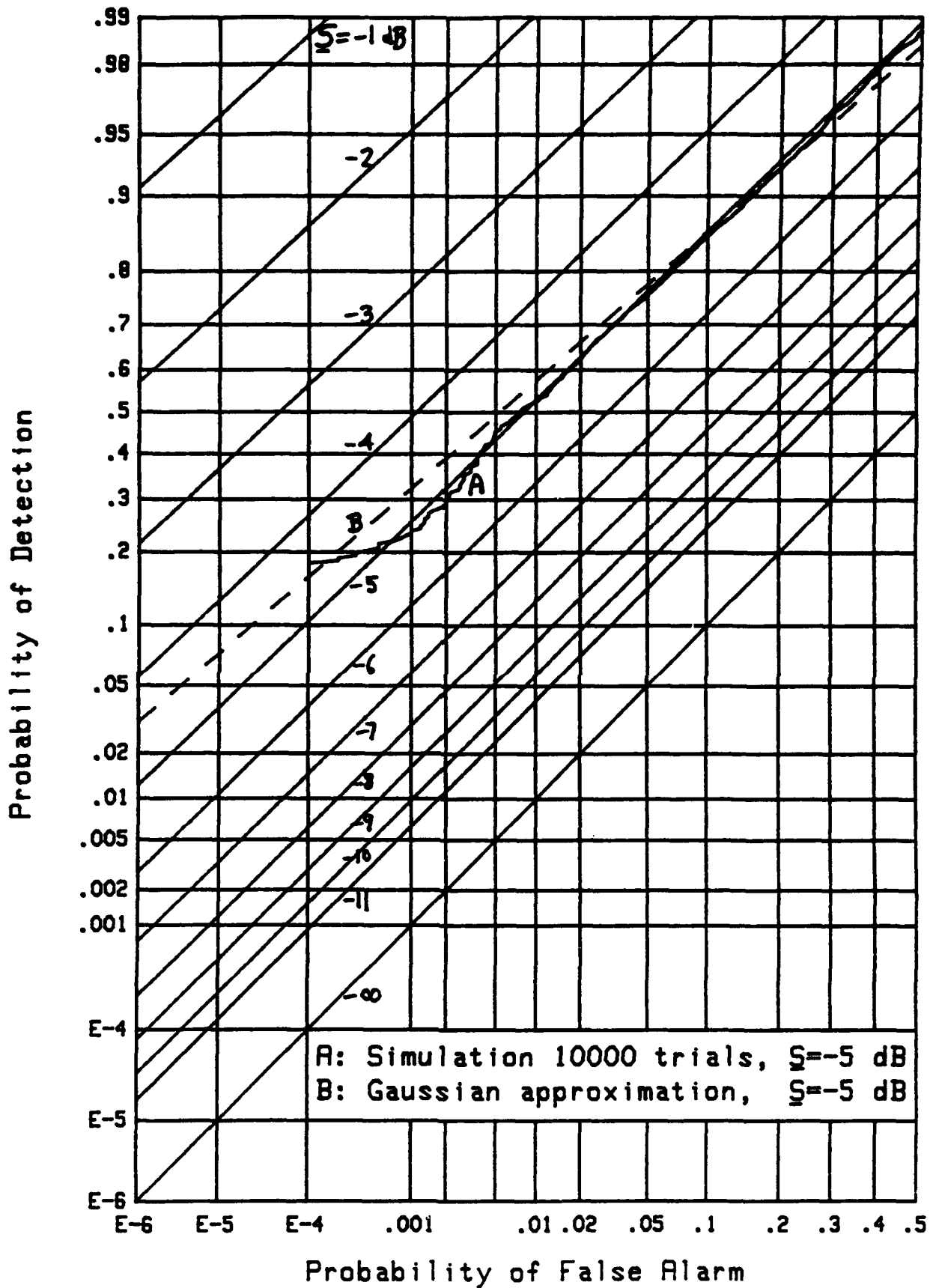
Figure 38. ROC for N=1024, M=256, Xo=1, FIT-4
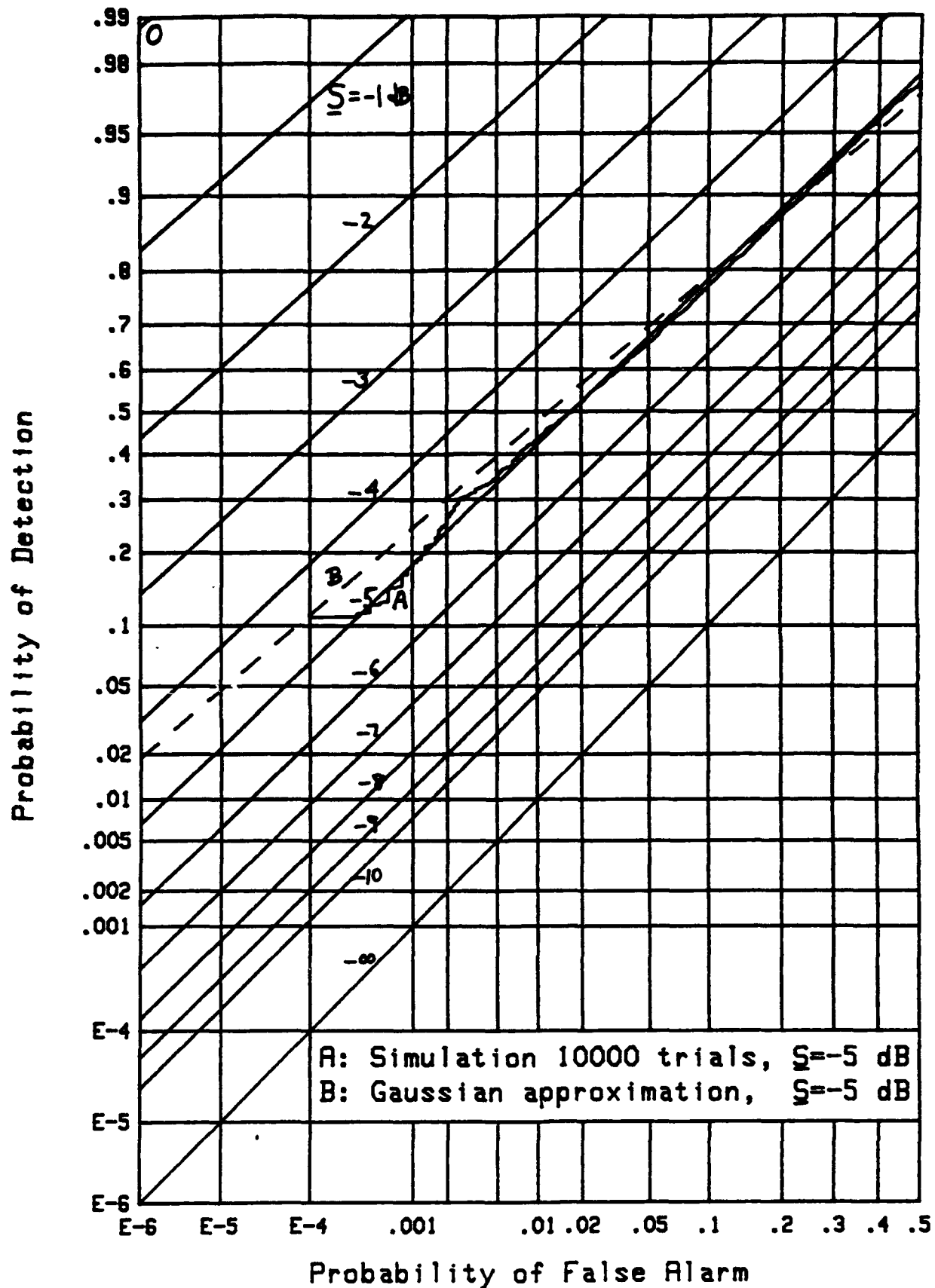
Figure 39. ROC for N=1024, M=256, Xo=3, FIT-4
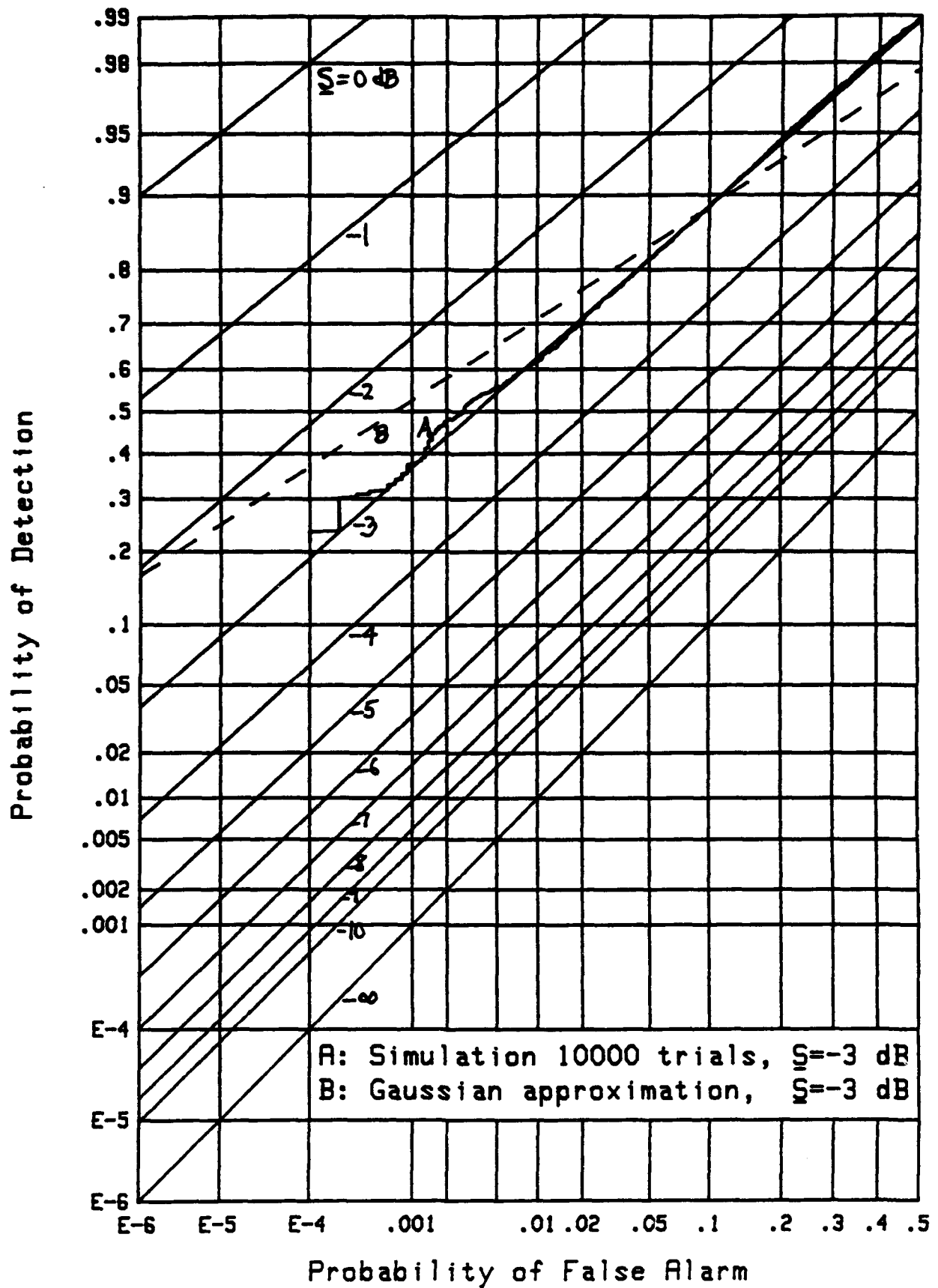
Figure 40. ROC for N=1024, M=256, Xo=5, FIT-4
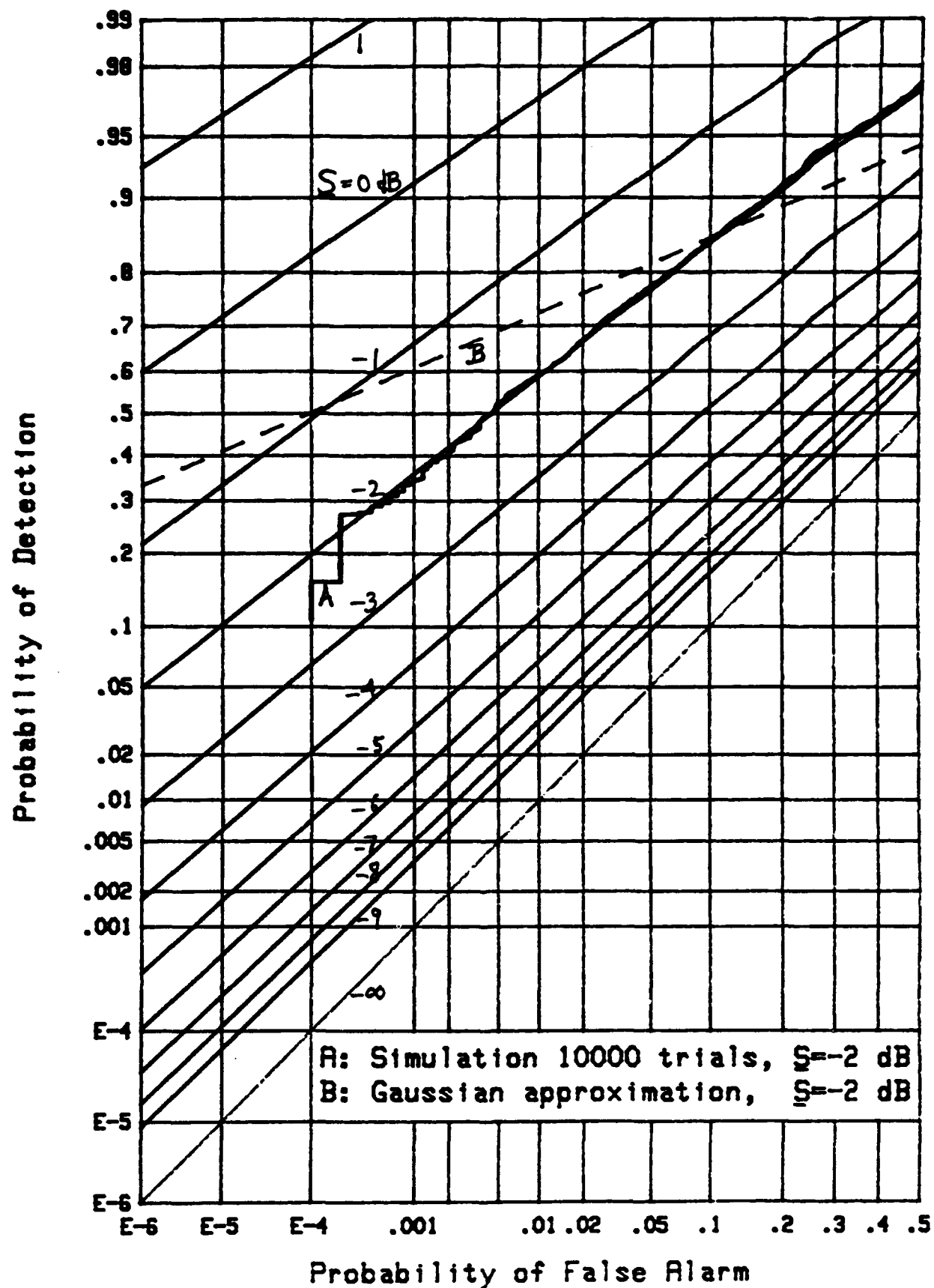
Figure 41. ROC for N=1024, M=256, Xo=7, FIT-2
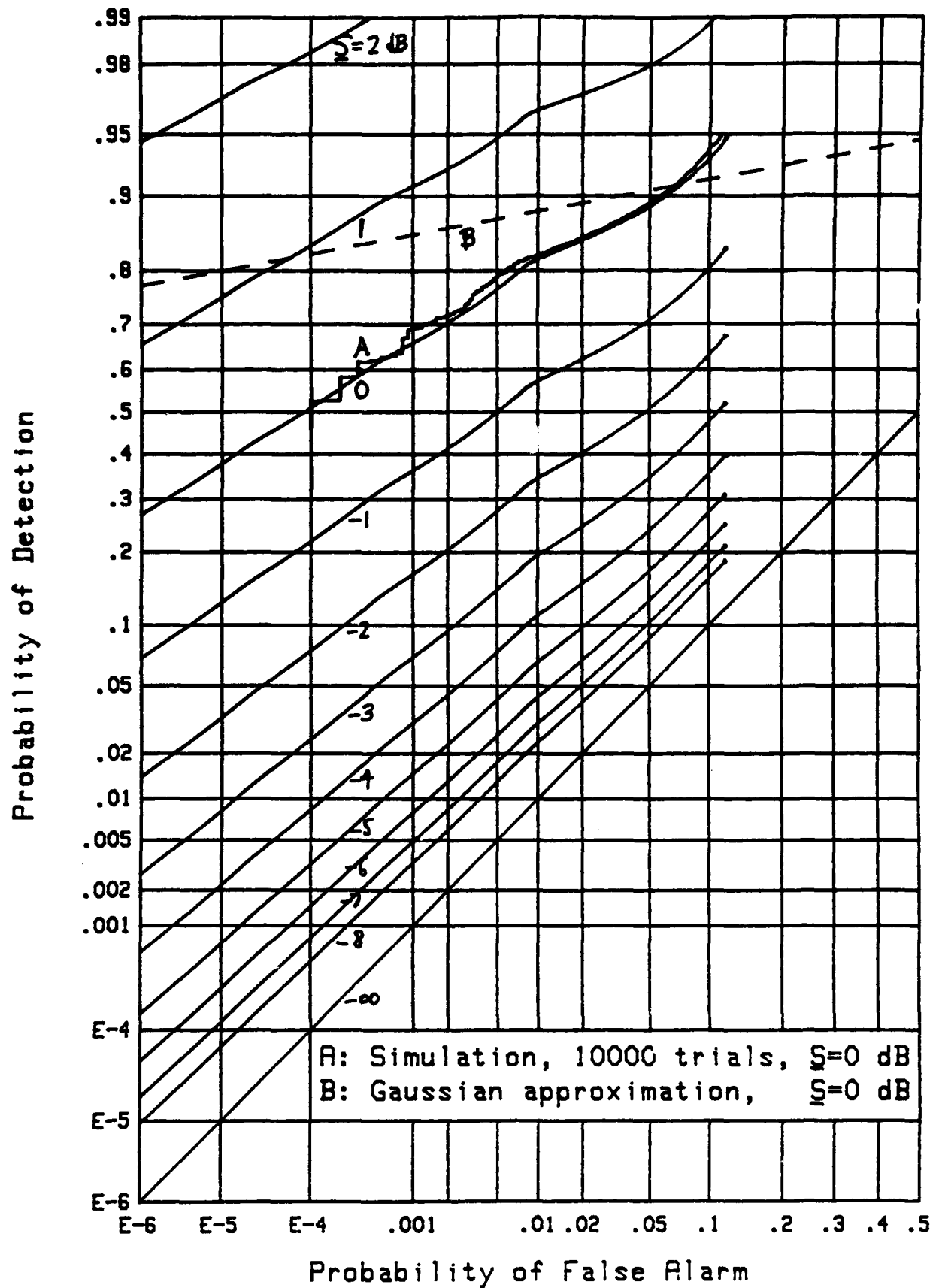
Figure 42. ROC for N=1024, M=256, Xo=9, FIT-2
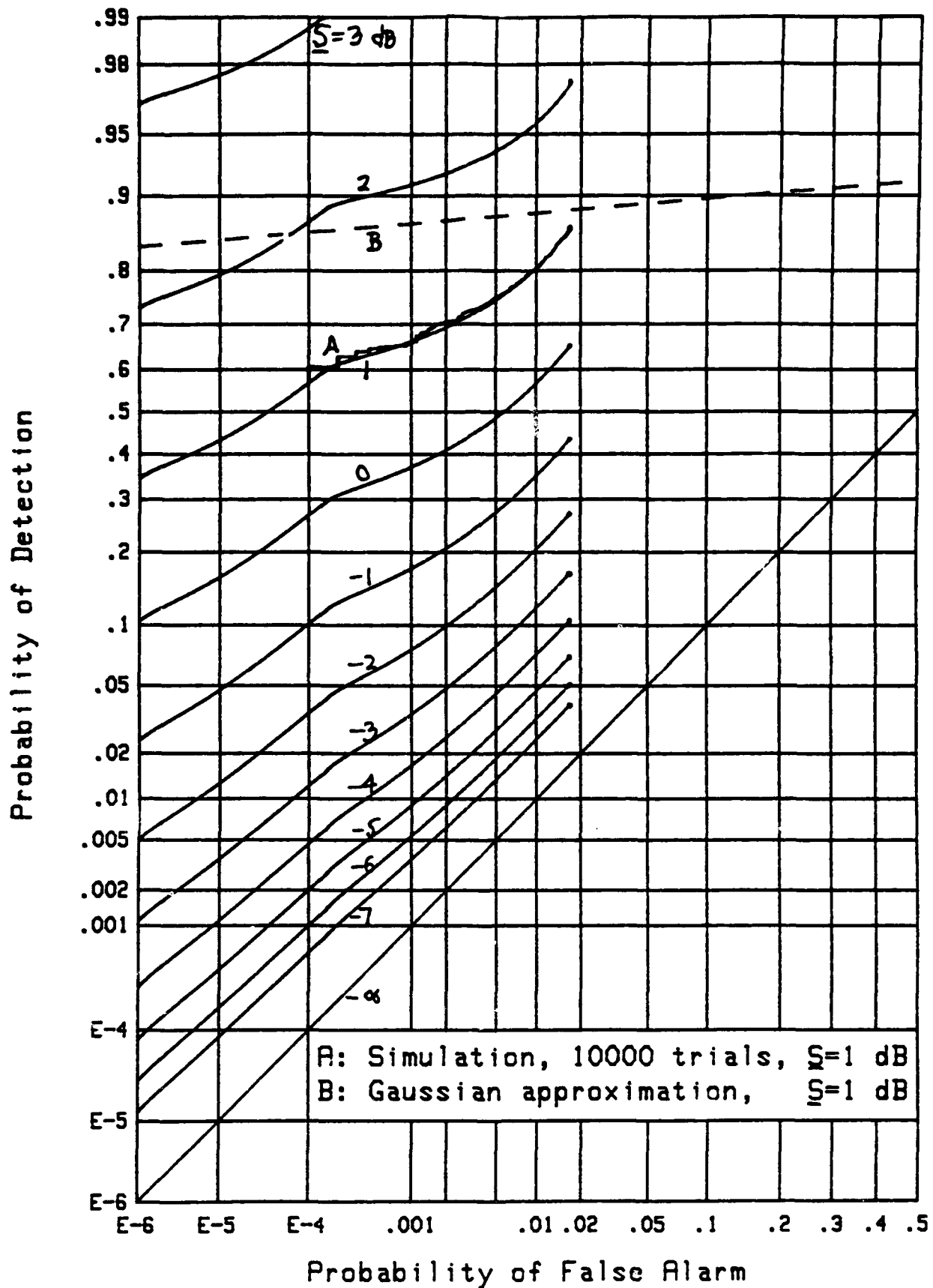
Figure 43. ROC for N=1024, M=256, Xo=11, FIT-2

VARIATION OF PERFORMANCE WITH N

All of the receiver operating characteristics in figures
8 - 43 above were computed for search size $N = 1024$. In order
to ascertain the dependence on N, without the same large-scale
computational investigation, we have computed the receiver
operating characteristics for $N = 512$ and $N = 256$, but only
for a few selected cases of M and x_o, namely

$$M = 8, \quad x_o = 11 , \tag{60}$$

$$M = 32, \quad x_o = 7 , \tag{61}$$

$$M = 256, \quad x_o = 1 . \tag{62}$$

These particular pairs were selected because they cover a wide
range of values of M, and they represent the best choices of
breakpoint x_o for each particular M; see tables 1 and 2.

The receiver operating characteristics for (60) are given in
figures 13, 44, and 45; those for (61) are given in figures 23,
46, and 47; while those for (62) are given in figures 38, 48, and
49. Simulations verify the theoretical analyses in every case.

The signal powers required in order to realize the two
operating points of interest are given in tables 3 and 4,
respectively. As N changes by a factor of 2, the differences in
required signal powers are 0.2 dB for $M = 8$ in (60); 0.5 dB for
$M = 32$ in (61); and 1.1 dB for $M = 256$ in (62). These
differences hold for both the low-quality and the high-quality
operating points. A very crude approximation to these

observations is $\frac{1}{2}$ log(M) - $\frac{1}{4}$. These results indicate that the cost of having to search a larger region is not significant, at least for these sets of parameter values.

Table 3. $\underline{S}$(dB) Required for $P_f = 10^{-3}$, $P_d = .5$

M	x_o	N = 1024	N = 512	N = 256
8	11	6.4	6.2	6.0
32	7	3.2	2.7	2.2
256	1	-4.0	-5.2	-6.3

Table 4. $\underline{S}$(dB) Required for $P_f = 10^{-6}$, $P_d = .9$

M	x_o	N = 1024	N = 512	N = 256
8	11	10.6	10.3	10.2
32	7	6.1	5.6	5.2
256	1	-1.1	-2.2	-3.2
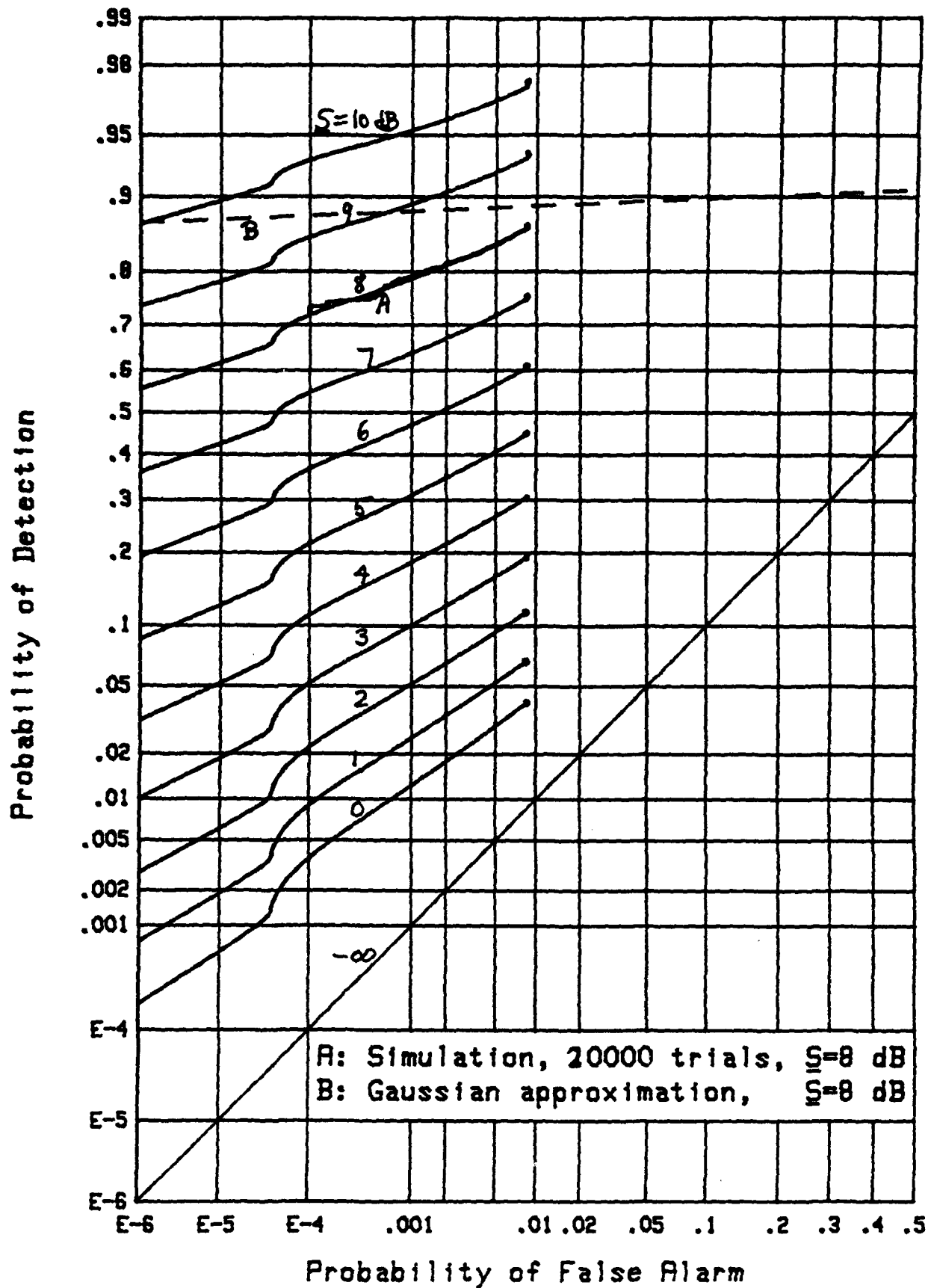
Figure 44. ROC for N=512, M=8, Xo=11, FIT-2
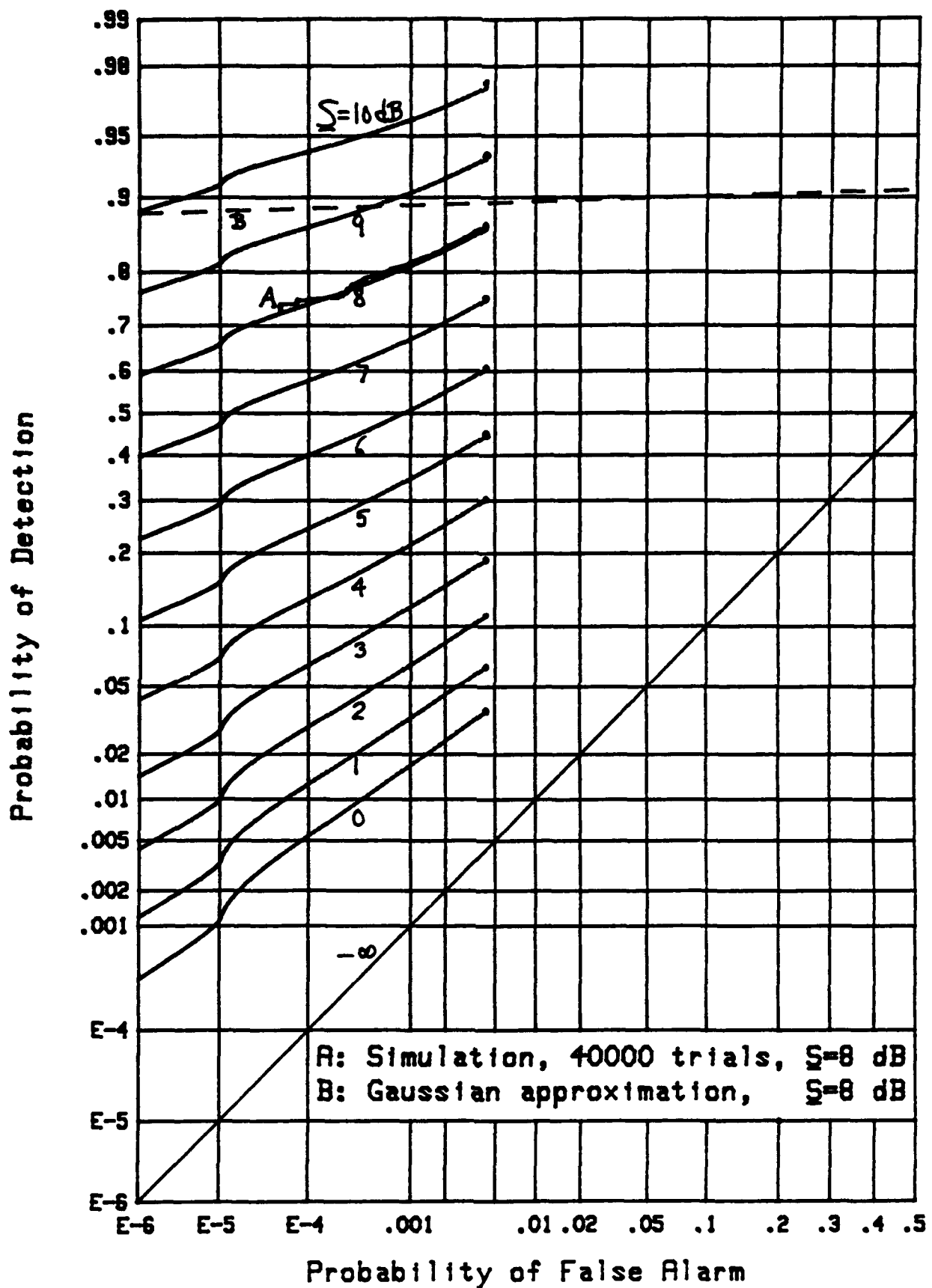
Figure 45. ROC for N=256, M=8, Xo=11, FIT-2
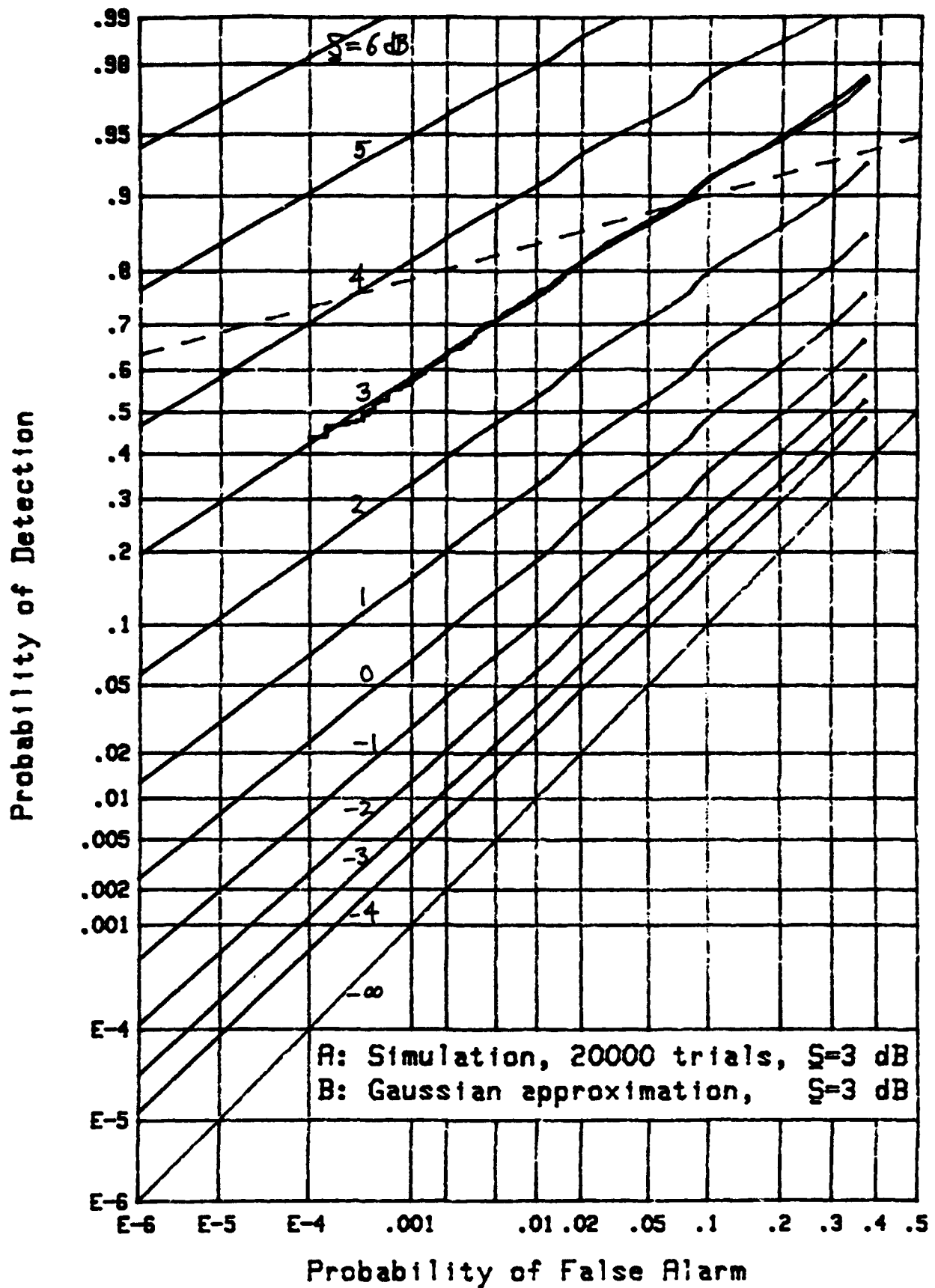
Figure 46. ROC for N=512, M=32, Xo=7, FIT-2
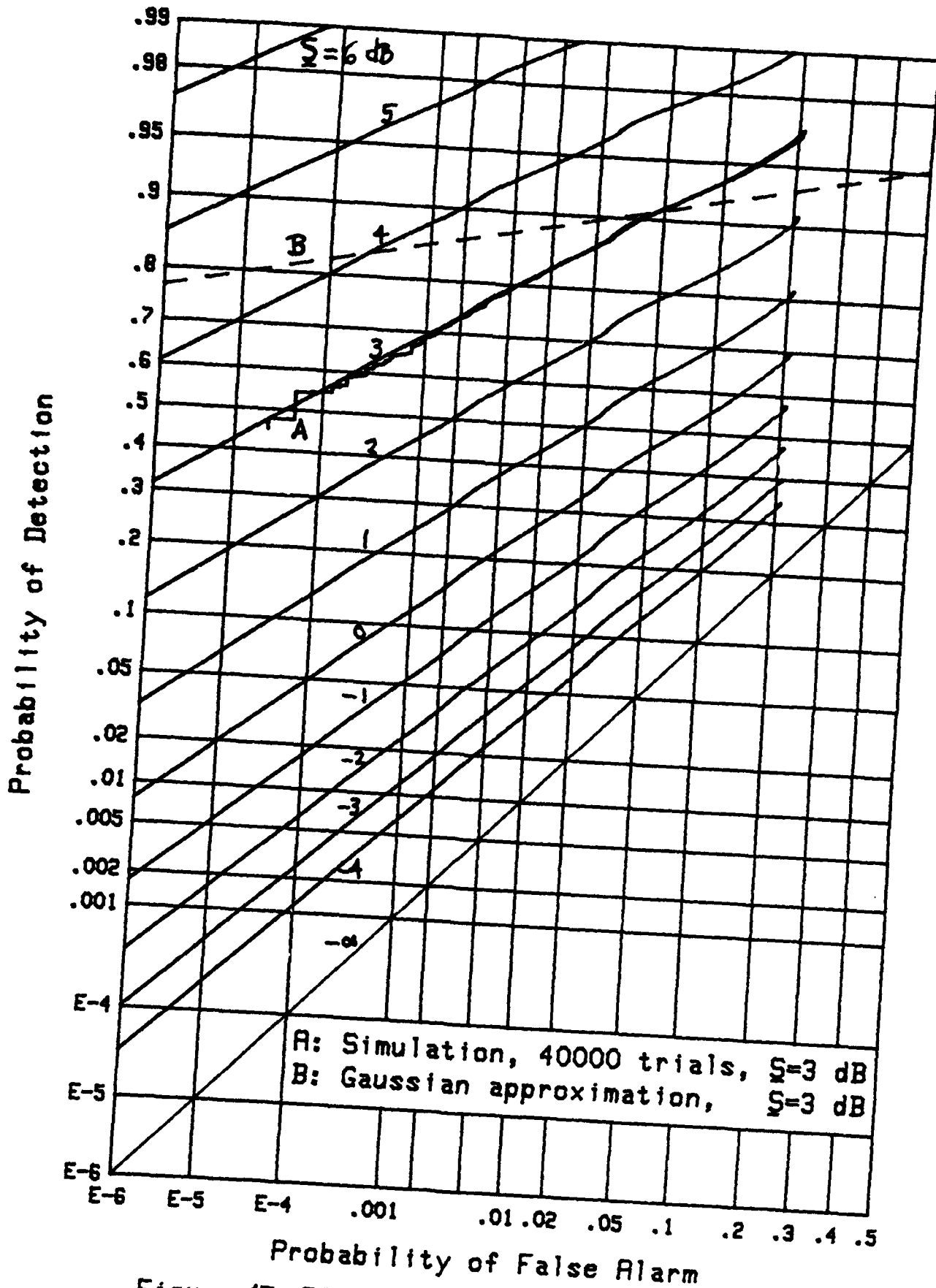
Figure 47. ROC for N=256, M=32, Xo=7, FIT-2

A: Simulation 10000 trials, S=-7 dB
B: Gaussian approximation, S=-7 dB
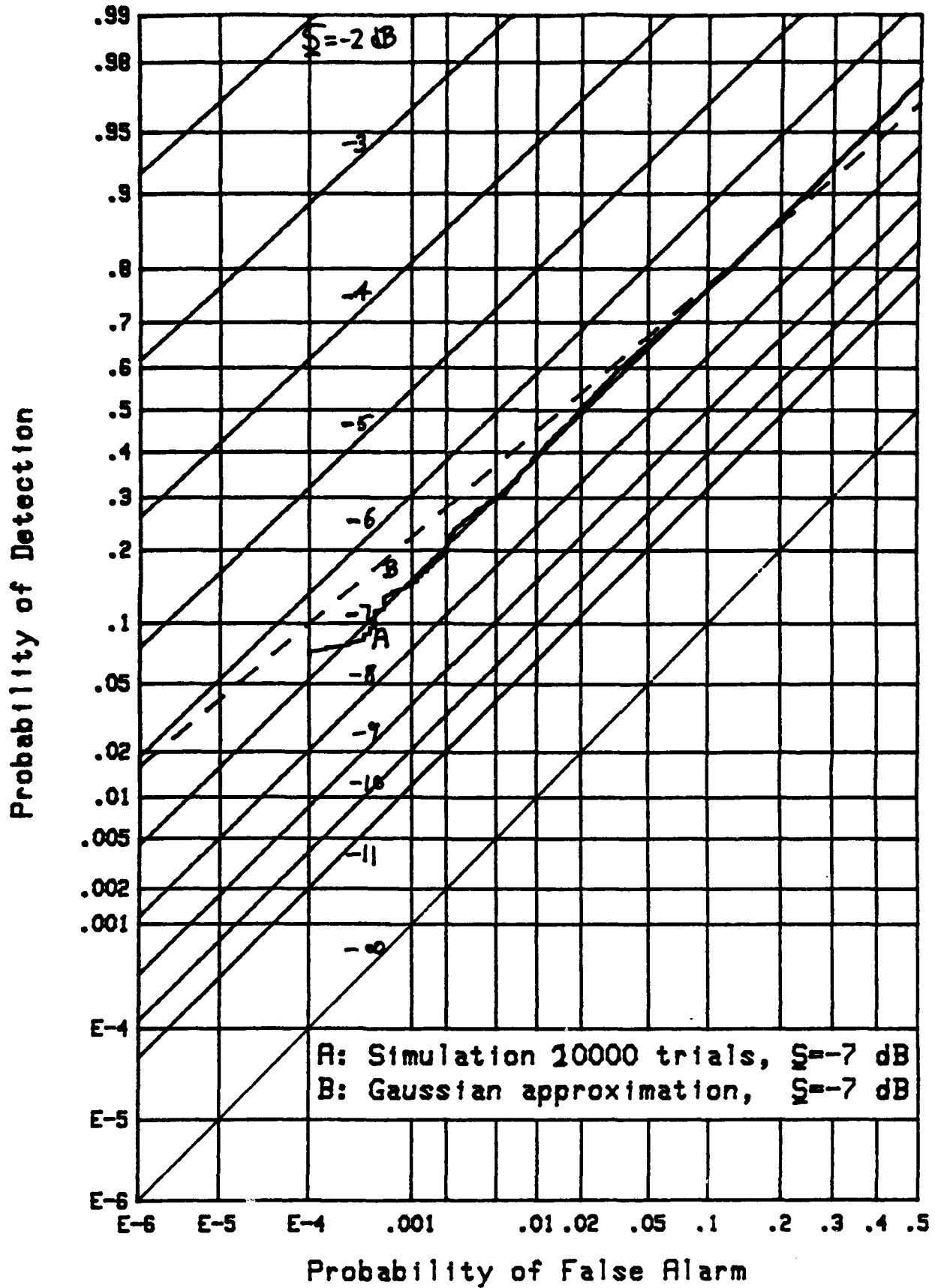
Figure 48. ROC for N=512, M=256, Xo=1, FIT-4
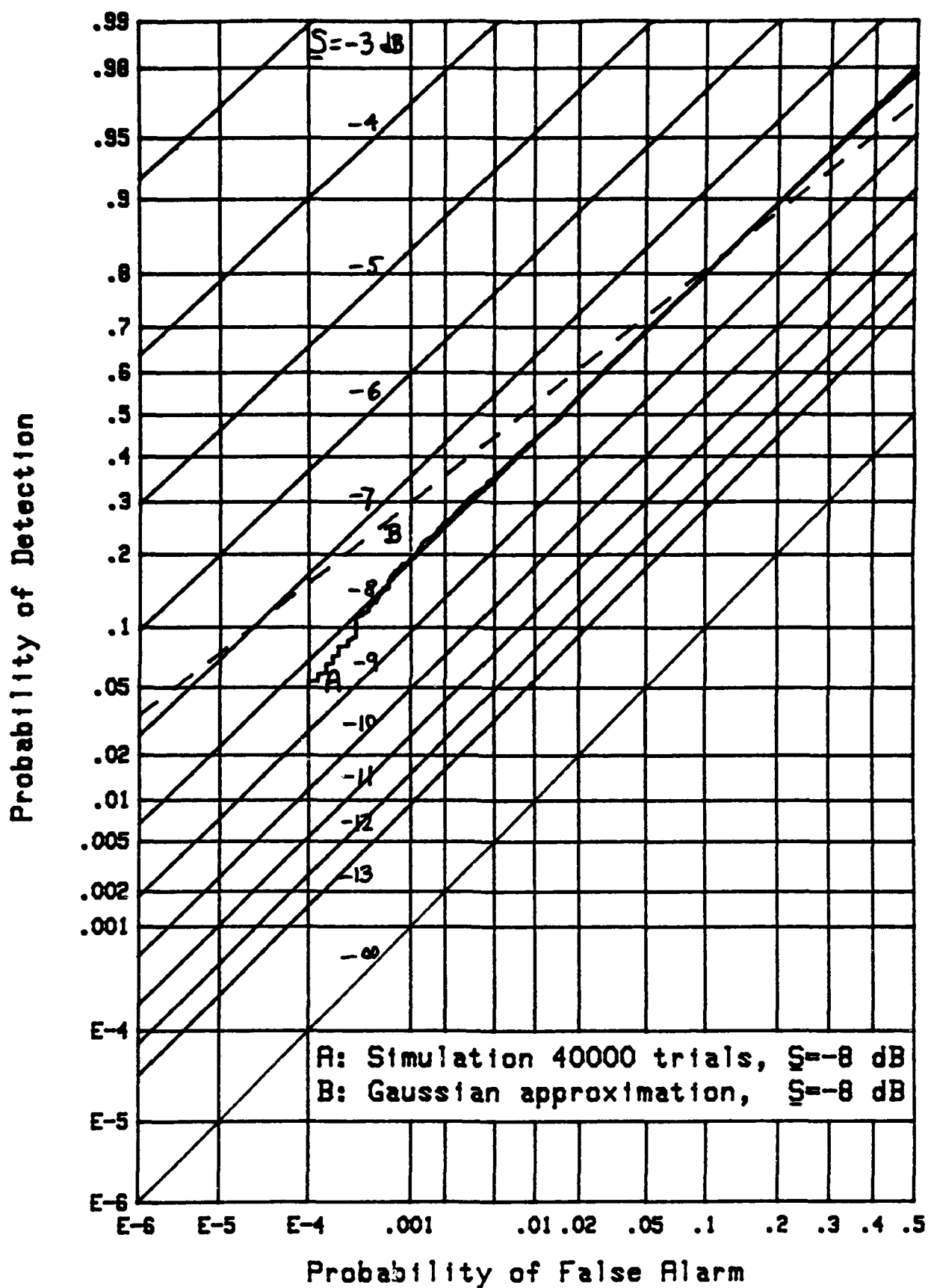
Figure 49. ROC for N=256, M=256, Xo=1, FIT-4

ENERGY DETECTOR CHARACTERISTICS

The energy detector was described in (52), and its characteristic function was presented in (53). The false alarm probability, given by (55), is plotted in figure 50 for search sizes N = 64, 128, 256, 512, 1024 for probability values down to the 10^{-6} level. The receiver operating characteristics were evaluated exactly, by the methods in [7], and are presented in figures 51 - 58 for N = 1024 and M = 8, 16, 32, 64, 128, 256, 512, 1024, respectively. The values of required signal power in tables 1 and 2 under the ED (energy detector) column were obtained from figures 51 - 58. Since these receiver operating characteristics were obtained by an exact analysis of the exact linear summation in (52), there is no need to resort to a simulation or a Gaussian approximation; hence, there are no overlays.
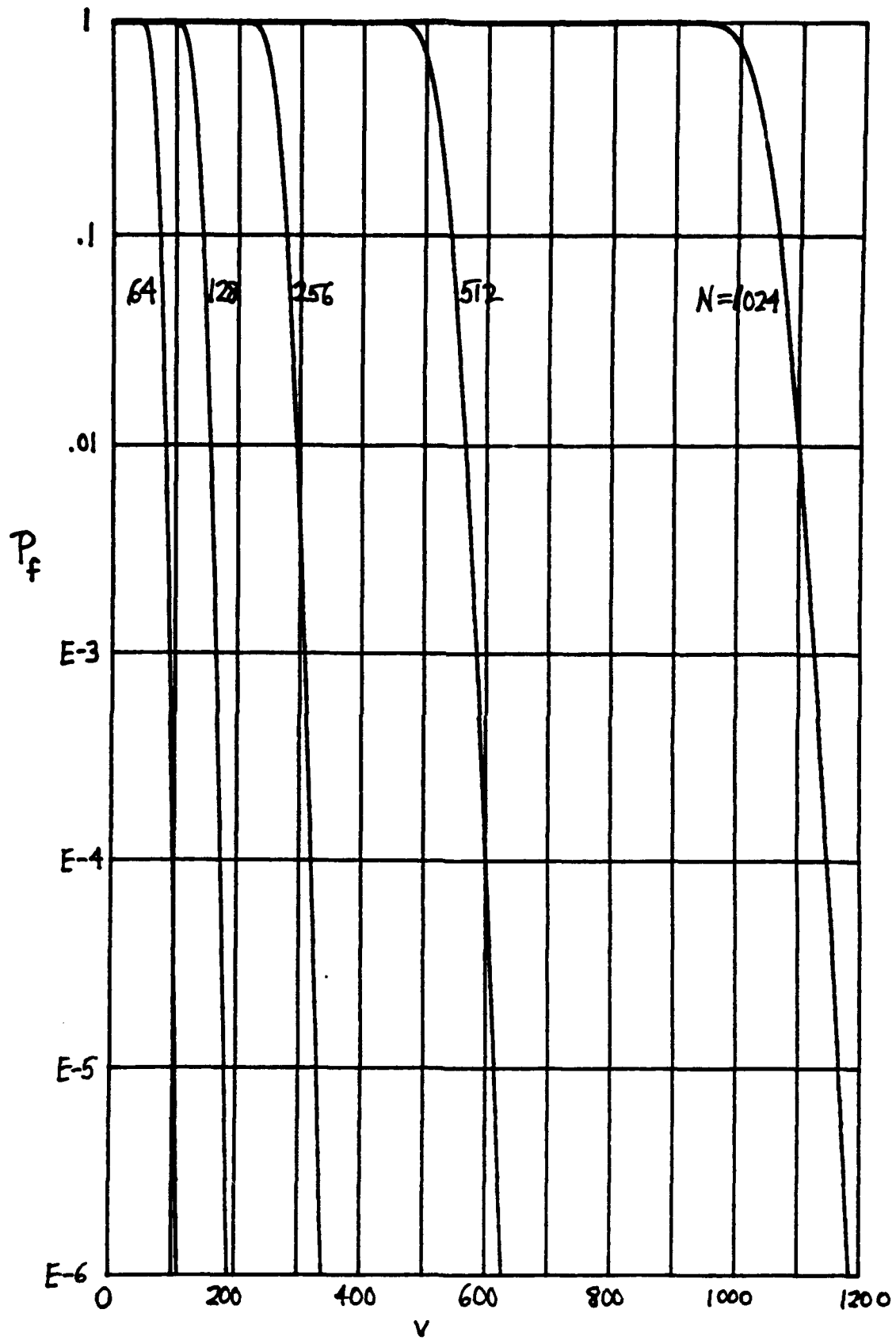
Figure 50. Energy Detector False Alarm Probability
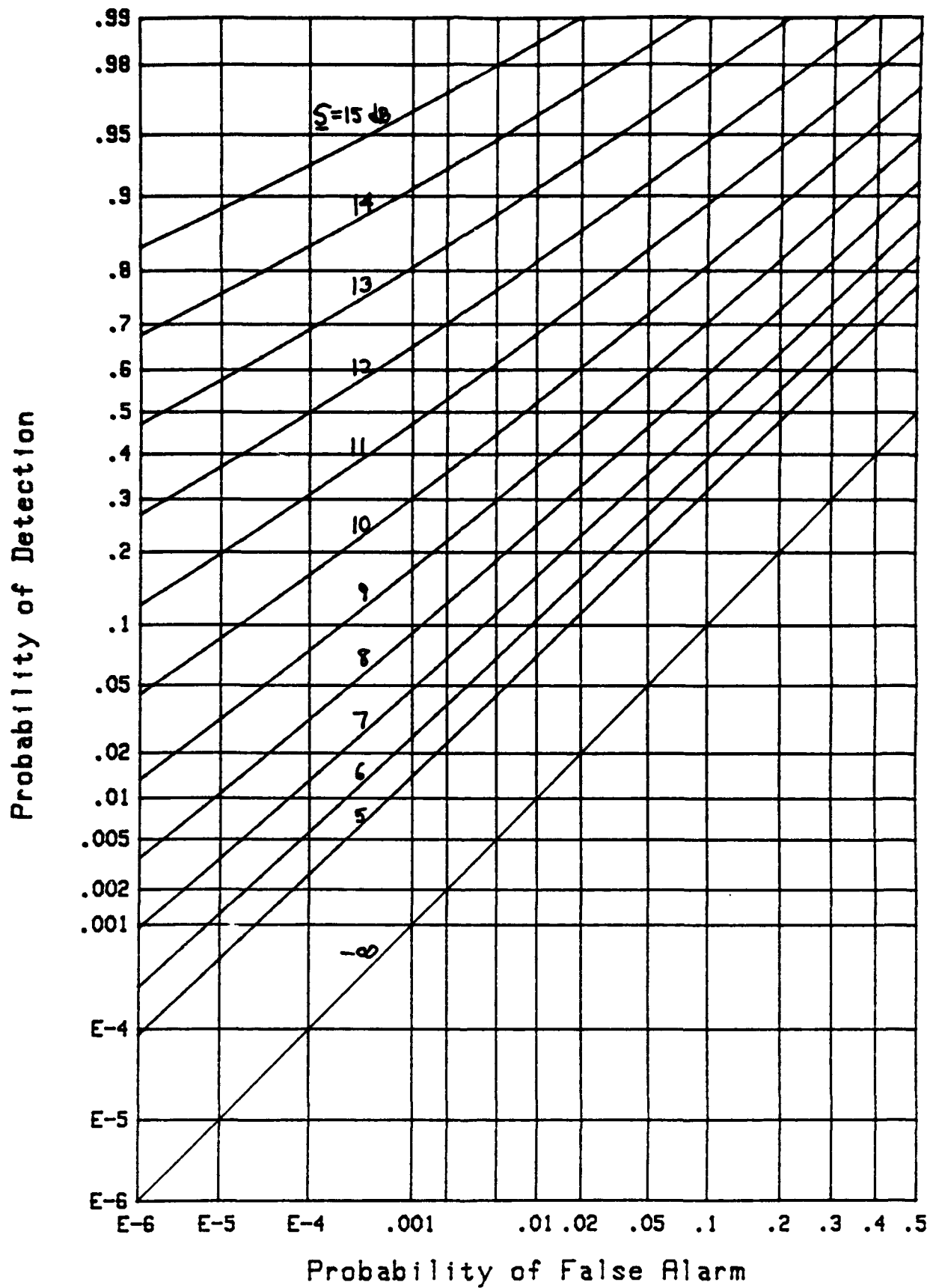
Figure 5l. Energy Detector ROC for N=1024, M=8
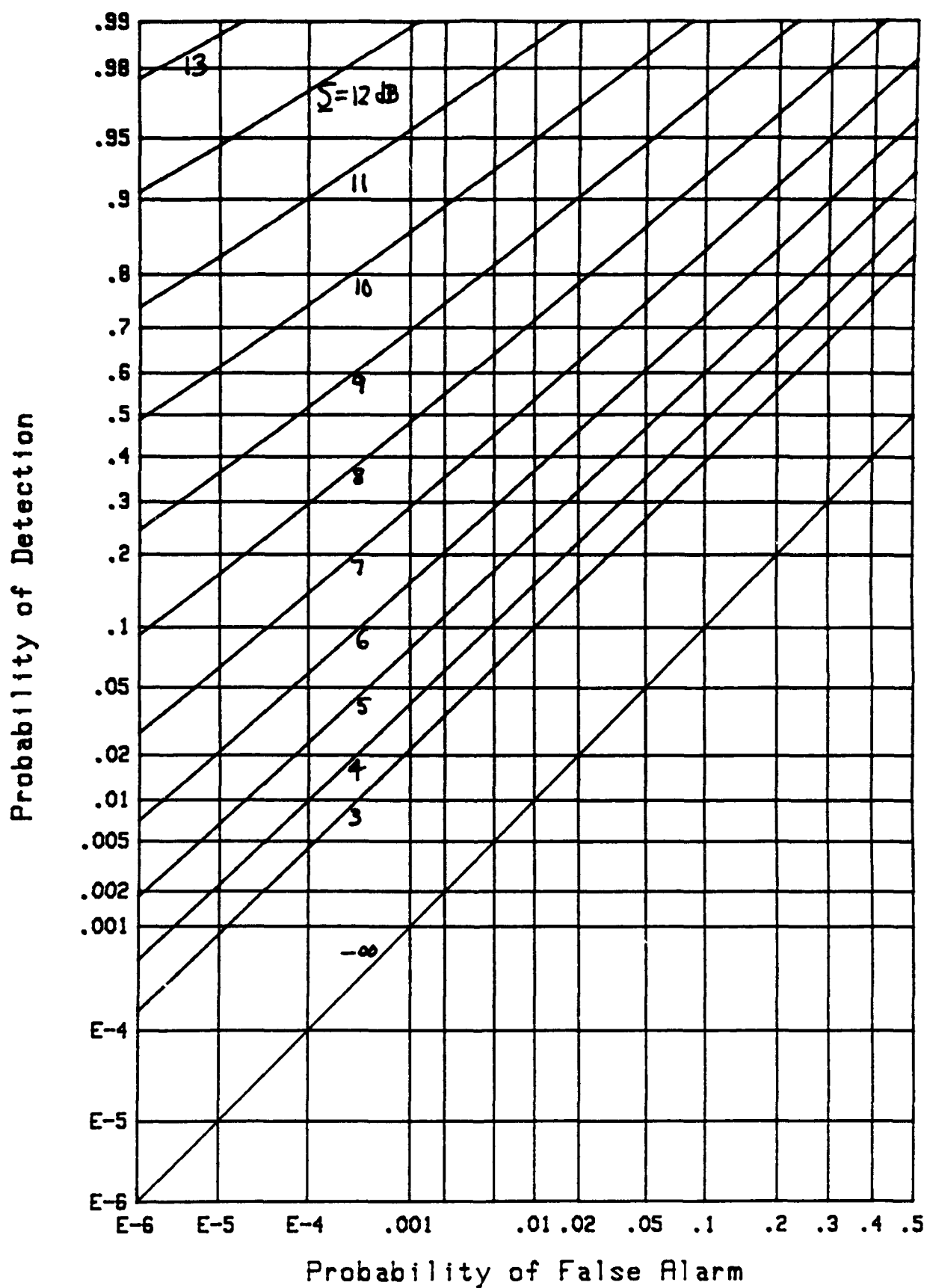
Figure 52. Energy Detector ROC for N=1024, M=16
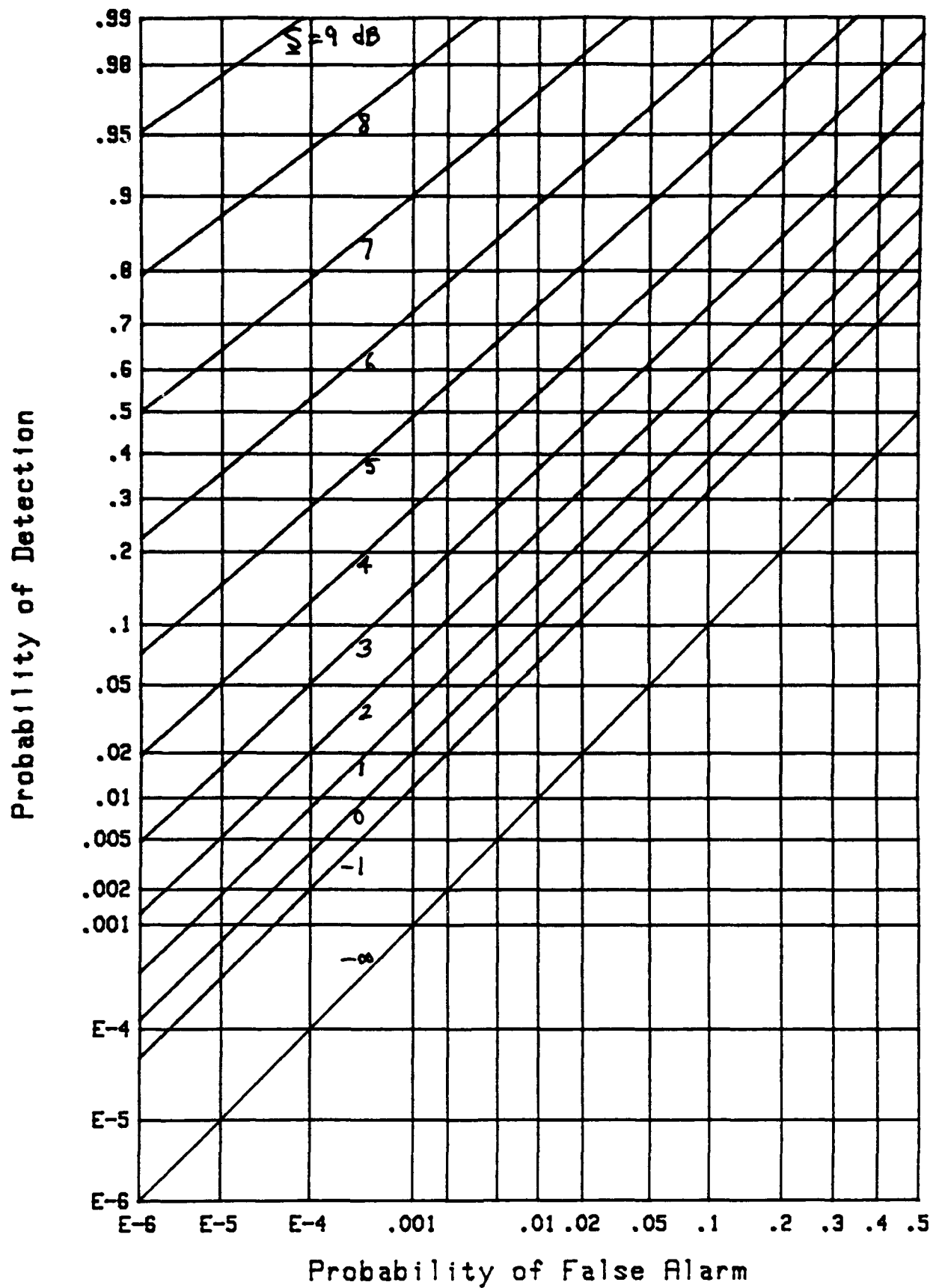
Figure 53. Energy Detector ROC for N=1024, M=32
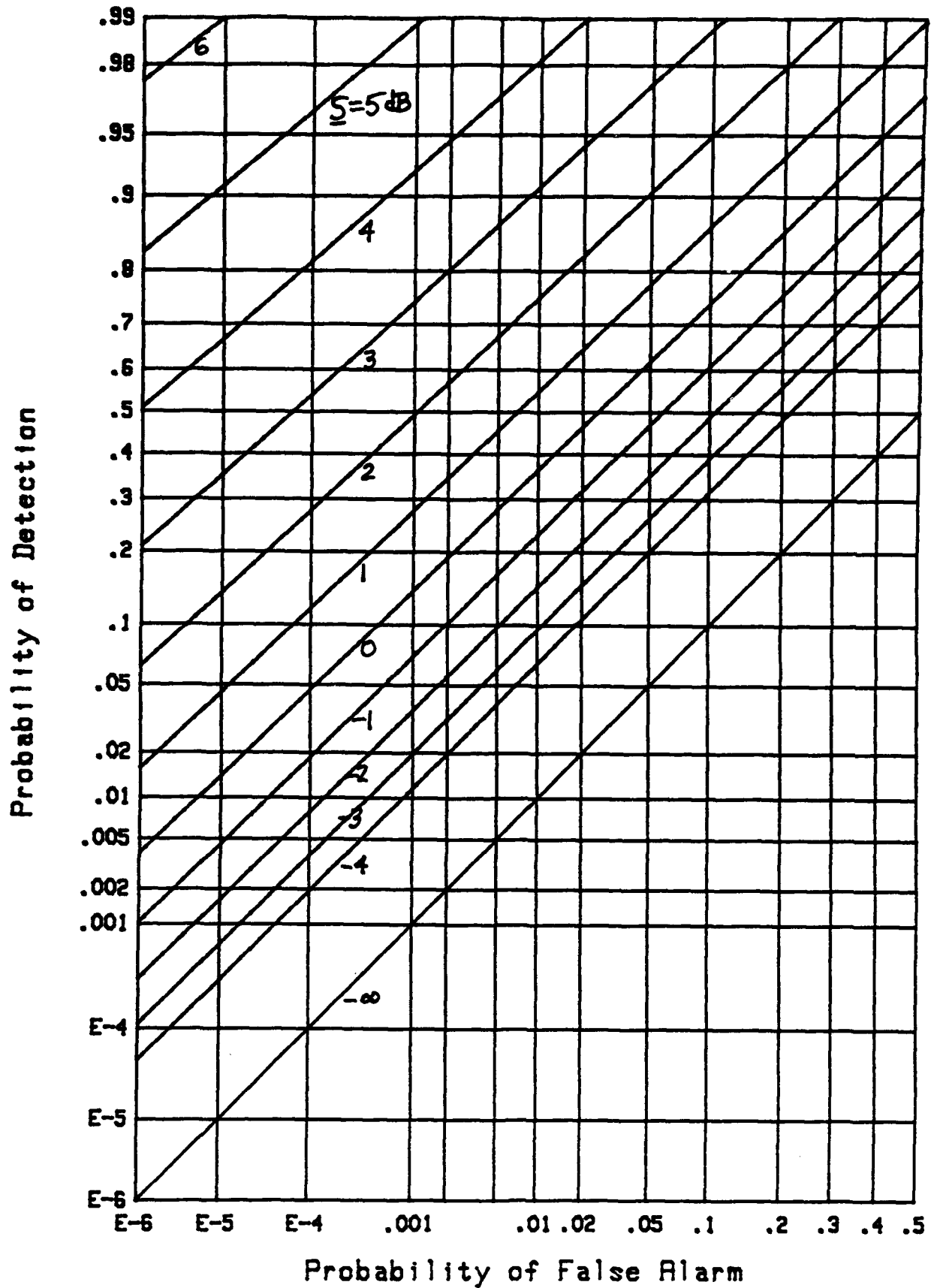
Figure 54. Energy Detector ROC for N=1024, M=64
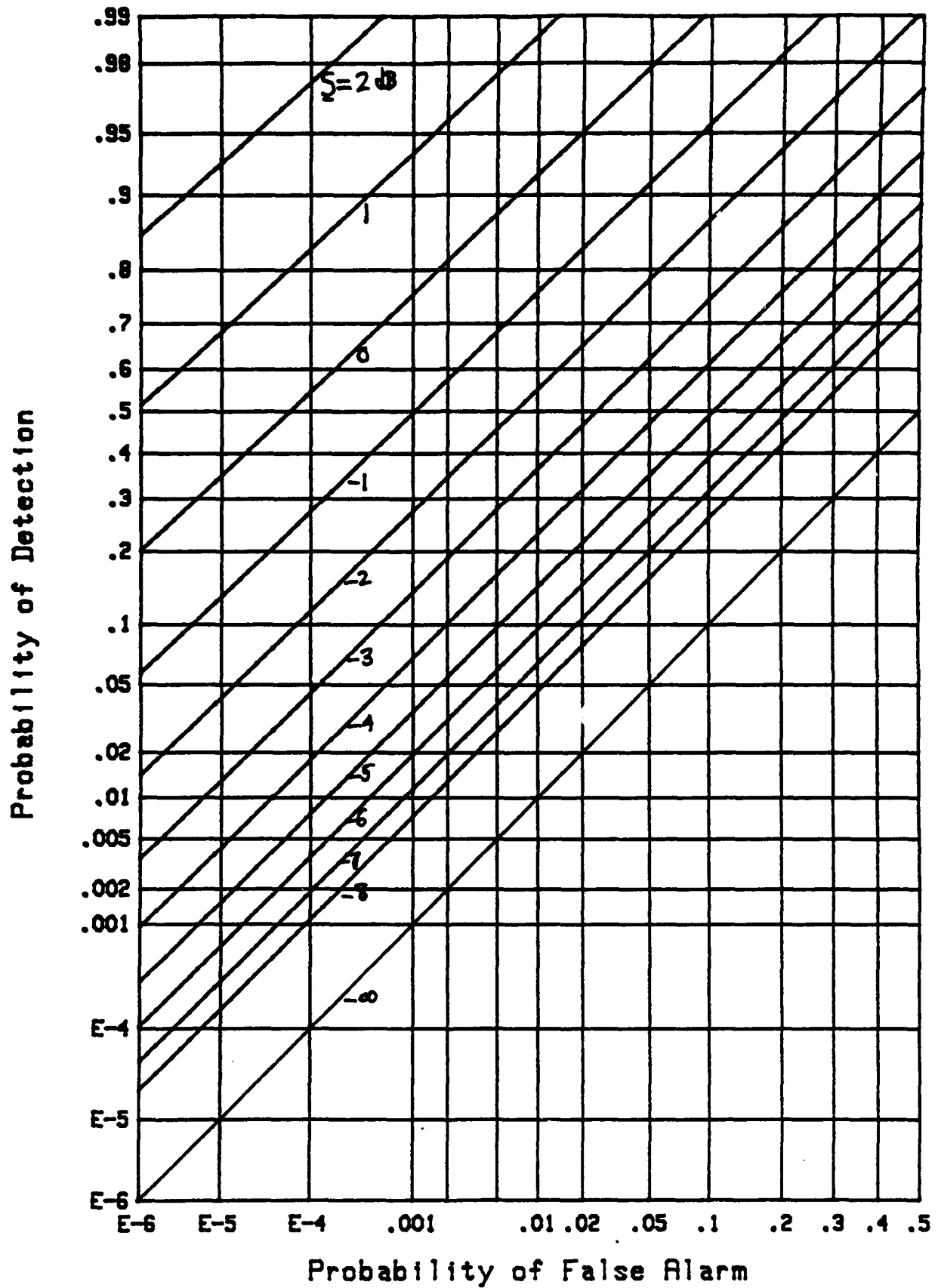
Figure 55. Energy Detector ROC for N=1024, M=128
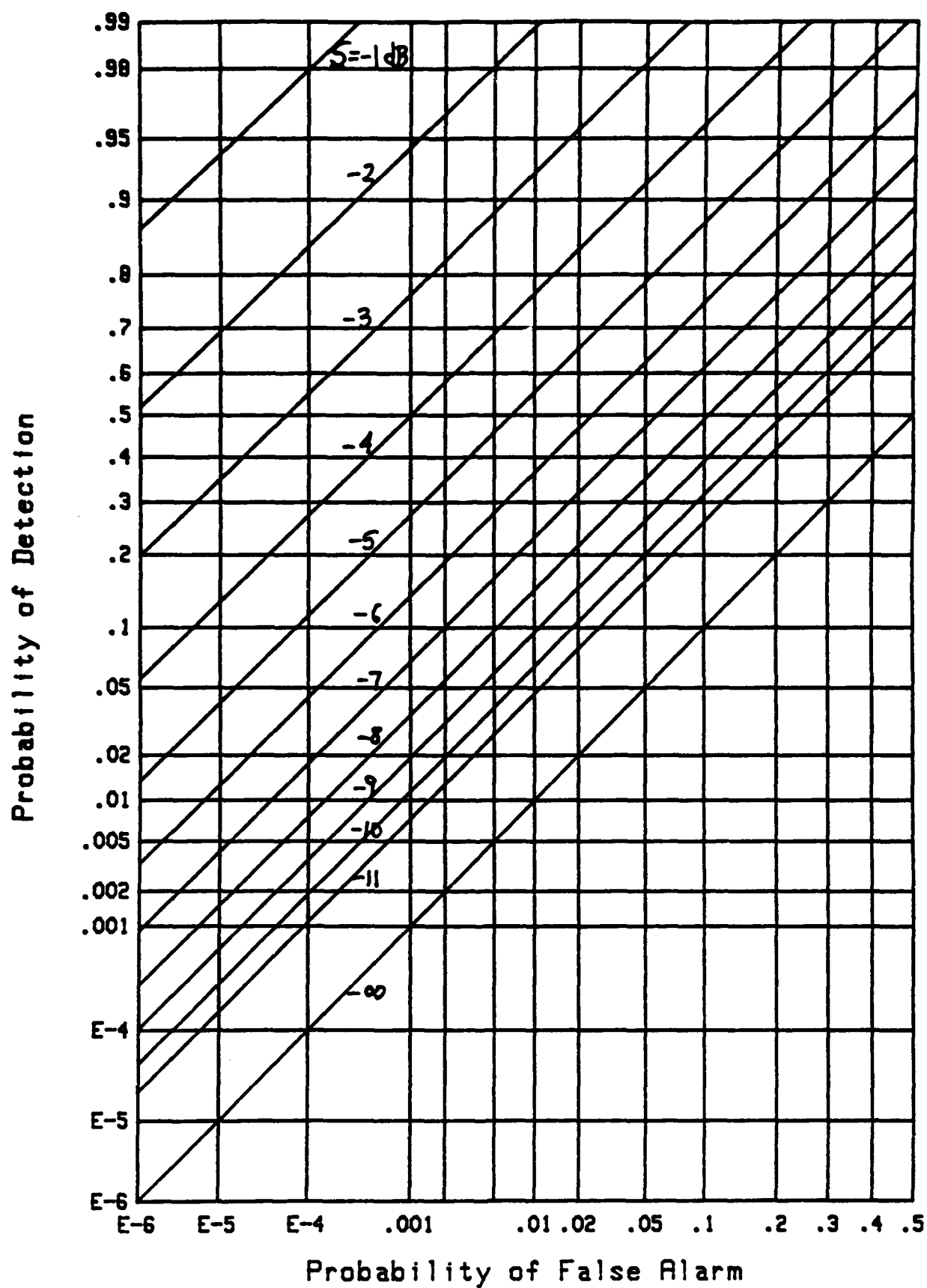
Figure 56. Energy Detector ROC for N=1024, M=256
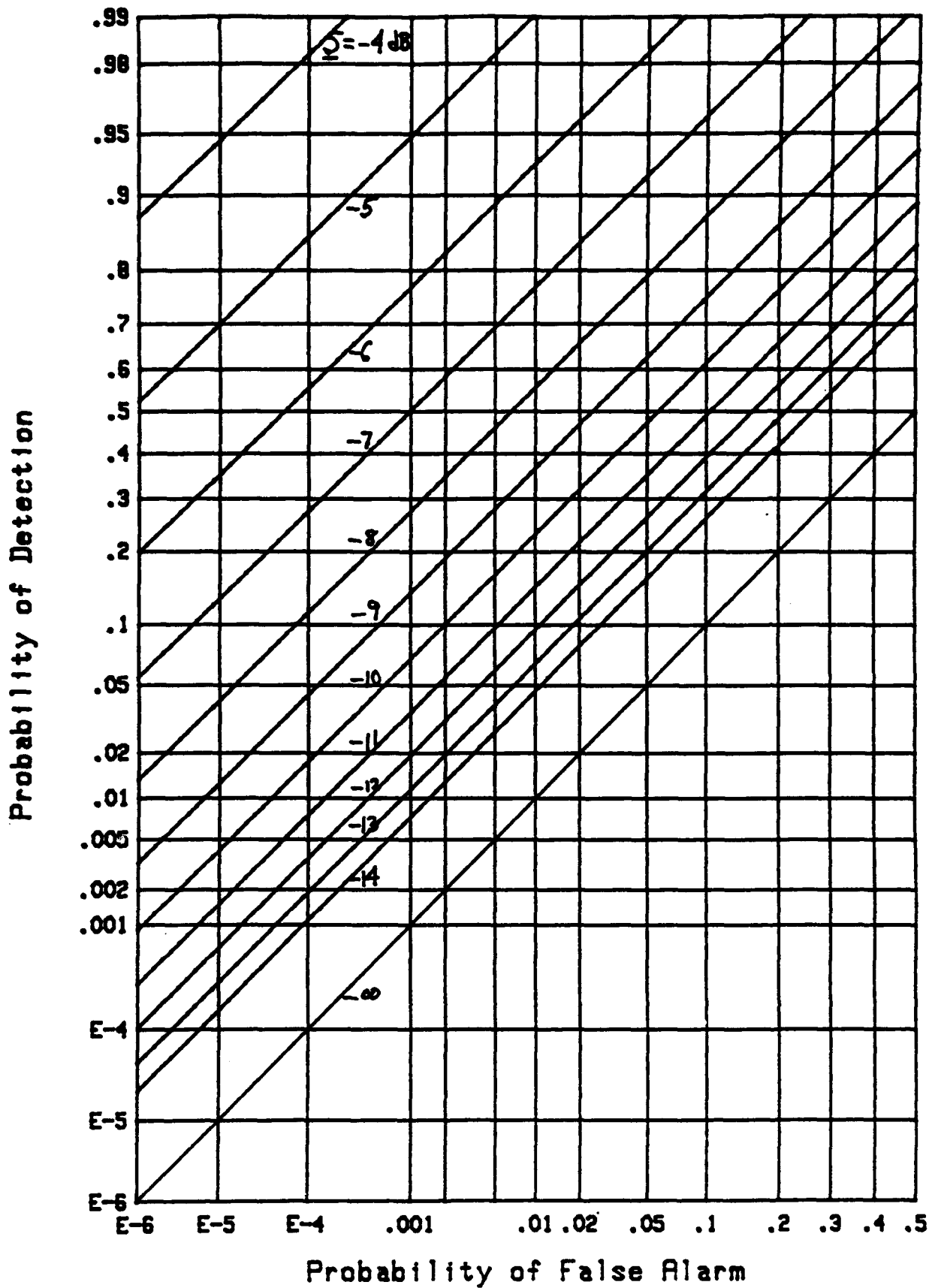
Figure 57. Energy Detector ROC for N=1024, M=512
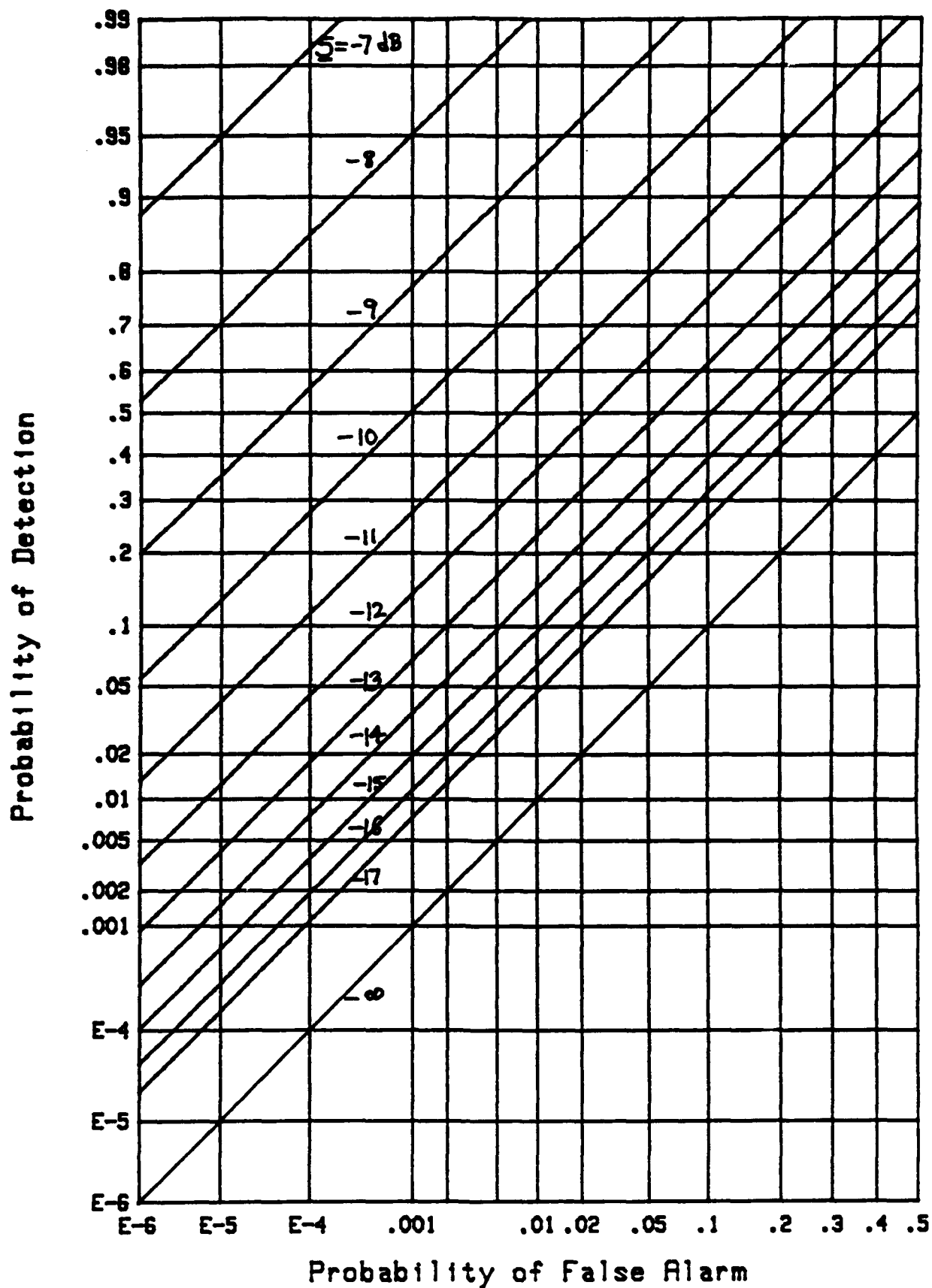
Figure 58. Energy Detector ROC for N=1024, M=1024

EXTENSION TO UNEQUAL SIGNAL POWERS

All the earlier results presumed that the M signal bins contained exactly the same signal power $\underline{S}$. In practice, the values of the signal powers in the various bins will be different. Instead of having to determine receiver operating characteristics for each particular set of unequal signal strengths $\{\underline{S}_m\}$, we will now determine effective values to replace $\underline{S}$ and/or M, that can be used with the existing results.

Let the signal power in the m-th signal bin be $\underline{S}_m$ for $1 \leq m \leq M$. We first consider an equivalent or effective signal power $\underline{S}_e$ to be used in place of the set $\{\underline{S}_m\}$. The number of signal bins is kept at value M in this particular approach.

An alternative approach, where an effective number, M_e, of signal bins is defined instead, while the signal power set $\{\underline{S}_m\}$ is replaced by its peak value, is considered next. Finally, a two-parameter extraction procedure, where both $\underline{S}_e$ and M_e are simultaneously determined, is presented.

MATCHING OF MEAN OUTPUTS

For breakpoint nonlinearity $g(x) = x - 1 - \ln(x)$ for $x > x_o$, define the following mean function, with $\underline{a} = 1/(1 + \underline{S})$,

$$\mu(\underline{S}, x_o) = \int_{x_o}^{\infty} du \; \underline{a} \; \exp(-\underline{a}u) \; [u - 1 - \ln(u)] =$$

$$= \exp(-\underline{a}x_o) \left(\frac{1}{\underline{a}} - 1 + x_o - \ln(x_o)\right) - E_1(\underline{a}x_o) \; . \tag{63}$$

A plot of this function is given in figure 59. The asymptotic behavior for large $\underline{S}$ is approximately linear, being given by [8; 5.1.11]

$$\mu(\underline{S}, x_o) \sim \underline{S} - \ln(1 + \underline{S}) + \gamma - x_o\left(\frac{1}{2}x_o - \ln(x_o)\right)/\underline{S} \quad \text{as} \quad \underline{S} \to \infty \; . \tag{64}$$

Without loss of generality, assume that the signal is in bins [1,M]. The mean of the output y_m of nonlinearity $g(x)$, for the m-th signal input, is $\mu(\underline{S}_m, x_o)$. The corresponding mean of summer output z is exactly

$$\mu_z = \sum_{m=1}^{M} \mu(\underline{S}_m, x_o) + (N - M) \; \mu(0, x_o) \; . \tag{65}$$

On the other hand, if all the signal powers, $\{\underline{S}_m\}$, are replaced by an effective signal power value, $\underline{S}_e$, over all the M signal bins, we obtain mean value

$$\mu_z = M \; \mu(\underline{S}_e, x_o) + (N - M) \; \mu(0, x_o) \; . \tag{66}$$

If we match these two expressions in (66) and (65) for the mean

output, we obtain the following equation that $\underline{S}_e$ must satisfy:

$$\mu(\underline{S}_e, x_o) = \frac{1}{M} \sum_{m=1}^{M} \mu(\underline{S}_m, x_o) . \tag{67}$$

Once the right-hand side of (67) has been computed from the specified M, $\{\underline{S}_m\}$, and x_o, the required $\underline{S}_e$ to realize equality in (67) can be found from figure 59. The use of closed form (63) makes the numerical summation in (67) a simple computer task, once a routine for exponential integral $E_1(z)$ is available.

If all $\{\underline{S}_m\}$ are equal to $\underline{S}$, then (67) yields $\underline{S}_e = \underline{S}$, as expected. However, in general, the quadratic behavior of mean function $\mu(\underline{S}, x_o)$ near $\underline{S} = 0$ indicates that the smaller signal powers $\underline{S}_m$ are suppressed relatively, the more so for larger x_o. The example M = 4, $\underline{S}_m = m$ for $1 \leq m \leq M$, yields effective signal powers $\underline{S}_e = 2.554, 2.557, 2.586, 2.638, 2.700, 2.763$ for $x_o = 1, 3, 5, 7, 9, 11$, respectively.

This replacement approach of $\{\underline{S}_m\}$ by $\underline{S}_e$ takes account of the specific nonlinearity g(x), the breakpoint value x_o, and all of the individual signal powers $\{\underline{S}_m\}$ for $1 \leq m \leq M$. However, it does require the solution of (67) for argument $\underline{S}_e$ which leads to equality with the computed right-hand side.

Instead of keeping M fixed throughout this replacement, we could instead define an effective number, M_e, to be used with the replacement of the set of signal powers, $\{\underline{S}_m\}$, by its peak value $\underline{S}_p = \max\{\underline{S}_m\}$. In this latter case, the first term on the right-hand side of (65) becomes $M_e \mu(\underline{S}_p, x_o)$. When we equate this expression to the corresponding term in (65), we have an explicit

result for the effective number M_e of signal bins as

$$M_e = \sum_{m=1}^{M} \frac{\mu(\underline{S}_m, x_o)}{\mu(\underline{S}_p, x_o)} \, . \qquad (68)$$

This result, in conjunction with expression (63), allows for rapid and simple evaluation of M_e, once x_o and set $\{\underline{S}_m\}$ are specified. For the same numerical example above, namely M = 4, $\underline{S}_m$ = m for $1 \le m \le M$, we find $\underline{S}_p$ = 4 and M_e = 2.409, 2.343, 2.184, 2.020, 1.876, 1.756 for x_o = 1, 3, 5, 7, 9, 11, respectively.

MATCHING OF FIRST TWO MOMENTS

We now derive an effective number, M_e, of signal bins, in addition to an effective signal power, $\underline{S}_e$, for the set $\{\underline{S}_m\}$ for $1 \le m \le M$. These effective parameters would then be used in place of M and $\underline{S}$ in the results of previous sections, and would be expected to have wider applicability than using just $\underline{S}_e$.

For nonlinearity g(x) = x - 1 - ln(x) for $x > x_o$, define the following functions:

$$\sigma^2(\underline{S}, x_o) = \int_{x_o}^{\infty} du \, \underline{a} \, \exp(-\underline{a}u) \, [u - 1 - \ln(u)]^2 - \mu^2(\underline{S}, x_o) \, , \qquad (69)$$

$$R(\underline{S}, x_o) = \frac{\sigma^2(\underline{S}, x_o) - \sigma^2(0, x_o)}{\mu(\underline{S}, x_o) - \mu(0, x_o)} \, . \qquad (70)$$

Plots of the three functions in (70) are given below, namely the denominator, the numerator, and the ratio $R(\underline{S}, x_o)$, in figures 60, 61, and 62, respectively. (If desired, the integral in (69) can be evaluated by use of the results in appendix F.)

The mean and variance of the output, y_m, of nonlinearity, $g(x)$, for the m-th signal input, are $\mu(\underline{S}_m, x_o)$ and $\sigma^2(\underline{S}_m, x_o)$, respectively. The corresponding first two cumulants of summer output z are

$$\mu_z = \sum_{m=1}^{M} \mu(\underline{S}_m, x_o) + (N - M)\, \mu(0, x_o) =$$

$$= \sum_{m=1}^{M} \left[\mu(\underline{S}_m, x_o) - \mu(0, x_o) \right] + N\, \mu(0, x_o) , \tag{71}$$

$$\sigma_z^2 = \sum_{m=1}^{M} \sigma^2(\underline{S}_m, x_o) + (N - M)\, \sigma^2(0, x_o) =$$

$$= \sum_{m=1}^{M} \left[\sigma^2(\underline{S}_m, x_o) - \sigma^2(0, x_o) \right] + N\, \sigma^2(0, x_o) , \tag{72}$$

respectively.

On the other hand, if all the signal powers, $\{\underline{S}_m\}$, are replaced by an effective value, $\underline{S}_e$, for an effective number, M_e, of signal bins, we obtain

$$\mu_z = M_e \left[\mu(\underline{S}_e, x_o) - \mu(0, x_o) \right] + N\, \mu(0, x_o) , \tag{73}$$

$$\sigma_z^2 = M_e \left[\sigma^2(\underline{S}_e, x_o) - \sigma^2(0, x_o) \right] + N\, \sigma^2(0, x_o) . \tag{74}$$

Equating (73) to (71), and (74) to (72), it follows that we must

satisfy

$$R(\underline{S}_e, x_o) = \frac{\sum_{m=1}^{M} \left(\sigma^2(\underline{S}_m, x_o) - \sigma^2(0, x_o) \right)}{\sum_{m=1}^{M} \left(\mu(\underline{S}_m, x_o) - \mu(0, x_o) \right)} . \tag{75}$$

Since the value of the right-hand side of (75) is known, once M, $\{\underline{S}_m\}$, and x_o are specified, this is a transcendental equation for effective signal power $\underline{S}_e$. That is, $\underline{S}$ in (70) is varied until the value in (75) is realized; this can be easily done by use of figure 62. Then, effective number M_e follows according to

$$M_e = \frac{\sum_{m=1}^{M} \left(\mu(\underline{S}_m, x_o) - \mu(0, x_o) \right)}{\mu(\underline{S}_e, x_o) - \mu(0, x_o)} . \tag{76}$$

It should be noted that this approach accounts for the specific nonlinearity $g(x)$, the breakpoint value x_o, and all of the individual signal powers $\{\underline{S}_m\}$ for $1 \le m \le M$, through the quantities in (75), which in turn utilize (63) and (69). This approach does not employ an ad hoc definition of effective values; however, it does require a numerical solution to the transcendental equation (75) for $\underline{S}_e$, or the use of figure 62.

The number of search bins N is not altered by any of these replacements, and need not be changed in utilizing the earlier plots. Rather, the values of M and/or $\underline{S}$ to be employed in using the previously plotted receiver operating characteristics are those given by M_e and/or $\underline{S}_e$ here, respectively.
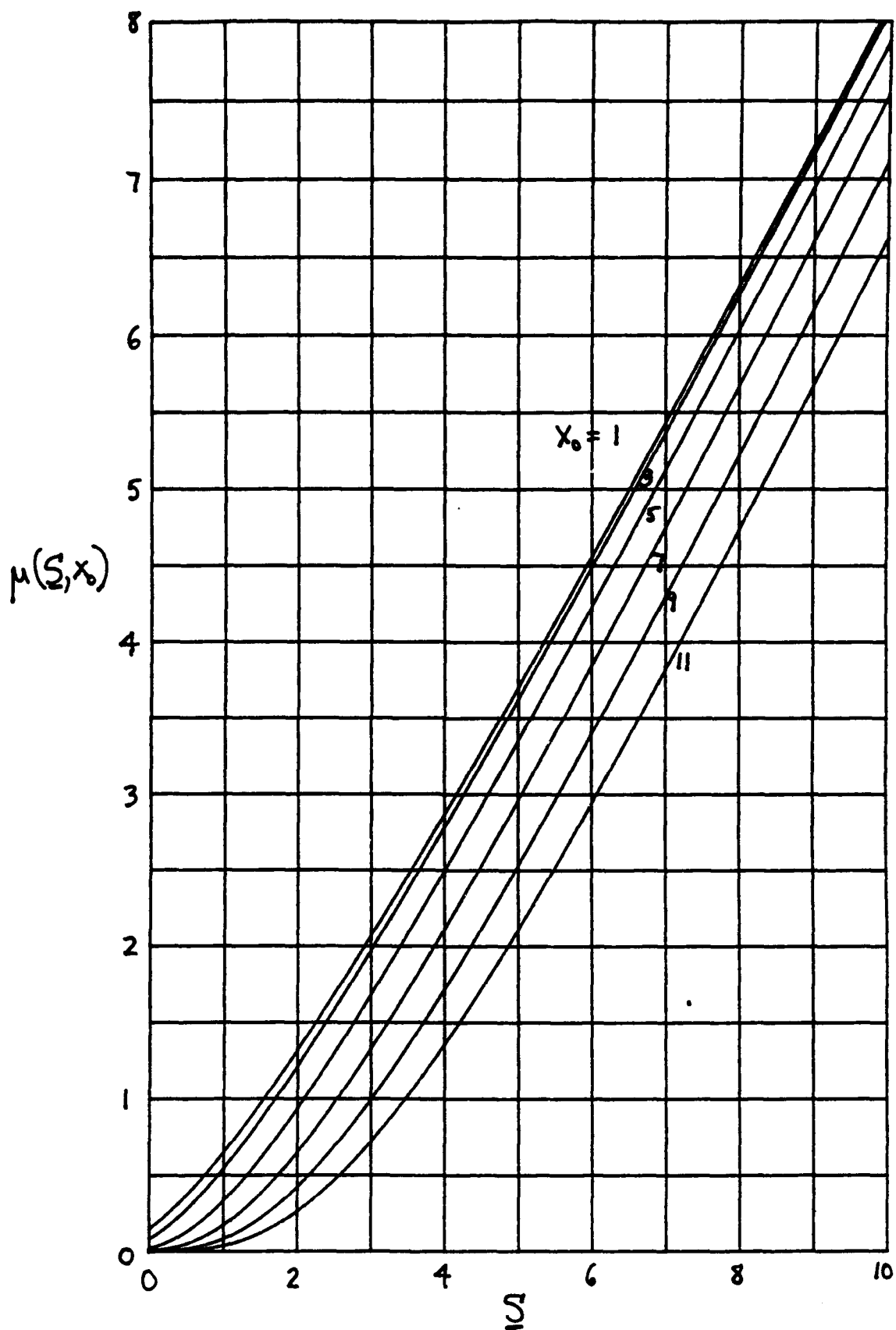
Figure 59.   Mean $\mu(\underline{S}, x_0)$ versus Signal Power $\underline{S}$
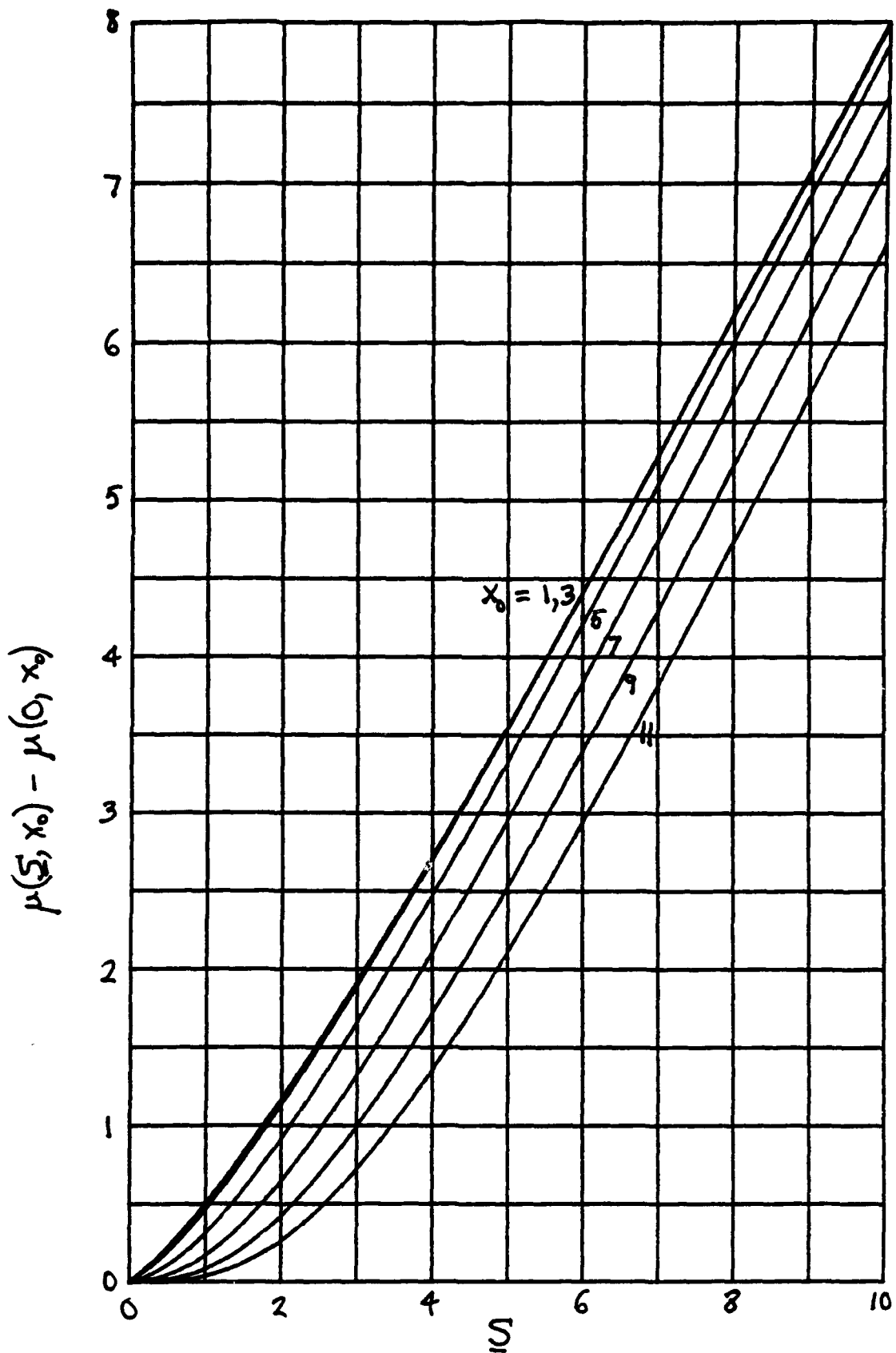
Figure 60. Difference of Means versus Signal Power $\underline{S}$
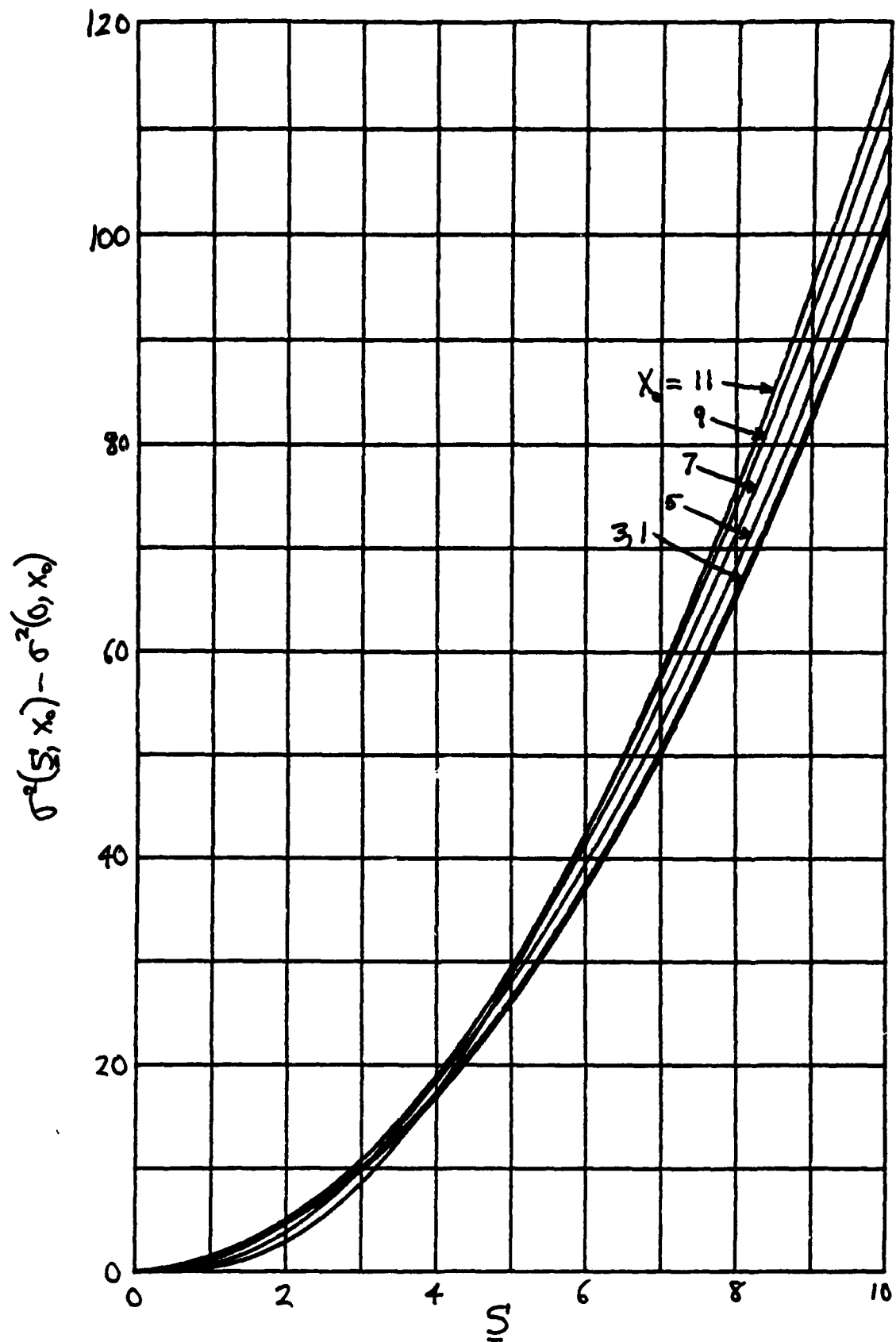
Figure 61. Difference of Variances versus Signal Power $\underline{S}$
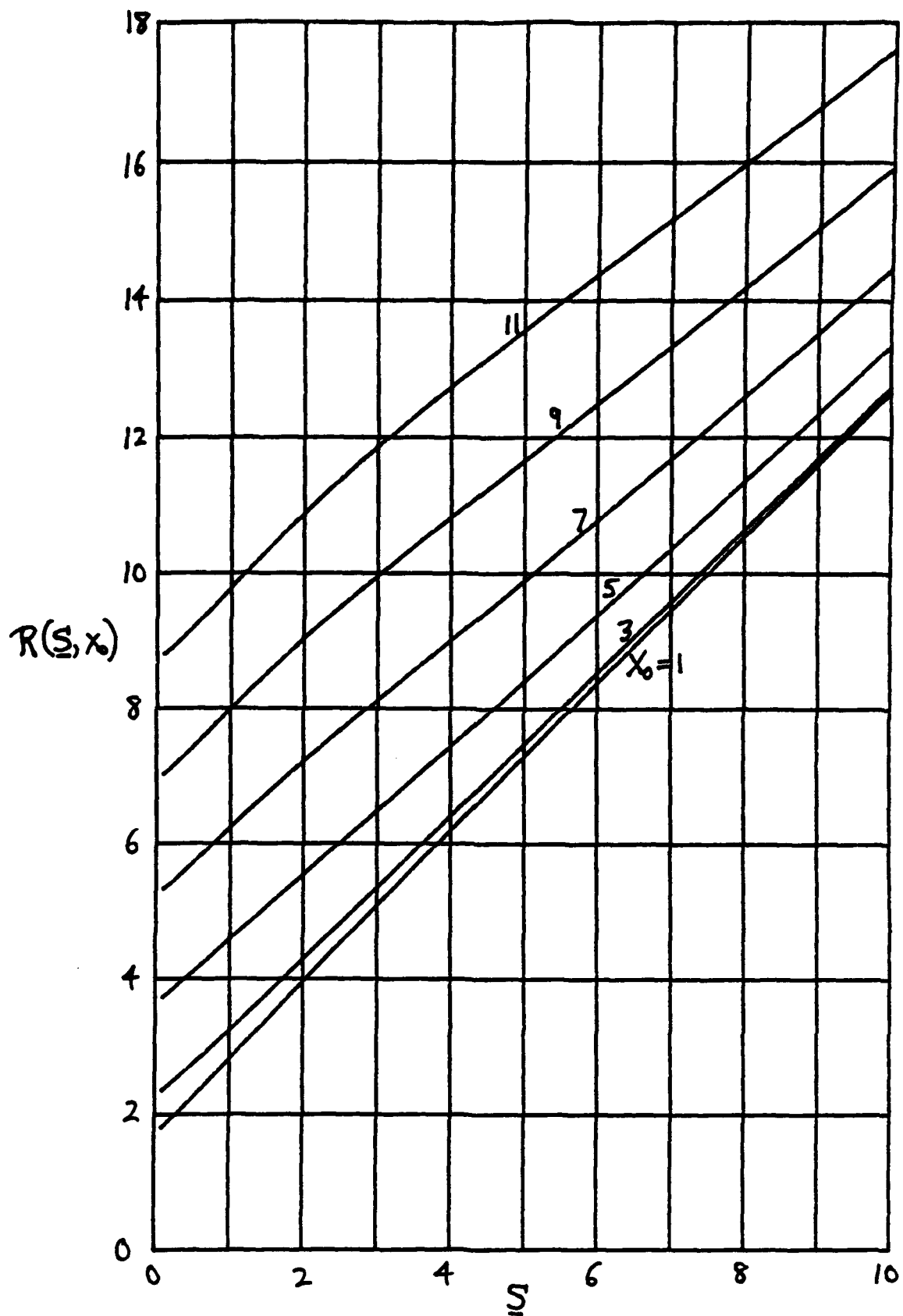
Figure 62.   Ratio R($\underline{S}$,x_o) versus Signal Power $\underline{S}$

SUMMARY

The MGLR processor has been analyzed and numerically evaluated in terms of its false alarm and detection probabilities P_f, P_d, over a wide range of parameter values. In particular, plots of P_f versus threshold v for search sizes N = 1024, 512, 256, 128, 64 and breakpoint x_o = 1(1)11 have been presented. These numerical results allow for accurate determination of required threshold settings in order to realize specified false alarm probability values.

In addition, receiver operating characteristics, P_d versus P_f, for N = 1024, signal set sizes M = 8, 16, 32, 64, 128, 256, and breakpoint values x_o = 1, 3, 5, 7, 9, 11 have been plotted, with the signal power $\underline{S}$ varied over a range sufficient to cover the practical range of performance values. All of these results have been checked by simulation; the discrepancy is usually less then 0.1 dB in terms of required signal power.

The energy detector has been analyzed and evaluated exactly, and can serve as a basis of comparison with the MGLR processor. Receiver operating characteristics for N = 1024 and M = 8, 16, 32, 64, 128, 256, 512, 1024 have been plotted. The corresponding plot of P_f versus threshold v is also given.

The analysis of performance has been accomplished by a combination of two methods. A piecewise-linear approximation works best for large breakpoint values, x_o, while a fourth-order moment fitting procedure is more appropriate for small x_o values. The piecewise-linear approach can actually be used for small

breakpoint values, such as $x_o = 3$; however, the time of execution is sometimes excessive, and there is the danger of loss of significance, due to the large alternating terms encountered in the series expansions. Accordingly, the fourth-order moment fit has been used in the region of small breakpoint values x_o. An alternative is investigated in appendix G.

One possible objection to use of these results for the performance of the MGLR processor, in practice, is that M will often not be known, meaning that the best breakpoint x_o cannot be selected. This raises the question of how to process, in general, when M is unknown. Also, the use of large breakpoint values, x_o, (as suggested here for small values of M) causes us to reject some very strong signal power estimates, which is unsatisfactory and counter intuitive. In fact, the question of whether we should employ a breakpoint at all is a meaningful one that requires further investigation.

It is worthwhile to derive the true generalized likelihood ratio tests for the situations where M is unknown, as well as when M is known to be less than N, but the signal occupancy pattern is unknown. Also, if partial information about the signal structure is available, like its bandwidth, how should this information be incorporated in the generalized likelihood ratio test? Comparisons with the optimum likelihood ratio processors or near-optimum processors in each case would be very worthwhile and should be pursued. This is the subject of a current investigation which will appear in a NUWC technical report [3].

APPENDIX A. MODIFIED GENERALIZED LIKELIHOOD RATIO PROCESSOR

In this appendix, we will derive the form of the modified generalized likelihood ratio processor. Since the actual signal power per bin, $\underline{S}_n$, is unknown, we hypothesize parameter value S_n and estimate it from the observation set (random variables) $\{x_n\}$. We also define the signal power parameter $a_n = 1/(1 + S_n)$. Since we will only allow signal power $S_n \geq 0$, then we must have $a_n \leq 1$.

According to (2), the joint probability density function of observation $\{x_n\}$ under hypothesis H_1 is, for <u>hypothesized</u> parameter values $\{a_n\}$,

$$q_1(u_1, \ldots, u_N) = \prod_{n=1}^{N} \{a_n \exp(-a_n u_n)\} \quad \text{for } u_n > 0 , \qquad \text{(A-1)}$$

where we have allowed the possibility of signal being present in all N search bins. This is tantamount to assuming M = N, for the time being; the method by which the estimated number of signal bins is reduced below the value N will be indicated below.

For observation $\{x_n\}$, the density in (A-1) takes on value

$$q_1(x_1, \ldots, x_N) = \prod_{n=1}^{N} \{a_n \exp(-a_n x_n)\} . \qquad \text{(A-2)}$$

This quantity is to be maximized by choice of all $\{a_n\}$. It can be seen that the best choice of each parameter is (random variable) $a_n = \min\{1, 1/x_n\}$, where we have accounted for the constraint $a_n \leq 1$. This translates into tne signal power estimate $S_n = \max\{0, x_n - 1\}$. However, since values of random

variable x_n near 1 are typical (even for the noise-alone case H_0 where $E\{x_n\}$ is 1), we will reject signal power estimates which are below some minimum acceptable level, S_o. Thus, our __modified__ signal power estimate is

$$S_n = \begin{Bmatrix} x_n - 1 & \text{for } x_n - 1 \geq S_o \\ 0 & \text{otherwise} \end{Bmatrix} ; \quad S_o \geq 0 . \qquad \text{(A-3)}$$

This is equivalent to the modification

$$a_n = \begin{Bmatrix} 1/x_n & \text{for } x_n \geq x_o \\ 1 & \text{otherwise} \end{Bmatrix} ; \quad x_o = 1 + S_o \geq 1 . \qquad \text{(A-4)}$$

Now, let L be the set of n values in (A-4) for which $x_n \geq x_o$. Then, upon maximization, the n-th term in (A-2) becomes $1/(x_n e)$ for $n \, \varepsilon \, L$, and $\exp(-x_n)$ otherwise. The generalized likelihood ratio is then given by

$$\text{GLR} = \frac{\max q_1}{q_o} = \prod_{n \varepsilon L} \left(\frac{1}{x_n} \exp(x_n - 1) \right) = \prod_{n \varepsilon L} \{ \exp[x_n - 1 - \ln(x_n)] \} =$$

$$= \exp \left(\sum_{n \varepsilon L} [x_n - 1 - \ln(x_n)] \right) = \exp \left(\sum_{n=1}^{N} g(x_n) \right) , \qquad \text{(A-5)}$$

where nonlinearity $g(x)$ is defined as

$$g(x) = \begin{Bmatrix} x - 1 - \ln(x) & \text{for } x \geq x_o \\ 0 & \text{otherwise} \end{Bmatrix} . \qquad \text{(A-6)}$$

This nonlinearity has a breakpoint at $x = x_o$, which is never less than 1; that is, from (A-4), $x_o = 1 + S_o \geq 1$, since minimum acceptable signal power level S_o is never negative.

Comparison of the generalized likelihood ratio in (A-5) with a threshold is equivalent to the test

$$z = \sum_{n=1}^{N} g(x_n) \underset{<}{>} v . \qquad (A-7)$$

Since breakpoint x_o of nonlinearity $g(x)$ rejects any input values x_n which are less than x_o, the number of nonzero contributors to output z in (A-7) is less than N. In fact, if x_o is significantly larger than 1, then very few terms will contribute to the output z in (A-7).

The selection of breakpoint x_o in this MGLR processor is its way of restricting the estimated number of signal bins to be less than N. However, unfortunately, there is no simple way of deciding on the best value of breakpoint x_o for each hypothesized value of M. We must conduct a complete analysis of performance of processor (A-7) in terms of the false alarm and detection probabilities in order that the best x_o for each specified M can be determined. However, this still does not address the problem of what to do when M is unknown in practice. This is a fundamental limitation of the MGLR processor.

APPENDIX B. PIECEWISE-LINEAR FIT TO NONLINEARITY g(x)

Nonlinearity $g(x)$ is zero for $x < x_o$, and otherwise arbitrary for $x \geq x_o$, where x_o is called the breakpoint. Function $g(x)$ is to be approximated by a piecewise-linear fit $h(x)$, which is also zero for $x < x_o$, but which is linear for $x \geq x_o$. In particular, let

$$h(x) = c + b(x - x_o) \text{ for } x \geq x_o , \qquad \text{(B-1)}$$

where c is the ordinate of $h(x)$ at breakpoint x_o, and b is the slope of $h(x)$ for $x > x_o$. A variety of choices for b and c are possible and will be developed below.

The input to nonlinearity $g(x)$ is a random variable x, with probability density function $p_x(u)$. The (random) error between the outputs of the two devices is

$$e = g(x) - h(x) = g(x) - c - b(x - x_o) \text{ for } x \geq x_o , \qquad \text{(B-2)}$$

and $e = 0$ for $x < x_o$. Initially, the constants b and c in fit $h(x)$ will be chosen so as to minimize the mean squared error

$$E = \overline{e^2} = \overline{\left(g(x) - h(x)\right)^2} = \int du \, p_x(u) \left(g(u) - h(u)\right)^2 =$$

$$= \int_{x_o}^{\infty} du \, p_x(u) \left(g(u) - c - b(u - x_o)\right)^2 ; \qquad \text{(B-3)}$$

this is called FIT-2, because two parameters are optimized.

When we set the two partial derivatives of E to zero, the best values of b and c are found to be given by

$$\tilde{b} = \frac{L_0 R_1 - L_1 R_0}{L_0 L_2 - L_1^2} , \quad \tilde{c} = \frac{R_0 L_2 - R_1 L_1}{L_0 L_2 - L_1^2} , \quad \text{(B-4)}$$

where

$$L_n = \int\limits_{x_0}^{\infty} du \, p_x(u) \, (u - x_0)^n ,$$

$$R_n = \int\limits_{x_0}^{\infty} du \, p_x(u) \, g(u) \, (u - x_0)^n . \quad \text{(B-5)}$$

In the special case where probability density function $p_x(u)$ is exponential with signal power parameter $\underline{a}$, namely

$$p_x(u) = \underline{a} \exp(-\underline{a}u) \quad \text{for } u > 0 , \quad \underline{a} = \frac{1}{1 + \underline{S}} , \quad \text{(B-6)}$$

the expression for L_n simplifies (for $x_0 \geq 0$) to

$$L_n = n! \, \exp(-\underline{a}x_0)/\underline{a}^n . \quad \text{(B-7)}$$

Correspondingly, the optimum parameter values simplify to

$$\tilde{b} = \underline{a}^2 \int\limits_{0}^{\infty} dt \, \exp(-\underline{a}t) \, (\underline{a}t - 1) \, g(x_0 + t) ,$$

$$\tilde{c} = \underline{a} \int\limits_{0}^{\infty} dt \, \exp(-\underline{a}t) \, (2 - \underline{a}t) \, g(x_0 + t) . \quad \text{(B-8)}$$

These optimum values, $\tilde{b}$ and $\tilde{c}$, obviously depend on both the breakpoint x_0 as well as the probability density signal power parameter $\underline{a}$. For signal power $\underline{S} = 0$, then $\underline{a} = 1$, and $\tilde{b}$, $\tilde{c}$ are denoted by $\tilde{b}_0$, $\tilde{c}_0$, which depend only on x_0.

There are cases where it is desirable to fix ordinate c, a priori, and to minimize mean square error E solely by choice of slope b; this is called FIT-1. For example, ordinate $\bar{c}$ above can turn out to be negative, even though original nonlinearity g(x) is always positive for $x \geq x_o$. If this is undesirable, c could be set to zero, for example, and the best slope b selected. When we set the derivative of mean square error E (with respect to b) equal to zero, the optimum slope (for fixed $c = \bar{c}$) is given by

$$\bar{b} = \int_{x_o}^{\infty} du\, p_x(u)\, [g(u) - \bar{c}]\, (u - x_o) \Big/ \int_{x_o}^{\infty} du\, p_x(u)\, (u - x_o)^2 \, . \quad \text{(B-9)}$$

In the special case of an exponential probability density function $p_x(u)$, as in (B-6) above, there follows (for $x_o \geq 0$)

$$\bar{b} = \frac{1}{2}\, \underline{a}^3 \int_0^{\infty} dt\, \exp(-\underline{a}t)\, t\, [g(x_o + t) - \bar{c}] \, . \quad \text{(B-10)}$$

This optimum value, $\bar{b}$, depends on x_o, $\underline{a}$, and $\bar{c}$. For signal power $\underline{S} = 0$, then $\underline{a} = 1$, and we denote $\bar{c}$ by $\bar{c}_o$, and $\bar{b}$ by $\bar{b}_o$ which depends on x_o and $\bar{c}_o$.

Finally, the parameters b and c in fit h(x) can be chosen arbitrarily, with no specific optimization in mind; this case, where zero parameters are optimized, is called FIT-0. For example, we might take $\underline{c} = g(x_o)$, the initial ordinate, and take $\underline{b} = g'(x_o)$, the initial slope; this corresponds to the tangent line to g(x) at x_o. (This particular choice takes no account of the signal power $\underline{S}$.) Generally, $\underline{b}$ and $\underline{c}$ can depend on parameter $\underline{a}$ as well as x_o. When $\underline{S} = 0$, then $\underline{a} = 1$, and we denote $\underline{b}$ and $\underline{c}$

by $\underline{b}_0$ and $\underline{c}_0$, respectively, which depend only on x_0. Some of the coefficients, c and b, are tabulated below for the various fit procedures.

The mean square error E for FIT-2 is always smaller than those for the other two fits. However, there is the possibility of a negative ordinate $\tilde{c}$ or $\tilde{c}_0$, which may or may not be damaging. On the other hand, FIT-1 may be poor for large signal powers $\underline{S}$, where large values of random variable x are frequently encountered. Finally, FIT-0 can be very unsatisfactory, (as for example by using the tangent,) since the output of $h(x)$ might always underestimate the true nonlinearity $g(x)$; this could be especially damaging for large $\underline{S}$.

One way around this shortcoming of the approximation $h(x)$ used in (B-1) is to use several breakpoints in approximating $g(x)$ with piecewise-linear fits. One possible problem with this latter approach is the tractability of the Fourier transform of input probability density function $p_x(u)$ over an arbitrary finite segment. For an exponential probability density function, this is not a problem. However, a more significant problem will arise in determining the dominant asymptotic decay of the characteristic function of the output of nonlinearity $h(x)$, so that it can be subtracted out for rapid convergence of the FFT required for numerical evaluation of the exceedance distribution function. This procedure has already been carried out for a nonlinearity with a single breakpoint. Although tedious, this is a workable approach for accurately approximating the detection characteristics of any nonlinear memoryless device.

OPTIMUM COEFFICIENT $\bar{b}$ FOR FIT-1, $g(x) = x - 1 - \ln(x)$

S	x_o	$\bar{b}$	$\bar{c}$
0	1	.50000 00000	$g(x_o)=0$
1	1	.63463 61709	0
2	1	.70479 93293	0
3	1	.74929 19895	0
4	1	.78053 21002	0
5	1	.80390 29111	0
6	1	.82216 51352	0
7	1	.83689 78455	0
8	1	.84907 68432	0
9	1	.85934 10855	0
10	1	.86812 82760	0
16	1	.90265 28405	0
0	2	.83409 07182	0
1	2	.82671 32049	0
2	2	.84136 46500	0
3	2	.85567 46879	0
4	2	.86781 56014	0
5	2	.87797 07329	0
6	2	.88652 82066	0
7	2	.89382 42960	0
8	2	.90011 88888	0
9	2	.90560 86911	0
10	2	.91044 31283	0
16	2	.93065 54450	0
0	2	.68066 43084	$g(x_o)=1-\ln(2)$
1	2	.75000 00000	$g(x_o)$
2	2	.79022 25134	$g(x_o)$
3	2	.81731 80855	$g(x_o)$
4	2	.83713 03195	$g(x_o)$
5	2	.85239 96646	$g(x_o)$
6	2	.86461 01481	$g(x_o)$
7	2	.87464 59948	$g(x_o)$
8	2	.88307 15099	$g(x_o)$
9	2	.89026 60501	$g(x_o)$
10	2	.89649 52728	$g(x_o)$
16	2	.92163 03621	$g(x_o)$

OPTIMUM COEFFICIENT $\bar{b}$ FOR FIT-1, $g(x) = x - 1 - \ln(x)$

$\underline{S}$	x_o	$\bar{b}$	$\bar{c}$
0	1	.50000 00000	$g(x_o)$
0	2	.68066 43084	$g(x_o)$
0	3	.76208 37403	$g(x_o)$
0	4	.80951 84749	$g(x_o)$
0	5	.84084 43526	$g(x_o)$
0	6	.86316 90731	$g(x_o)$
0	7	.87992 32882	$g(x_o)$
0	8	.89297 87374	$g(x_o)$
0	9	.90344 78223	$g(x_o)$
0	10	.91203 50027	$g(x_o)$
0	11	.91920 88943	$g(x_o)$

OPTIMUM COEFFICIENTS FOR FIT-2, $g(x) = x - 1 - \ln(x)$

$\underline{S}(dB)$	x_o	$\check{b}$	$\check{c}$
$-\infty$	11	.92225 95675	7.5960 03381
-4	11	.92620 52679	7.5912 90368
-3	11	.92714 32728	7.5899 30861
-2	11	.92828 10207	7.5881 49569
-1	11	.92964 98384	7.5858 06201
0	11	.93128 09423	7.5827 13409
1	11	.93320 30816	7.5786 23271
2	11	.93543 95228	7.5732 12010
3	11	.93800 45899	7.5660 64105
4	11	.94090 01605	7.5566 57775
5	11	.94411 26969	7.5443 54565
6	11	.94761 14546	7.5283 96232
7	11	.95134 84273	7.5079 11992
8	11	.95526 03258	7.4819 38230
9	11	.95927 24991	7.4494 51068
10	11	.96330 43057	7.4094 10003
$-\infty$	9	.90775 76002	5.7941 55867
-4	9	.91315 09831	5.7877 17092
-3	9	.91441 81751	5.7858 80522
-2	9	.91594 78247	5.7834 85744
-1	9	.91777 76590	5.7803 53285
0	9	.91994 35729	5.7762 46689
1	9	.92247 62583	5.7708 57817
2	9	.92539 71647	5.7637 91177
3	9	.92871 41971	5.7545 49005
4	9	.93241 77882	5.7425 19630
5	9	.93647 81265	5.7269 72270
6	9	.94084 42937	5.7070 61457
7	9	.94544 58154	5.6818 43574
8	9	.95019 66890	5.6503 06459
9	9	.95500 14422	5.6114 10871
10	9	.95976 23429	5.5641 40375

OPTIMUM COEFFICIENTS FOR FIT-2, $g(x) = x - 1 - \ln(x)$

S(dB)	x_o	$\tilde{b}$	$\tilde{c}$
$-\infty$	7	.88648 76725	4.0409 61082
-7	7	.89059 83768	4.0364 46787
-6	7	.89160 15654	4.0352 17624
-5	7	.89283 16788	4.0336 38712
-4	7	.89433 08847	4.0316 04404
-3	7	.89614 47388	4.0289 75636
-2	7	.89832 03044	4.0255 69793
-1	7	.90090 32451	4.0211 48392
0	7	.90393 38303	4.0154 02859
1	7	.90744 20032	4.0079 39227
2	7	.91144 19462	3.9982 63354
3	7	.91592 68934	3.9857 69096
4	7	.92086 51677	3.9697 32518
5	7	.92619 84553	3.9493 15412
6	7	.93184 30742	3.9235 80802
7	7	.93769 44685	3.8915 21627
8	7	.94363 44925	3.8521 01661
9	7	.94954 04350	3.8043 05370
10	7	.95529 43858	3.7471 91510
$-\infty$	5	.85211 08814	2.3680 29030
-4	5	.86465 39431	2.3530 81233
-3	5	.86748 93493	2.3489 72161
-2	5	.87085 95380	2.3436 96494
-1	5	.87481 86148	2.3369 20078
0	5	.87940 72956	2.3282 21660
1	5	.88464 55460	2.3170 78963
2	5	.89052 54537	2.3028 58079
3	5	.89700 56821	2.2848 09313
4	5	.90400 89311	2.2620 72753
5	5	.91142 35093	2.2336 96167
6	5	.91910 93940	2.1986 66239
7	5	.92690 81996	2.1559 51865
8	5	.93465 55879	2.1045 55788
9	5	.94219 41367	2.0435 68946
10	5	.94938 46865	1.9722 21122

OPTIMUM COEFFICIENTS FOR FIT-2, $g(x) = x - 1 - \ln(x)$

$\underline{S}$(dB)	x_o	$\mathfrak{b}$	$\mathfrak{c}$
$-\infty$	3	.78625 12208	.85305 27503
-4	3	.80999 00501	.82481 06427
-3	3	.81516 25120	.81731 52922
-2	3	.82122 36047	.80782 83112
-1	3	.82822 71199	.79584 26744
0	3	.83619 25020	.78074 60381
1	3	.84509 41622	.76181 49196
2	3	.85485 37960	.73821 72304
3	3	.86533 79676	.70902 61829
4	3	.87636 25481	.67324 74273
5	3	.88770 42542	.62985 91859
6	3	.89911 79023	.57786 25469
7	3	.91035 66214	.51633 66733
8	3	.92119 16319	.44449 22468
9	3	.93142 85042	.36171 64722
10	3	.94091 78565	.26760 44129
11	3	.94955 98168	.16197 38256
12	3	.95730 28205	.04486 33282
13	3	.96413 81279	-.08348 39910
14	3	.97009 17657	-.22264 79238
15	3	.97521 54947	-.37206 52497
$-\infty$	1	.59634 73623	-.19269 47246
-4	1	.66461 29941	-.27361 79847
-3	1	.67837 13161	-.29355 18221
-2	1	.69403 34922	-.31806 14225
-1	1	.71154 20343	-.34801 67111
0	1	.73072 76581	-.38436 59487
1	1	.75130 37657	-.42810 59470
2	1	.77287 66361	-.48023 95488
3	1	.79497 21515	-.54172 30324
4	1	.81707 57330	-.61340 88469
5	1	.83867 85685	-.69599 10057
6	1	.85932 16212	-.78996 07593
7	1	.87862 98970	-.89557 85961
8	1	.89633 24642	-1.0128 65645
9	1	.91226 74477	-1.1416 14117
10	1	.92637 43448	-1.2814 13515

APPENDIX C. PARTIAL FRACTION EXPANSION OF PRODUCT

For j and n integer, and complex parameters $\alpha \neq \beta$, define the quantities

$$\mu_{jn}(\alpha,\beta) = \frac{\alpha^j \ (-\beta)^n}{(\alpha-\beta)^{j+n}} \frac{(j)_n}{n!} \quad \text{for } j \geq 1 \ , \ n \geq 0 \ ; \qquad \text{(C-1)}$$

$$\nu_{jn}(\alpha,\beta) = \frac{\beta^j \ (-\alpha)^n}{(\beta-\alpha)^{j+n}} \frac{(j)_n}{n!} \quad \text{for } j \geq 1 \ , \ n \geq 0 \ . \qquad \text{(C-2)}$$

Then, $\nu_{jn}(\beta,\alpha) = \mu_{jn}(\alpha,\beta)$.

These quantities can be easily evaluated by recursions:

$$\mu_{j0}(\alpha,\beta) = \left(\frac{\alpha}{\alpha-\beta}\right)^j \quad \text{for } j \geq 1 \ ,$$

$$\mu_{jn}(\alpha,\beta) = \mu_{j,n-1}(\alpha,\beta) \ \frac{\beta}{\beta-\alpha} \ \frac{j-1+n}{n} \quad \text{for } n \geq 1 \ , \ j \geq 1 \ ; \qquad \text{(C-3)}$$

$$\nu_{j0}(\alpha,\beta) = \left(\frac{\beta}{\beta-\alpha}\right)^j \quad \text{for } j \geq 1 \ ,$$

$$\nu_{jn}(\alpha,\beta) = \nu_{j,n-1}(\alpha,\beta) \ \frac{\alpha}{\alpha-\beta} \ \frac{j-1+n}{n} \quad \text{for } n \geq 1 \ , \ j \geq 1 \ . \qquad \text{(C-4)}$$

Now, consider the partial fraction expansion of the product of the following two functions, where complex constants $\alpha \neq \beta$; for integers $m \geq 1$, $k \geq 1$, define the function of complex variable z,

$$f(z) = \frac{1}{(1+z\alpha)^m \ (1+z\beta)^k} \ . \qquad \text{(C-5)}$$

Develop f(z) according to partial fraction expansion

$$f(z) = \sum_{n=0}^{m-1} \frac{u_n}{(1+z\alpha)^{m-n}} + \sum_{n=0}^{k-1} \frac{v_n}{(1+z\beta)^{k-n}} . \qquad (C-6)$$

Multiply both sides of (C-6) by $(1+z\alpha)^m$ to obtain

$$\frac{1}{(1+z\beta)^k} = \sum_{n=0}^{m-1} u_n (1+z\alpha)^n + (1+z\alpha)^m \sum_{n=0}^{k-1} \frac{v_n}{(1+z\beta)^{k-n}} . \qquad (C-7)$$

Take the p-th derivative of (C-7) with respect to z, and then let $z = -1/\alpha$; the right-hand side becomes simply $u_p\, p!\, \alpha^p$, while the left-hand side is

$$\frac{\alpha^{k+p} (-\beta)^p}{(\alpha-\beta)^{k+p}} (k)_p . \qquad (C-8)$$

Equating the two sides, we recognize that coefficient u_p in (C-6) is equal to $\mu_{kp}(\alpha,\beta)$ defined in (C-1). A similar treatment for coefficients $\{v_n\}$ in (C-6) yields the following expansion: for $m \geq 1$, $k \geq 1$, $\alpha \neq \beta$,

$$\frac{1}{(1+z\alpha)^m (1+z\beta)^k} = \sum_{n=0}^{m-1} \frac{\mu_{kn}(\alpha,\beta)}{(1+z\alpha)^{m-n}} + \sum_{n=0}^{k-1} \frac{v_{mn}(\alpha,\beta)}{(1+z\beta)^{k-n}} . \qquad (C-9)$$

Observe that expansion coefficients $\{\mu_{kn}(\alpha,\beta)\}$ do not depend on m, and that expansion coefficients $\{v_{mn}(\alpha,\beta)\}$ do not depend on k. It should also be noted that numerical difficulties can be expected with series expansion (C-9) when m and k are large, and α is close to β, due to the alternating character of the terms. Although the terms themselves can be calculated very accurately by means of (C-1) and (C-2), the sums in (C-9) will lose significance due to cancellation effects.

APPENDIX D. TWO ALTERNATIVE EXACT ANALYSIS METHODS

HIGH-ORDER MOMENT APPROACH

We can use the methods of [4; page 88] to determine the exact exceedance distribution function of summer output z in (4), provided that we can accurately evaluate the higher-order moments of the summer inputs $\{y_n\}$. These moments can be obtained as follows; for $x_o \geq 1$, and $g(x) = x - 1 - \ln(x)$ for $x > x_o$, zero otherwise, the k-th moment of y_n is given exactly by

$$\overline{y_n^k} = \overline{g(x_n)^k} = \int du \, p_x(u) \, g(u)^k = \int_{x_o}^{\infty} du \, p_x(u) \, (u - 1 - \ln(u))^k \quad \text{(D-1)}$$

for $k \geq 1$. For the exponential density (2) of input random variables $\{x_n\}$, this k-th moment becomes

$$\overline{y_n^k} = \int_{x_o}^{\infty} du \, \underline{a} \exp(-\underline{a}u) \, (u - 1 - \ln(u))^k \quad \text{for } k \geq 1 , \quad \text{(D-2)}$$

which depends on k, x_o, and $\underline{a}$. Since the integrand is positive for all u, regardless of k and $\underline{a}$, these integrals can be conducted very accurately to high order k, and used in the recursive procedures of [4] to get the cumulants of $\{y_n\}$ and z.

The major stumbling block to this approach is the round-off error encountered in transforming moments to cumulants. Double precision arithmetic is a necessity for useful numerical results. For $k = 1$, a closed form result is available; see (63). For $k = 2$, (D-2) could be evaluated from the results in appendix F.

CHARACTERISTIC FUNCTION APPROACH

An alternative approach is to directly numerically evaluate the characteristic function of $\{y_n\}$, which is given exactly by

$$f_y(\xi) = \overline{\exp(i\xi y_n)} = \overline{\exp(i\xi g(x_n))} = \int du \, p_x(u) \, \exp(i\xi g(u)) =$$

$$= \int_{-\infty}^{x_o} du \, p_x(u) + \int_{x_o}^{\infty} du \, p_x(u) \, \exp(i\xi[u - 1 - \ln(u)]) . \qquad (D-3)$$

When probability density function $p_x(u)$ is exponential, this reduces, for $x_o > 0$, to

$$f_y(\xi) = 1 - \exp(-\underline{a}x_o) + \underline{a} \int_{x_o}^{\infty} du \, \exp(-\underline{a}u + i\xi[u - 1 - \ln(u)]) . \quad (D-4)$$

The integral depends on ξ, $\underline{a}$, and x_o. It must be numerically evaluated very accurately for numerous values of ξ.

The major drawback with this approach is the lack of decay of characteristic function $f_y(\xi)$ with ξ. Namely, $f_y(\xi)$ behaves as the constant, $1 - \exp(-\underline{a}x_o)$, as $\xi \to \pm\infty$. In order to numerically Fourier transform $f_z(\xi)$, which is given in terms of powers of $f_y(\xi)$, we must determine the dominant asymptotic behaviors of $f_y(\xi)$ and $f_z(\xi)$. In fact, it will be necessary to determine several of the leading terms in the asymptotic expansion of $f_y(\xi)$, at least to the point where the remainder decays fast enough to ensure that the termination of the Fourier integral, on the remainder of $f_z(\xi)$, contributes insignificantly to the truncation error. The asymptotic behavior of $f_y(\xi)$ is now considered.

ASYMPTOTIC BEHAVIOR OF CHARACTERISTIC FUNCTION
FOR IMPULSIVE PROBABILITY DENSITY FUNCTION

The generic problem is as follows: a given probability density function $p_y(u)$ has an impulse of area A_1 at the origin, and a distributed component which is nonzero only for $u \geq y_o$, where $y_o = g(x_o)$. Furthermore, $p_y(u)$ is smooth for $u > y_o$ and decays to zero for large u. The corresponding characteristic function is

$$f_y(\xi) = A_1 + \int_{y_o}^{\infty} du \ \exp(i\xi u) \ p_y(u) \ . \qquad (D-5)$$

We integrate by parts, letting (for $u > y_o$)

$$U = \exp(\alpha u) \ p_y(u) \equiv h(u) \ , \quad dV = du \ \exp(-(\alpha-i\xi)u) \ , \qquad (D-6)$$

where positive real constant α is yet to be chosen. Then,

$$dU = du \ h'(u) \ , \quad V = - \frac{\exp(-(\alpha-i\xi)u)}{\alpha-i\xi} \ , \qquad (D-7)$$

leading to

$$f_y(\xi) = A_1 + \frac{\exp(-(\alpha-i\xi)y_o)}{\alpha-i\xi} \ h(y_o) + \frac{1}{\alpha-i\xi} \int_{y_o}^{\infty} du \ \exp(-(\alpha-i\xi)u) \ h'(u). \qquad (D-8)$$

Repeated integrations by parts yields the asymptotic expansion of characteristic function $f_y(\xi)$ as

$$f_y(\xi) \sim A_1 + \sum_{n=1}^{\infty} \frac{\exp(i\xi y_o)}{(\alpha-i\xi)^n} \ \exp(-\alpha y_o) \ h^{(n-1)}(y_o) \quad \text{as } \xi \to \pm\infty \ . \qquad (D-9)$$

Strictly, the functions and derivatives are evaluated at $u = y_o+$.

Because $h(u) = \exp(\alpha u)\, p_y(u)$, the derivatives required above can be evaluated as follows; for $u > y_0$,

$$h'(u) = \exp(\alpha u)\,[\alpha\, p_y(u) + p_y'(u)] \,, \tag{D-10}$$

$$h''(u) = \exp(\alpha u)\,[\alpha^2\, p_y(u) + 2\alpha\, p_y'(u) + p_y''(u)] \,. \tag{D-11}$$

Then, the asymptotic expansion for characteristic function $f_y(\xi)$ becomes explicitly, to third order, $f(\xi) \sim f_3(\xi)$ as $\xi \to \pm\infty$, where

$$f_3(\xi) = A_1 + \exp(i\xi y_0)\left[\frac{P_1}{1-i\xi/\alpha} + \frac{P_2}{(1-i\xi/\alpha)^2} + \frac{P_3}{(1-i\xi/\alpha)^3}\right] \,, \tag{D-12}$$

and

$$P_1 = \frac{1}{\alpha}\, p_y(y_0) \,, \qquad P_2 = \frac{1}{\alpha^2}\Big(\alpha\, p_y(y_0) + p_y'(y_0)\Big) \,, \tag{D-13}$$

$$P_3 = \frac{1}{\alpha^3}\Big(\alpha^2\, p_y(y_0) + 2\alpha\, p_y'(y_0) + p_y''(y_0)\Big) \,. \tag{D-14}$$

One possible choice for α is to make the coefficient, P_2, of $(1-i\xi/\alpha)^{-2}$ equal to zero; that is, take $\alpha = -p_y'(y_0)/p_y(y_0)$, or approximately so. Another is to let $\exp(-\alpha u)$ duplicate the asymptotic behavior of $p_y(u)$; that is, have $h(u)$ approach a constant as $u \to +\infty$. The choice of α does not seem critical.

The individual terms in $f_3(\xi)$ can be easily Fourier transformed analytically. The leading term is an impulse at $u = 0$, as before. The next term is a decaying exponential starting at $u = y_0$. The $(1-i\xi/\alpha)^{-2}$ term leads to a $u\exp(-u)$ type term, also delayed to $u = y_0$. The last term behaves as $u^2\exp(-u)$, but starting at $u = y_0$.

We are also interested in the asymptotic decay of a power of $f_y(\xi)$. Letting $z = (1-i\xi/\alpha)^{-1}$, we have the k-th power

$$f_y^k(\xi) \sim f_3^k(\xi) = \left(A_1 + \exp(i\xi y_0)\left(P_1 \, z + P_2 \, z^2 + P_3 \, z^3\right)\right)^k =$$

$$\sim A_1^k + k \, A_1^{k-1} \exp(i\xi y_0)\left(P_1 \, z + P_2 \, z^2 + P_3 \, z^3\right) + \binom{k}{2} A_1^{k-2} \times$$

$$\times \exp(i\xi 2y_0)\left(P_1^2 \, z^2 + 2 \, P_1 \, P_2 \, z^3\right) + \binom{k}{3} A_1^{k-3} \exp(i\xi 3y_0) \, P_1^3 \, z^3 \, ,$$

$$\text{(D-15)}$$

as $z \to 0$, to third order. Substituting for z,

$$f_y^k(\xi) \sim f_{3k}(\xi) = A_1^k + k \, A_1^{k-1} \exp(i\xi y_0)\left(\frac{P_1}{1-i\xi/\alpha} + \frac{P_2}{(1-i\xi/\alpha)^2} + \right.$$

$$\left. + \frac{P_3}{(1-i\xi/\alpha)^3}\right) + \binom{k}{2} A_1^{k-2} \exp(i\xi 2y_0)\left(\frac{P_1^2}{(1-i\xi/\alpha)^2} + \frac{2 \, P_1 \, P_2}{(1-i\xi/\alpha)^3}\right) +$$

$$+ \binom{k}{3} A_1^{k-3} \exp(i\xi 3y_0) \, \frac{P_1^3}{(1-i\xi/\alpha)^3} \quad \text{as } \xi \to \pm\infty \, . \qquad \text{(D-16)}$$

This is the desired result for the asymptotic behavior of the k-th power of characteristic function $f_y(\xi)$.

The corresponding cumulative distribution function is

$$A_1^k \, C_0(v) + k \, A_1^{k-1}\left(P_1 \, C_1(v_1) + P_2 \, C_2(v_1) + P_3 \, C_3(v_1)\right) +$$

$$+ \binom{k}{2} A_1^{k-2}\left(P_1^2 \, C_2(v_2) + 2 \, P_1 \, P_2 \, C_3(v_2)\right) + \binom{k}{3} A_1^{k-3} \, P_1^3 \, C_3(v_3) \, ,$$

$$\text{(D-17)}$$

where

$$v_n = \alpha(v - ny_0) \, . \qquad \text{(D-18)}$$

EVALUATION OF DERIVATIVES OF $p_y(u)$

In order to use the results in (D-12) and (D-14), we need to know the derivatives of probability density function $p_y(u)$ at $u = y_0+$, where $y_0 = g(x_0)$. Random variable y_n is obtained by nonlinear transformation $g(x_n)$, where nonlinearity $g(x)$ is presumed to be strictly monotonically increasing for $x > x_0$, and to be zero for $x < x_0$. We now relate the desired derivatives of $p_y(u)$ to those of $p_x(u)$ and the nonlinear transformation $g(x)$. This will enable us to determine the constants P_1, P_2, P_3 required in (D-14).

For $v > y_0$, the exceedance distribution function of random variable y_n is given by

$$E_y(v) = \Pr(y_n > v) = \Pr(g(x_n) > v) = \Pr(x_n > \tilde{g}(v)) = E_x(\tilde{g}(v)) \ . \tag{D-19}$$

Here, $\tilde{g}(y)$ is the inverse function to $g(x)$, at least for $y > y_0$; that is,

if $y = g(x)$ for $x > x_0$, then $x = \tilde{g}(y)$ for $y > y_0 = g(x_0)$. (D-20)

A useful relation follows from the fact that $g(\tilde{g}(y)) = y$. Taking a derivative with respect to y, we have $g'(\tilde{g}(y)) \, \tilde{g}'(y) = 1$, or

$$\tilde{g}'(y) = \frac{1}{g'(\tilde{g}(y))} \ . \tag{D-21}$$

The probability density function of random variable y_n is given by

$$p_y(u) = -\frac{d}{du} E_y(u) = -\frac{d}{du} E_x(\breve{g}(u)) = p_x(\breve{g}(u))\ \breve{g}'(u) =$$

$$= \frac{p_x(\breve{g}(u))}{g'(\breve{g}(u))} \quad \text{for } u > y_0 , \tag{D-22}$$

where we used (D-21). If we now let $u = g(t)$, this latter relation takes on the desired very useful form:

$$p_y(g(t)) = \frac{p_x(t)}{g'(t)} . \tag{D-23}$$

Substitution of $t = x_0$ yields $p_y(y_0) = p_x(x_0)/g'(x_0)$, which is one of the results required for (D-14). Notice that inverse function $\breve{g}(y)$ is not required or used in (D-23) or the sequel.

We now take two successive derivatives of (D-23) with respect to t, to get

$$p_y'(g(t)) = \frac{g'(t)\ p_x'(t) - p_x(t)\ g''(t)}{g'(t)^3} , \tag{D-24}$$

$$p_y''(g(t)) = \frac{g'^2\ p_x'' - 3\ g'\ g''\ p_x' + \left(3\ g''^2 - g'\ g'''\right)\ p_x}{g'^5} , \tag{D-25}$$

where all the quantities in the last equation are to be evaluated at argument t. When we substitute $t = x_0$, we obtain expressions for $p_y'(y_0)$ and $p_y''(y_0)$ in terms of quantities easily available from the given functions $p_x(u)$ and $g(x)$. There is no need to evaluate inverse function $\breve{g}(y)$ or its derivatives at all.

For example, we have, for $x > x_0$ and for $u > 0$,

$$g(x) = x - 1 - \ln(x), \quad g'(x) = 1 - \frac{1}{x}, \quad g''(x) = \frac{1}{x^2}, \quad (D-26)$$

$$p_x(u) = \underline{a} \exp(-\underline{a}u), \quad p_x'(u) = -\underline{a}^2 \exp(-\underline{a}u), \quad p_x''(u) = \underline{a}^3 \exp(-\underline{a}u).$$

APPENDIX B. TABLES OF FIRST FOUR CUMULANTS OF y_n

FIRST FOUR CUMULANTS OF y_n FOR $x_o = 1$

$\underline{S}$(dB)	$X_y(1,x_o,\underline{S})$	$X_y(2,x_o,\underline{S})$	$X_y(3,x_o,\underline{S})$	$X_y(4,x_o,\underline{S})$
$-\infty$	.14849 55068	.17363 54789	.36390 41244	1.1105 77108
-3	.37232 63923	.67739 77766	2.1866 54609	10.222 37915
-2	.44083 61060	.87450 33444	3.0742 91858	15.641 93753
-1	.53192 32228	1.1641 73519	4.5105 69661	25.281 35153
0	.65328 77247	1.5963 40984	6.9002 68199	43.135 87531
1	.81510 93535	2.2499 35901	10.982 78191	77.532 33382
2	1.0307 05214	3.2500 85125	18.129 05704	146.29 59138
3	1.3173 12381	4.7954 26841	30.913 39282	288.51 60247
4	1.6970 24416	7.2014 17458	54.221 46053	591.76 61973
5	2.1979 28595	10.968 93324	97.408 56056	1255.9 48815
6	2.8555 11925	16.892 91290	178.52 20929	2744.8 30537
7	3.7144 26320	26.234 42995	332.59 30788	6149.3 66839
8	4.8307 25577	40.993 28950	627.96 80417	14066. 27845
9	6.2747 10254	64.339 96462	1198.5 59409	32737. 77500
10	8.1345 44258	101.30 01036	2307.6 61144	77293. 54256
11	10.520 84245	159.83 93733	4474.4 34247	18465 5.1198
12	13.572 47552	252.58 28253	8724.9 42288	44542 8.8106
13	17.463 89993	399.53 99358	17090. 91588	10829 81.677

FIRST FOUR CUMULANTS OF y_n FOR $x_o = 2$

$\underline{S}$(dB)	$X_y(1,x_o,\underline{S})$	$X_y(2,x_o,\underline{S})$	$X_y(3,x_o,\underline{S})$	$X_y(4,x_o,\underline{S})$
$-\infty$	.12796 27858	.17574 47137	.37421 11513	1.1387 25648
-3	.34822 40437	.69043 82072	2.2305 06064	10.384 05135
-2	.41655 24216	.89094 29992	3.1298 99242	15.860 39913
-1	.50764 21649	1.1850 11999	4.5823 63547	25.584 30823
0	.62925 97917	1.6227 77524	6.9941 24512	43.565 01106
1	.79164 09435	2.2833 42973	11.106 35405	78.149 58412
2	1.0081 35006	3.2919 45145	18.291 97917	147.19 16125
3	1.2959 77672	4.8472 32578	31.127 31394	289.81 88541
4	1.6772 24228	7.2645 48258	54.499 84453	593.65 45829
5	2.1798 91997	11.044 52901	97.766 23265	1258.6 63214
6	2.8393 78415	16.981 77103	178.97 45759	2748.6 86124
7	3.7002 41138	26.336 94483	333.15 58187	6154.7 66460
8	4.8184 48437	41.109 44269	628.65 56484	14073. 72632
9	6.2642 33059	64.469 36116	1199.3 85027	32747. 89234
10	8.1257 12529	101.44 20408	2308.6 36021	77307. 08684
11	10.513 47608	159.99 29258	4475.5 67530	18467 3.0099
12	13.566 38612	252.74 69308	8726.2 41019	44545 2.1601
13	17.458 90366	399.71 34719	17092. 38514	10830 11.838

FIRST FOUR CUMULANTS OF y_n FOR $x_o = 3$

$\underline{S}$(dB)	$X_y(1,x_o,\underline{S})$	$X_y(2,x_o,\underline{S})$	$X_y(3,x_o,\underline{S})$	$X_y(4,x_o,\underline{S})$
$-\infty$	.08161 61389	.15797 37056	.38690 96395	1.2208 51895
-3	.27666 02014	.69156 35364	2.3702 27986	11.036 89414
-2	.34121 53043	.90194 63156	3.3221 83512	16.774 78383
-1	.42874 07666	1.2104 17015	4.8501 33315	26.896 18335
0	.54736 75223	1.6685 94431	7.3691 87760	45.481 75146
1	.70773 91341	2.3571 33468	11.631 37379	80.982 51465
2	.92358 84667	3.4026 30423	19.021 84015	151.39 81523
3	1.2124 28857	5.0045 81998	32.129 31540	296.05 40638
4	1.5964 18859	7.4783 77694	55.852 29933	602.83 07406
5	2.1034 74853	11.323 74546	99.555 41783	1272.0 15276
6	2.7687 09493	17.333 46922	181.29 04235	2767.8 40967
7	3.6362 73368	26.765 75330	336.08 70650	6181.8 14926
8	4.7616 84723	41.617 23609	632.28 52476	14111. 29939
9	6.2147 55389	65.055 34614	1203.7 86484	32799. 24592
10	8.0832 59751	102.10 31337	2313.8 71014	77376. 20297
11	10.477 54291	160.72 42975	4481.6 84888	18476 4.7253
12	13.536 32086	253.54 ?5985	8733.2 76884	44557 2.3351
13	17.433 99077	400.56 68463	17100. 36401	10831 67.581

FIRST FOUR CUMULANTS OF y_n FOR $x_o = 4$

$\underline{S}$(dB)	$X_y(1,x_o,\underline{S})$	$X_y(2,x_o,\underline{S})$	$X_y(3,x_o,\underline{S})$	$X_y(4,x_o,\underline{S})$
$-\infty$	.04409 23362	.11669 06448	.35266 30056	1.2490 58964
-3	.19680 45752	.62991 50503	2.4586 33259	11.977 52732
-2	.25275 52920	.84403 91675	3.4874 09776	18.216 44483
-1	.33098 77685	1.1623 08487	5.1381 14630	29.139 34394
0	.44016 13655	1.6398 93287	7.8490 33261	48.998 37207
1	.59167 89225	2.3618 68137	12.402 31198	86.492 11951
2	.80018 53326	3.4596 25997	20.218 49273	159.95 79889
3	1.0841 03120	5.1369 50753	33.922 84360	309.15 65917
4	1.4663 01430	7.7119 13587	58.445 51834	622.50 32500
5	1.9750 40621	11.684 38786	103.17 17742	1300.9 23790
6	2.6453 34913	17.844 38888	186.15 89727	2809.4 09138
7	3.5208 35504	27.444 78839	342.42 69507	6240.3 71327
8	4.6562 93538	42.475 26777	640.29 29312	14192. 26152
9	6.1206 54795	66.095 85133	1213.6 27511	32909. 34237
10	8.0008 77841	103.32 27879	2325.6 76461	77523. 73434
11	10.406 63981	162.11 42758	4495.5 51594	18495 9.8717
12	13.476 17733	255.09 01757	8749.2 70217	44582 7.5304
13	17.383 59317	402.25 69708	17118. 52208	10834 97.984

FIRST FOUR CUMULANTS OF y_n FOR $x_o = 5$

$\underline{S}$(dB)	$X_y(1,x_o,\underline{S})$	$X_y(2,x_o,\underline{S})$	$X_y(3,x_o,\underline{S})$	$X_y(4,x_o,\underline{S})$
$-\infty$	.02169 71321	.07429 15920	.27629 23357	1.1378 38302
-6	.06315 81464	.23428 94293	.96935 98872	4.5748 10040
-5	.07820 10435	.29577 38500	1.2557 42634	6.1234 69370
-4	.09966 37988	.38597 79652	1.6911 30853	8.5814 32049
-3	.13059 80027	.52048 20797	2.3690 78533	12.613 56291
-2	.17548 64274	.72384 98638	3.4491 59992	19.453 18457
-1	.24077 73591	1.0346 12281	5.2064 25434	31.446 96885
0	.33548 43650	1.5126 74268	8.1193 82192	53.177 35907
1	.47177 85899	2.2502 13248	13.028 97303	93.844 08351
2	.66549 58331	3.3878 89404	21.432 66966	172.47 94233
3	.93653 73661	5.1397 44742	36.043 12414	329.71 05887
4	1.3092 61848	7.8329 42384	61.872 58912	654.91 96171
5	1.8130 90353	11.972 72241	108.36 34174	1350.0 16099
6	2.4835 95568	18.348 79645	193.58 95155	2880.9 67995
7	3.3642 83219	28.207 60768	352.54 26287	6341.2 44308
8	4.5091 48759	43.527 50601	653.47 59357	14330. 61359
9	5.9860 00189	67.454 60329	1230.1 76332	33095. 11689
10	7.8805 39970	104.99 11600	2345.8 02719	77769. 26471

APPENDIX F.   INDEFINITE INTEGRAL OF EXPONENTIAL INTEGRAL

The integral of interest here is, for $x > 0$,

$$E_{11}(x) \equiv \int_x^\infty \frac{dt}{t} E_1(t) = \int_1^\infty \frac{dt}{t} \ln(t) \exp(-xt) . \qquad (F-1)$$

A series expansion for $E_{11}(x)$, which is good for small x, is given by [9; pages 258 - 259]:

$$E_{11}(x) = \frac{1}{2}[\ln(x)+\gamma]^2 + \frac{\pi^2}{12} + \sum_{n=1}^\infty \frac{(-x)^n}{n^2 \, n!} \quad \text{for } x > 0 . \qquad (F-2)$$

However, for large x, this series loses significance, and an asymptotic expansion is required.

We begin with the second form in (F-1) and express

$$\frac{\ln(t)}{t} = \frac{\ln(1 + t-1)}{1 + t-1} = \sum_{n=1}^\infty (-1)^{n-1} \gamma_n \, (t-1)^n \quad \text{for } |t-1| < 1 , \quad (F-3)$$

where

$$\gamma_n \equiv 1 + \frac{1}{2} + \frac{1}{3} + \cdots + \frac{1}{n} \quad \text{for } n \geq 1 . \qquad (F-4)$$

Then, as $x \to +\infty$,

$$E_{11}(x) \sim \int_1^\infty dt \, \exp(-xt) \sum_{n=1}^\infty (-1)^{n-1} \gamma_n \, (t-1)^n =$$

$$= \frac{\exp(-x)}{x^2} \sum_{n=1}^\infty \frac{n! \, \gamma_n}{(-x)^{n-1}} . \qquad (F-5)$$

The leading terms of (F-5) are given by

$$E_{11}(x) \sim \frac{\exp(-x)}{x^2} \left[1 - \frac{3}{x} + \frac{11}{x^2} - \frac{50}{x^3} + \frac{274}{x^4} - \cdots \right] \quad \text{as } x \to +\infty . \quad \text{(F-6)}$$

A program for $E_{11}(x)$ for $x > 0$, incorporating series expansion (F-2) and asymptotic expansion (F-5), is given below in BASIC. The switch between the two expansions is done at $x = 13$, which res_lts in 6 significant digits in result $E_{11}(x)$. A recursion for n! γ_n is built into the program in lines 190 - 200.

```
10   DEF FNE11(X)
20   IF X>13. THEN 150
30   Tol=1.E-14
40   T=LOG(X)+.577215664490153286
50   S=.5*T*T+PI*PI/12.
60   T=1.
70   Sn=0.
80   FOR N=1 TO 100
90   T=-T*X/N
100  R=T/(N*N)
110  Sn=Sn+R
120  IF ABS(R)<Tol*ABS(Sn) THEN 140
130  NEXT N
140  RETURN S+Sn
150  T=-1./X
160  A=1.E10
170  H=G=P=S=1.
180  FOR N=2 TO 100
190  H=H*(N-1)
200  G=G*N+H
210  P=P*T
220  Ao=A
230  A=G*P
240  IF ABS(A)>ABS(Ao) THEN 270
250  S=S+A
260  NEXT N
270  S=S-.5*Ao
280  RETURN S*EXP(-X)*T*T
290  FNEND
```

APPENDIX G. DIRECT EVALUATION OF EXACT EXCEEDANCE DISTRIBUTION

The _exact_ characteristic function of output $y_n = g(x_n)$ in (4), of the nonlinear device in (3), can be found with the aid of (2). For the case, H_1, of the signal-present bins with equal signal powers $\underline{S}_n = \underline{S}$, it is given by the integral expression

$$f_y^{(1)}(\xi) = \overline{\exp(i\xi y_n)} = \overline{\exp(i\xi g(x_n))} = \int du\, q_1(u)\, \exp(i\xi g(u)) =$$

$$= 1 - \exp(-\underline{a}x_0) + \int_{x_0}^{\infty} du\, \underline{a}\, \exp(-\underline{a}u)\, \exp(i\xi[u - 1 - \ln(u)]) \ , \quad \text{(G-1)}$$

where $\underline{a} = 1/(1 + \underline{S})$. For case H_0, replace $\underline{a}$ by 1. The characteristic function of decision variable z in (4), for signal present in M bins, is then given by

$$f_z(\xi) = \left(f_y^{(1)}(\xi)\right)^M \left(f_y^{(0)}(\xi)\right)^{N-M} . \quad \text{(G-2)}$$

This result can be evaluated numerically by brute force from (G-1) for numerous values of ξ, and used in the fast accurate procedure of [7] to directly obtain the exceedance distribution function of decision variable z, at least for some cases of breakpoint x_0 and large N. An example for $\underline{S} = 0$, $x_0 = 1$, and N = 1024 is given in figure G-1, where we evaluated integral (G-1) at increment $\Delta_\xi = \pi/120$, up to $\xi = 1$. This plot is the false alarm probability and should be compared with the corresponding simulation curve in figure 3. Agreement is excellent, but we are now able to investigate down to the 10^{-6} level.
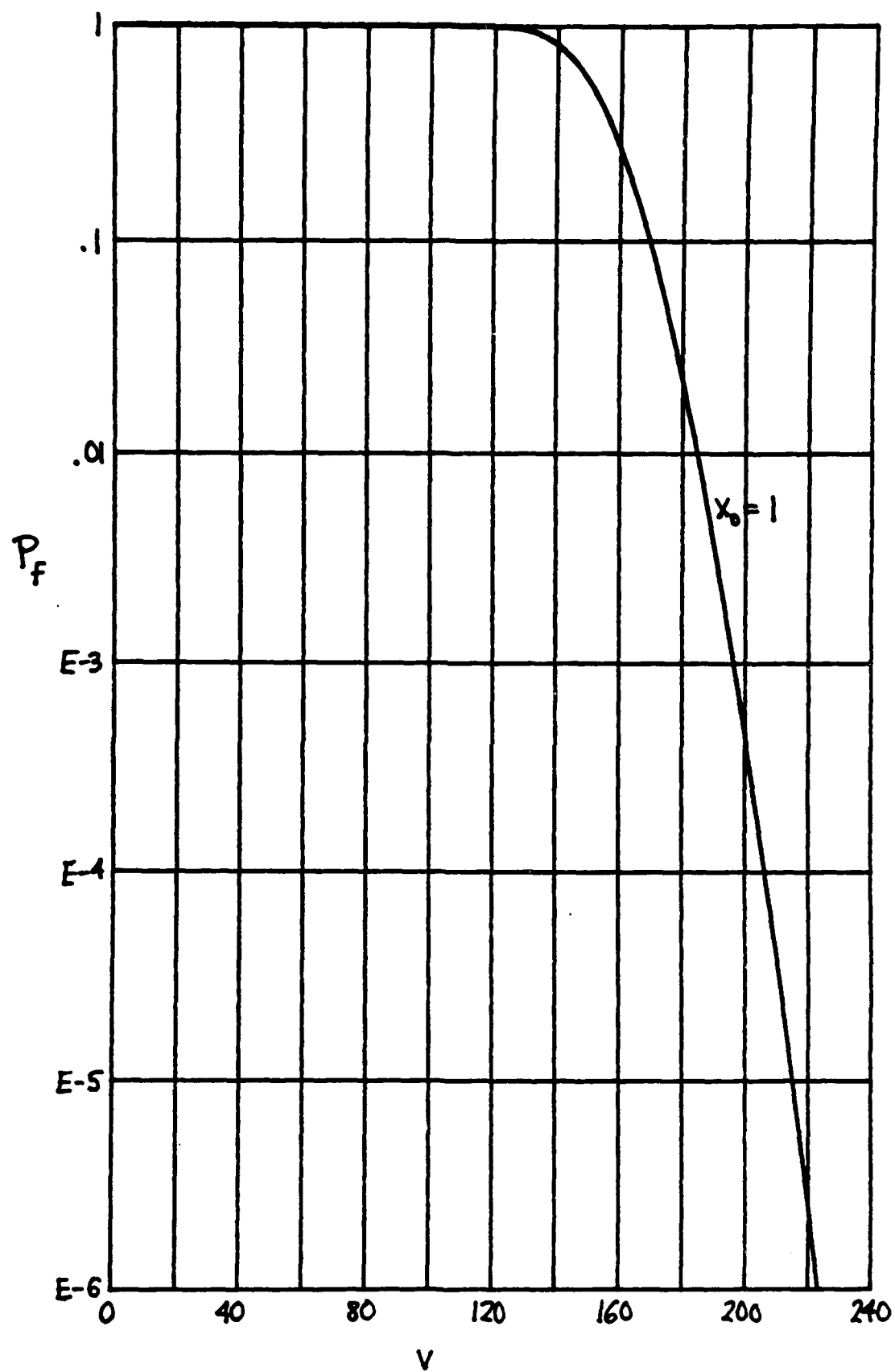
Figure G-1. False Alarm Probability for N = 1024, x_o = 1

REFERENCES

[1] J. J. Wolcin, personal communication, August 1983.

[2] A. H. Nuttall, Operating Characteristics for Combiner With a Dead Zone in Each Channel, NUSC Technical Report 8595, Naval Underwater Systems Center, New London, CT, 10 August 1989.

[3] A. H. Nuttall, Generalized Likelihood Ratio Processors and Near-Optimum Processors under Various Degrees of Knowledge of Signal Structure, NUWC Technical Report, Naval Undersea Warfare Center, New London, CT, to be published.

[4] A. H. Nuttall, Evaluation of Densities and Distributions via Hermite and Generalized Laguerre Series Employing High-Order Expansion Coefficients Determined Recursively via Moments or Cumulants, NUSC Technical Report 7377, Naval Underwater Systems Center, New London, CT, 28 February 1985.

[5] A. H. Nuttall, Operating Characteristics for Weighted Energy Detector with Gaussian Signals, NUSC Technical Report 8753, Naval Underwater Systems Center, New London, CT, 16 July 1990.

[6] A. H. Nuttall, Exact Performance of Filtered and Weighted Energy Detector with Mismatched Frequency and Time Locations and Characteristics, NUSC Technical Report 8913, Naval Underwater Systems Center, New London, CT, 29 July 1991.

[7] A. H. Nuttall, Accurate Efficient Evaluation of Cumulative or Exceedance Probability Distributions Directly From Characteristic Functions, NUSC Technical Report 7023, Naval Underwater Systems Center, New London, CT, 1 October 1983.

[8]   Handbook of Mathematical Functions, U. S. Department of Commerce, National Bureau of Standards, Applied Mathematics Series, number 55, U. S. Government Printing Office, Washington, DC, June 1964.

[9]   V. Kourganoff, Basic Methods in Transfer Problems, Dover Publications Inc., New York, NY, 1963.

INITIAL DISTRIBUTION LIST

Addressee	Number of Copies
Center for Naval Analyses, VA	1
Coast Guard Academy, CT	
J. Wolcin	1
Defense Nuclear Agency, VA	
J. Meyers	1
Defense Technical Information Center, VA	12
National Radio Astronomy Observatory, VA	
F. Schwab	1
National Security Agency, MD	
J. Maar	1
National Technical Information Service, VA	10
Naval Air Warfare Center, PA	
Commander	1
L. Allen	1
T. Madera	1
A. Witt	1
Naval Command Control and Ocean Surveillance Center, HI	1
Naval Command Control and Ocean Surveillance Center, CA	
Commanding Officer	1
J. Alsup	1
D. Hanna	1
W. Marsh	1
P. Nachtigall	1
C. Persons	1
J. Silva	1
C. Tran	1
Naval Environmental Prediction Research Facility, CA	1
Naval Intelligence Command, DC	1
Naval Oceanographic and Atmospheric Research Laboratory, CA	
M. Pastore	1
Naval Oceanographic and Atmospheric Research Laboratory, MS	
Commanding Officer	1
B. Adams	1
R. Fiddler	1
E. Franchi	1
R. Wagstaff	1
Naval Oceanographic Office, MS	1
Naval Personnel Research and Development Center, CA	1
Naval Postgraduate School, CA	
Superintendent	1
C. Therrien	1
Naval Research Laboratory, FL	1
Naval Research Laboratory, DC	
Commanding Officer	1
D. Bradley	1
W. Gabriel	1
A. Gerlach	1

INITIAL DISTRIBUTION LIST (CONT'D)

Addressee	Number of Copies
Naval Research Laboratory, DC	
D. Steiger	1
E. Wald	1
N. Yen	1
Naval Sea Systems Command, DC	
SEA-00; -63; -63D; -63X; -92R; PMS-402	6
Naval Surface Warfare Center, FL	
Commanding Officer	1
E. Linsenmeyer	1
D. Skinner	1
Naval Surface Warfare Center, MD	
W. Phillips	1
P. Prendergast	1
Naval Surface Warfare Center, VA	
J. Gray	1
Naval Surface Weapons Center, FL	1
Naval Surface Weapons Center, MD	
Officer in Charge	1
M. Strippling	1
Naval Surface Weapons Center, VA	
Commander	1
H. Crisp	1
D. Phillips	1
T. Ryczek	1
Naval Technical Intelligence Center, DC	
Commanding Officer	1
D. Rothenberger	1
Naval Undersea Warfare Center, FL	
Officer in Charge	1
R. Kennedy	1
Naval Weapons Center, CA	1
Office of the Chief of Naval Research, VA	
OCNR-00; -10; -11; -12; -13; -20; -21; -22; -23 (3)	11
P. Abraham	1
N. Gerr	1
D. Johnson	1
A. Wood	1
Space and Naval Warfare System Command, DC	
SPAWAR-00; -04; -005; PD-80; PMW-181	5
R. Cockerill	1
L. Parrish	1
U. S. Air Force, Maxwell Air Force Base, AL	
Air University Library	1
U. S. Department of Commerce, CO	
A. Spaulding	1
Wright Patterson Air Force Base, OH	
R. Leonard	1